Aus der Medizinischen Klinik mit
Schwerpunkt Rheumatologie und Klinische Immunologie
der Medizinischen Fakultät
Charité-Universitätsmedizin Berlin

In Kooperation mit
The ANZAC Research Institute
The University of Sydney, Australia

DISSERTATION

Fracture Healing and Glucocorticoids in HSD2 Transgenic Mouse Model

zur Erlangung des akademischen Grades
Doctor medicinae (Dr. med.)

vorgelegt der Medizinischen Fakultät
Charité-Universitätsmedizin Berlin

von

Agnes Johanna Weber
aus Berlin

Gutachter: 1. Prof. Dr. med. F. Buttgereit
2. Prof. Dr. med. F. Jakob
3. Prof. Dr. med. P. Oelzner

Datum der Promotion: 24.02.2012

Abstract

Objective:

Glucocorticoids administered at pharmacological doses have been shown to interfere with fracture repair in humans. The role of endogenous glucocorticoids in fracture healing is not well understood. We examined whether endogenous glucocorticoids affect bone healing in an *in vivo* model of cortical defect repair.

Methods:

Experiments were performed using a mouse model in which intracellular glucocorticoid signalling was disrupted in osteoblasts at the pre-receptor level through transgenic over-expression of 11ß-hydroxysteroid-dehydrogenase type 2 (11ßHSD2) under the control of a collagen type I promoter (Col2.3-11ßHSD2). Unicortical bone defects (Ø 0.8 mm) were created in the tibiae of 7-week-old male transgenic mice and their wild-type littermates. Repair was assessed via histomorphometry, immunohistochemistry, microcomputed tomography (micro-CT) analysis performed at one, two and three weeks after defect initiation.

Results:

At week 1, micro-CT images of the defect demonstrated formation of mineralized intramembranous bone which increased in volume and density by week 2. At week 3, healing of the defect was nearly complete in all animals. Analysis by histomorphometry and micro-CT revealed that repair of the bony defect was similar in Col2.3-11ßHSD2 transgenic animals and their wild-type littermates at all time points.

Conclusion:

Disrupting endogenous glucocorticoid signalling in mature osteoblasts does not affect intramembranous fracture healing in a tibia defect repair model. It remains to be shown whether glucocorticoid signalling has a role in endochondral fracture healing.

Keywords: Osteoblasts, Steroid Hormones: Glucocorticoids, Fracture Repair

Zusammenfassung

Hintergrund:
Glucocorticoide in pharmakologischer Dosierung interferieren mit Frakturheilungsprozessen. Hingegen ist die Rolle der endogenen Glucocorticoide im Frakturheilungsprozess nur zum geringen Teil verstanden. Gegenstand der vorliegenden Arbeit war es, den Einfluss endogener Glucocorticoide auf die Frakturheilung in einem *in vivo* Modell von kortikaler Defektheilung zu untersuchen.

Methodik:
Für die Durchführung der Experimente wurde ein Mausmodell verwendet, in welchem der intrazelluläre Glucocorticoid-Signalweg spezifisch in Osteoblasten durch transgene Überexpression des 11ß-hydroxysteroid-dehydrogenase type 2 (11ßHSD2) Enzyms unter der Kontrolle des Kollagen Typ I Promoters (Col2.3-11ßHSD2) blockiert wurde. Kortikale Knochendefekte (Ø 0,8 mm) wurden in Tibiae von sieben Wochen alten männlichen transgenen und Wildtyp-Mäusen generiert. Die Auswertung der Frakturheilung erfolgte nach ein, zwei und drei Wochen der Defektinitiierung durch Histomorphometrie, Immunhistochemie und Mikro-Computertomographie (Mikro-CT) Analyse.

Ergebnisse:
Nach Woche 1 der Frakturheilung zeigten Mikro-CT Bilder des Defektes die Bildung von mineralisiertem, intramembranösem Knochen, welcher an Volumen und Densität bis Woche 2 zunahm. Die Woche 3 des Heilungsprozesses war durch die fast abgeschlossene Defektheilung gekennzeichnet. Die histomorphometrische und mikrocomputer-tomographische Analyse ergab keinen Unterschied in der Frakturheilung zwischen Col2.3-11ßHSD2 transgenen und Wildtyp-Mäusen zu allen Zeitpunkten.

Schlussfolgerung:
Die Blockade des intrazellulären Signalwegs endogener Glucocorticoide in ausgereiften Osteoblasten beeinflusst nicht die intramembranöse Frakturheilung in einem Tibia-Defekt-Reparaturmodell. Es bleibt zu zeigen, ob der Glucocorticoid-Signalweg eine Rolle im endochondralen Frakturheilungsprozess spielt.

Schlagworte: Osteoblasten, Steroidhormone: Glucocorticoide, Frakturheilung

Table of Contents

1 INTRODUCTION 9

2 LITERATURE REVIEW 10

2.1 Bone Biology 10

2.1.1 Bone 10

2.1.2 Bone Composition 12

2.1.3 Bone Cells 12

2.1.4 Bone Remodelling 13

2.1.5 Coupling of Bone Formation and Resorption 16

2.1.6 Osteoblast Differentiation 17

2.2 Fracture Healing 21

2.2.1 Primary Fracture Healing 21

2.2.2 Secondary Fracture Healing 22

2.3 Glucocorticoids and Bone 24

2.3.1 Glucocorticoids 24

2.3.2 Glucocorticoid-induced Osteoporosis 24

2.3.3 Catabolic Effects of Glucocorticoids 25

2.3.4 Anabolic Effects of Glucocorticoids 27

2.3.5 Glucocorticoid Signalling in Osteoblasts 29

2.4 The Col2.3-11ßHSD2 Transgenic Mouse Model 29

2.5 Fracture Healing and Glucocorticoids 32

2.6 Hypothesis 34

3 ANIMALS AND METHODS 35

3.1 Experimental Animals and Study Design 35

3.2 Genotype Analysis 35

3.3 Tibia Cortical Defect Repair Model 36

3.4 Sample Preparation 37

3.5 Staining Procedures 38

3.5.1 Hematoxylin and Eosin (H&E) 38

3.5.2 Tartrate Resistant Acid Phosphatase (TRAP) 38

3.5.3 Toluidine Blue 39

3.6 Analyses of Defect Repair 39
3.6.1 Microcomputed Tomography (micro-CT) Analysis 39
3.6.2 Histomorphometric Analysis 42
3.6.3 Second-harmonic Imaging Microscopy (SHIM) 44
3.7 Immunohistochemistry 46
3.8 Statistical Analysis 47
4 RESULTS 48
4.1 Tibia Defect Repair Model 48
4.2 Body Weight 48
4.3 The Sequence of Defect Repair 49
4.4 Analyses of Defect Repair 52
4.4.1 Microcomputed Tomography 52
4.4.2 Histomorphometry 54
4.4.3 Second-harmonic Imaging Microscopy 56
4.4.4 Summary of Analyses of Defect Repair 58
4.5 Immunohistochemistry 59
5 DISCUSSION 60
5.1 Discussion of Methods 60
5.2 Discussion of Results 62
6 SUMMARY 67
7 ZUSAMMENFASSUNG 69
8 REFERENCES 71
9 APPENDIX 85
9.1 Publications and Presentations 85
9.2 Curriculum Vitae 86
9.3 Acknowledgements 87
9.4 Statement/ Erklärung an Eides Statt 88

List of Abbreviations

11ßHSD1	11ß-hydroxysteroid-dehydrogenase type 1
11ßHSD2	11ß-hydroxysteroid-dehydrogenase type 2
ABC technique	avidin-biotin complex technique
ACTH	adrenocorticotropic hormone
AES	3-aminopropyltriethoxysilane
ALP	alkaline phosphatase
AME	apparent mineralcorticoid excess
BDS	brainstem-derived serotonin
bGH PA	bovine GH polyadenylation sequence
BMP-2	bone morphogenetic protein-2
BMU	basic multicellular units
BrdU	5-bromo-2'deoxyuridine
BSA	bovine serum albumin
CART	cocaine-and amphetamine-regulated transcript
cDNA	complementary DNA
cGRα	cytosolic glucocorticoid receptor α
CRH	corticotropin releasing hormone
DAB	3,3'-diaminobenzidine
dNTPs	desoxyribonucleoside triphosphates
EDTA	ethylene diamine tetraacetic acid
FGF	fibroblast growth factor
GC	glucocorticoids
GDS	gut-derived serotonin
GIO	glucocorticoid-induced osteoporosis
GREs	glucocorticoid response elements
HPA axis	hypothalamo-pituitary-adrenal axis
HSP	heat shock protein
Htr2c	5-hydroxytryptamine receptor 2c
IL-1	interleukin-1
LEF/TCF	lymphoid enhancer-binding factor 1/T cell-specific transcription factor

LRP5/6	low-density lipoprotein receptor-related proteins 5/6
M	Molar
M-CSF	macrophage-colony stimulating factor
mGR	membrane-bound glucocorticoid receptor
micro-CT	microcomputed tomography
mmp-13	matrix metalloproteinase-13
MR	mineralcorticoid receptor
MSCs	mesenchymal stem cells
NMU	neuromedin U
NPY	neuropeptide Y
OPG	osteoprotegerin
OPPG	osteoporosis pseudoglioma syndrome
Osx	osterix
PDGF	platelet derived growth factor
PFA	paraformaldehyde
PINP	N-terminal propeptide of type I collagen
PPARγ	peroxisome proliferator-activator receptor gamma
PTH	parathyroid hormone
RANK	receptor activator of nuclear factor kappa B
RANKL	receptor activator of nuclear factor kappa B ligand
ROI	region of interest
Runx2	runt-related transcription factor 2
SEM	standard error of the mean
SHG	second harmonic generation
SHIM	second-harmonic imaging microscopy
TAZ	transcriptional co-activator with PDZ-binding motif
Tg	transgenic
TGF-ß	transforming growth factor ß
TNF	tumor necrosis factor
TPEF	two-photon excited fluorescence
Tph1	tryptophan hydroxylase 1
Tph2	tryptophan hydroxylase 2
TRAP	tartrate resistant acid phosphatase
WT	wild-type

1 Introduction

Glucocorticoids (GC) are widely used in almost all fields of medicine. They provide therapeutic benefit to patients suffering from systemic inflammatory diseases, malignancies or transplant rejection. It is, however, well established that GC at pharmacological doses exert detrimental effects on bone, muscle, cartilage and skin, substantially affecting patient quality of life and posing a socio-economic problem. Despite their therapeutic utility, the mechanisms by which GC mediate beneficial as well as detrimental effects on cells and tissues are poorly understood. In particular, it is unclear how and through which cells GC affect bone.

Glucocorticoid-induced osteoporosis (GIO) is the most common form of secondary osteoporosis and up to 50% of patients receiving chronic GC therapy will suffer from fragility fractures.[1] Moreover, fracture healing may be significantly impaired in patients on high-dose exogenous GC.[2] In contrast, extensive *in vitro*[3-6] and *in vivo* studies[7] suggest that GC administered at physiological (i.e. endogenous-like) levels have anabolic effects on bone cells by promoting osteoblast differentiation and matrix mineralization. However, the role of endogenous GC in fracture repair has not been fully investigated.

In clinical practice, delayed fracture healing or non-union is a common complication occurring in up to 10% of all patients and their treatment poses a major challenge.[8] Thus, extensive research has been done in recent years leading to the identification of osteoinductive factors accelerating bone repair, including the growth factors bone morphogenetic protein-2 (BMP-2), insulin-like growth factor-I (IGF-I) and transforming growth factor-beta1 (TGF-ß1). However, at present there is still a need for effective therapies in managing skeletal injuries in patients as the majority of these factors remain to be validated in clinical trials.[9]

Thus, the understanding of the cellular and molecular events during the normal repair process and the identification of endogenous factors which physiologically interact with it provides a basis for the development of new therapy strategies to augment healing of complicated fractures. Against this background the present work addresses the main objective to further investigate the role of physiological, endogenous GC signalling in osteoblast differentiation and function during fracture repair by examining the bone healing of cortical defects in a unique transgenic mouse model of osteoblast-targeted disruption of the normal GC signalling pathway.

2 Literature Review

The following chapter gives a brief overview of basic bone biology, followed by a description of glucocorticoids and of the current knowledge about their interaction with bone cells, particularly osteoblasts. Building on that, the recently developed Col2.3-11ßHSD2 transgenic (tg) mouse model will be described. Overall, the use of this animal model allowed for further investigations into the role of GC in osteoblast differentiation and function under challenged conditions such as fracture repair.

2.1 Bone Biology

2.1.1 Bone

Bone is a dynamic,[10, 11] specialized form of connective tissue that has a number of functions essential to the human body. These include mechanical support of soft tissues, a lever for locomotion and protection of vital organs, such as the brain, the heart and the lungs. Moreover, bone is the primary site of adult hematopoiesis and contributes notably to the maintenance of serum-mineral homeostasis. The latter function is particularly due to the large reservoir for calcium, stored in the form of hydroxyapatite in the bone matrix.[12-15]

Based on the embryological developmental process, bones can be classified into flat and long bones.[16] Flat bones develop through intramembranous bone formation, a process in which osteoblasts are formed directly from mesenchymal cells through different stages of osteoblast precursors. This type of bone comprises the scapula, mandibles and the skull bones, with the calvaria representing a convenient site for experimental research. Long bones, in contrast, are formed through endochondral ossification which includes a cartilage template which is then gradually replaced by bone.[16-18] This type of bone includes the humerus, femur and tibia, the latter being the site used to create defects in this experimental study.[16]

Macroscopically, a longitudinal section through a tibia shows the thick, dense, calcified outer shell, known as the cortex, compact or cortical bone (Figure 1). In the diaphysis or shaft it encloses the hematopoietic bone marrow housed in the medullary cavity. Towards the joint surfaces, in the metaphysis and epiphysis, the compact bone becomes thinner and comprises the trabecular or cancellous bone. This three-dimensional spongy network comprising both plates and rods also houses the bone marrow.[16] Interestingly, the orientation of trabeculae follows the direction of stress trajectories, as first described by Julius Wolff in 1892.[13, 19] According to the

law bearing his name, bone tissue adapts to altering mechanical loading patterns by altering its structure and thus represents the principle of "form follows function" in biological systems.[20] Trabecular bone is generally regarded as the site for systemic metabolism, whereas the cortex provides the structural rigidity.[15] Two important surfaces are distinguished: the periosteum on the external surface and the endosteum on the inner surface.[21] Both are lined with osteogenic cells.[16] Altogether, due to its remarkable architectural design, bone achieves structural stiffness, strength, flexibility and lightness at the same time.[10, 21]

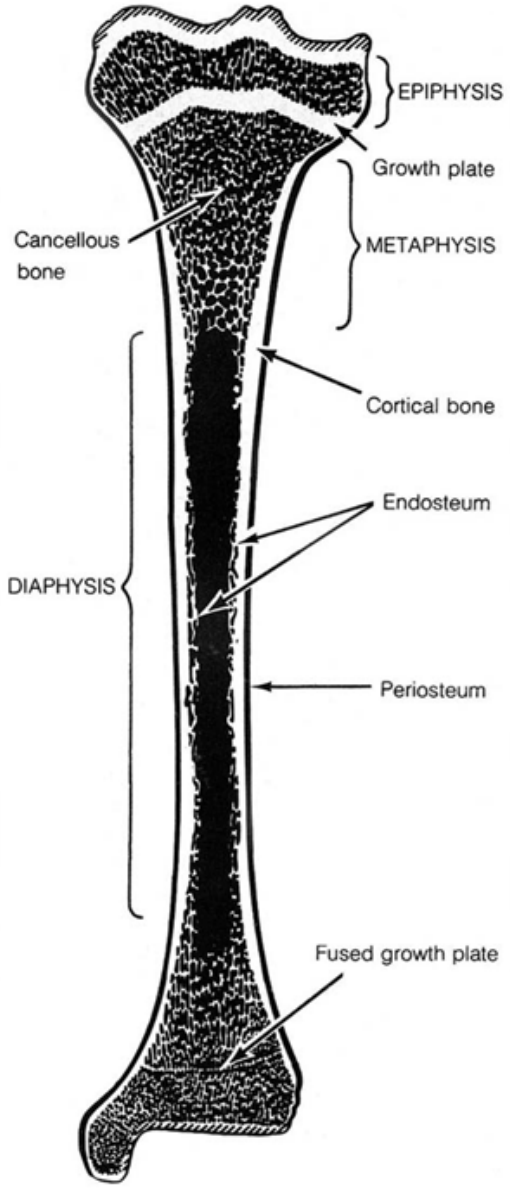

Figure 1: Schematic diagram of a longitudinal section of the tibia (from Webster SSJ. The skeletal tissues. In: Weiss L, ed. Histology, cell and tissue biology. New York: Elsevier Biomedical, 1983[22]).

2.1.2 Bone Composition

The characteristics of healthy bone are based on its material composition and structural design.[23] The stiffness and strength is achieved by the inorganic mineralized matrix, primarily consisting of calcium hydroxyapatite (Ca_{10} $(PO_4)_6$ $(OH)_2$) crystals.[14, 21] In contrast, flexibility is determined by the organic makeup. Here, triple helices of polypeptide chains form type I collagen fibrils as the predominant structure of this component.[15, 24] Two conformations of bone tissue are differentiated according to the orientation of collagen fibrils: lamellar and woven bone. Lamellar bone is characterized by an orderly arrangement of collagen fibrils forming concentric layers of bone matrix around central canals (Haversian systems) in cortical bone. By contrast, woven bone, with scattered, irregular collagen fibrils is formed during development and fracture healing.[15, 16] Further matrix constituents include the proteins osteocalcin, osteonectin, bone sialoprotein and proteoglycans.[14, 25]

2.1.3 Bone Cells

The bone matrix composition is modified by distinct cell types: osteoclasts, osteoblasts, osteocytes and bone lining cells. With the exception of osteoclasts, all these cell types are derived from the mesenchymal cell lineage.[15]

Osteoclasts are giant multinucleated cells of hematopoietic origin, formed by the fusion of circulating mononuclear progenitors of the monocyte/macrophage family.[10, 13, 14, 24, 26, 27] When carrying out their main function, the resorption of bone, osteoclasts attach to the bone surface.[27, 28] In that active state, the plasma membrane facing the bone surface infolds to form the “ruffled border”. Adjacent to this border is a sealing zone rich in filamentous actin, creating an isolated extracellular microenvironment of a low pH between the osteoclast and the bone surface. This acidic milieu leads first to the dissolution of the inorganic hydroxyapatite matrix and subsequently allows the lysosomal protease cathepsin K to degrade the organic components. All degradation products are then removed through a transcytotic vesicular pathway of the osteoclast.[14, 24, 28-30] Manifestations of resorptive activity include depressions and pits, known as “Howship’s lacunae”.[16]

The bone forming cells of the skeleton are the osteoblasts. These are specialized mesenchymal cells of cuboidal shape, often found in longitudinal clusters along the bone surface.[15, 31] The osteoblasts’ main function is the production and deposition of osteoid, the organic non-mineralized extracellular bone matrix, primarily consisting of type I collagen.

Moreover, non-collagenous proteins including osteocalcin, an important serum marker for bone turnover, are secreted by these cells.[18] Ultimately, the bone-forming cells become osteocytes, undergo apoptosis or become bone lining cells.[32]

Bone lining cells or "resting osteoblasts" are elongated, metabolic inactive cells covering bone surfaces.[15] Their exact function is still being investigated. Several authors propose a role as osteoblastic precursors, regulators of bone growth or building a barrier between extracellular fluid and bone.[15, 33]

Osteocytes are the most abundant bone cells, making up to more than 90% of all bone cells.[15] They are entrapped in spaces known as "lacunae" which are surrounded by bone matrix. The connection to adjacent osteocytes or bone lining cells is ensured by a canaliculi network, permeating the bone matrix. Microscopically, cytoplasmic processes are linked to each other mostly via gap junctions.[16, 34] This connection is thought to play an important role in cellular communication and nutrition by transporting cell signalling molecules, nutrients and waste products.[15]

2.1.4 Bone Remodelling

Bone resorption and bone formation are not independent functions of the skeletal cells; they are linked in the localized, dynamic physiological process of bone remodelling. It not only allows the maintenance of bone strength and mass during adult life but also the adaptation of its material composition and structure to loading requirements.[13, 31] However, it is also the process through which GC and other pharmacological and physiological factors might affect the bone's structural integrity.

In 1966, Frost described the underlying discrete temporary anatomic structures in the microscopic range, the "basic metabolizing units"[35], later termed "basic multicellular units (BMUs).[36] A BMU is formed by a group of osteoclasts, osteoblasts, blood vessels and connective tissue.[37, 38] The impulse of conversion of quiescent bone surface to a site of active remodelling has not yet been entirely understood. Presumably, microcracks on the bone surface or damaged osteocytic processes are sensed by osteocytes, mediated through the canalicular system.[39, 40] Subsequently, osteoclasts become activated and are recruited to the remodelling site assumedly via local factors from bone lining cells and osteocytes that may undergo apoptosis (Figure 2). Osteoclasts then begin with the removal of old bone, a process lasting about two to three weeks.[40] The resulting resorption lacunae in turn attract osteoblasts which refill the cavity through deposition of new bone matrix. As the average lifespan of an osteoclast is twelve days,

these cells need to be replaced continually.[37] The remodelling sequence is finally completed with the bone matrix being mineralized after three to five months. [41]

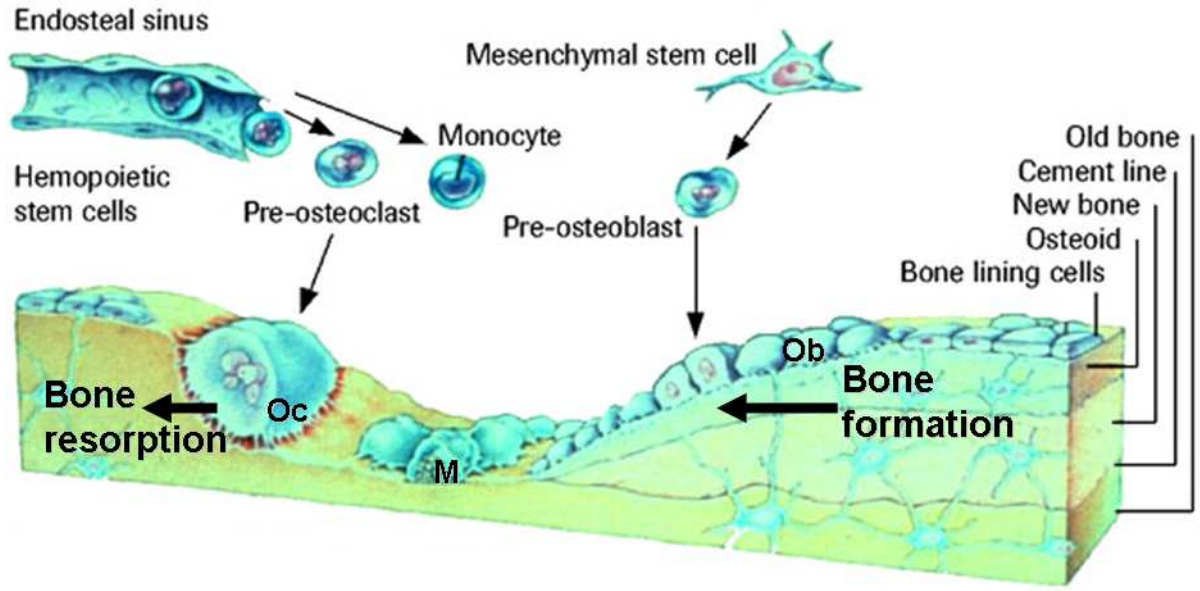

Figure 2: Bone remodelling. Oc-osteoclast, Ob-osteoblasts, M-macrophages (picture adapted from www.roche.com).

Bone remodelling occurs continuously and simultaneously at multiple locations, on endocortical, intracortical and trabecular surfaces in the adult skeleton with a BMU advancing about 25 µm/day.[37, 40] Thus, up to 10% of bone is remodelled each year, leading to a renewal of the entire skeleton every ten years.[14] However, this entails the balance of bone formation and bone resorption, quantitatively, temporally and spatially. In a simplified model, a negative balance with bone resorption relatively exceeding bone formation leads to osteoporosis, characterized by a loss of total bone mass and bone density.[42] By contrast to osteoporosis, in osteomalacia bones are softened due to a defective osteoid mineralisation as most commonly caused by a severe vitamin D deficiency.[43, 44] A positive balance favouring bone formation results in osteopetrosis, a disease possibly affecting bone marrow function due to an increased bone mass.[14] This illustrates the paramount importance of the orchestration of osteoblast and osteoclast activity, their appropriate number and coordination. Such factors determine the activation frequency and the duration of each bone remodelling unit, including the number of remodelling cycles.

At this point, GC, local (autocrine and paracrine factors; *e.g.* cytokines, growth factors) and systemic (*e.g.* endocrine hormones) factors might affect the homeostatic bone metabolism by

modulating the normal bone remodelling process via changing osteoblastic and osteoclastic cell replication, differentiation, apoptosis, function or life-span.

For example, estrogen has been shown to protect against bone loss. While inducing apoptosis of mature osteoclasts, shortening their life-span, osteoblasts' and osteocytes' lifespan is prolonged via estrogen-mediated anti-apoptotic effects.[45] Moreover, the activation frequency of BMUs is enhanced, expanding the remodelling space.[46] Hence, estrogen deficiency as commonly found in postmenopausal women might considerably account for the development of osteoporosis, as first hypothesized by Albright et al. in 1941 by causing opposing effects on bone cells.[47, 48] At present, this has been generally acknowledged as the cause for the accelerated early phase of bone loss in postmenopausal women. However, the role of estrogen and other factors in the late phase of slow bone loss is less clear.[47] Interestingly, estrogen deficiency might also contribute to bone loss in men as the bioavailable levels of estrogen also decline with aging.[46]

However, despite the great variety of factors regulating bone metabolism there seems to be a hierarchic order in which they might produce an effect. The main skeletal modulators are known to be sex steroids, mechanical usage and calcium mobilization, the latter encompassing the most pronounced effects.[12]

Ducy et al. proposed a new concept of central neuronal control of bone mass. Leptin, an adipocyte-derived peptide hormone known to affect energy metabolism via hypothalamic receptor binding was reported to induce an inhibitory effect on bone formation *in vivo*. Moreover, hypogonadic leptin-deficient and leptin-receptor deficient mice did not develop osteoporosis as commonly caused by a loss of gonadal function, but showed increased bone formation leading to high bone mass.[49] Recent studies by Karsenty and colleagues demonstrated an underlying mechanism of leptin's inhibitory regulation of bone mass. Leptin was found to decrease the synthesis and the release of serotonin by neurons of the brainstem. This brainstem-derived serotonin (BDS) physiologically acts as a neurotransmitter and favours bone mass accrual through its binding to 5-hydroxytryptamine receptor 2c receptors (Htr2c) expressed in ventromedial hypothalamic neurons. Accordingly, disruption of BDS synthesis through inactivation of its rate-limiting biosynthetic enzyme tryptophan hydroxylase 2 (Tph2) in mice resulted in a low bone mass phenotype with decreased bone formation parameters and increased bone resorption parameters.[50] By contrast, gut-derived serotonin (GDS) produced in enterochromaffin cells of the duodenum acts a as a hormone and was shown to exert opposite influences on bone remodelling. In particular, it decreased osteoblast proliferation and bone formation while not affecting bone resorption.[51] Thus, it was concluded that pharmacological inhibition of GDS biosynthesis might be an anabolic means to treat osteoporosis. Recently,

Yadav et al. synthesized LP533401, a small-molecule inhibitor of the rate-limiting tryptophan hydroxylase 1 (Tph1) enzyme in the GDS biosynthetic pathway. Supporting the concept, this inhibitor not only prevented the development of ovariectomy-induced osteoporosis in rodents but also rescued existing ovariectomy-induced osteopenia.[52]

Further *in vivo* studies support the hypothesis of a cross-talk between bones and brain by also revealing a bone-regulating central function for neuropeptides including neuromedin U (NMU), neuropeptide Y (NPY) and cocaine- and amphetamine-regulated transcript (CART).[53-55]

2.1.5 Coupling of Bone Formation and Resorption

Despite the complexity of factors regulating bone mass such as cytokines, growth factors and endocrine hormones, the cell type most commonly affected by these factors seems to be the osteoblast. These specialized skeletal cells are not only responsible for bone matrix formation but also play a pivotal role in the regulation of osteoclastogenesis, mainly through their direct interaction with osteoclasts. This results in a sequential coordination of bone resorption and bone formation, known as coupling (Figure 3).[56]

Osteoclastogenesis of monocyte/macrophage precursor cells and their maturation into polykaryotic osteoclasts is primarily governed by the macrophage-colony stimulating factor (M-CSF or CSF-1) and the receptor activator of nuclear factor kappa B ligand (RANKL or osteoprotegerin ligand (OPGL).[57-59] Both are membrane-bound cytokines, produced and expressed by osteoblasts and stromal cells.[60]

The cytokine M-CSF is a crucial modulator of early osteoclastogenesis.[58] Binding to its receptor, c-fms, on early stem cell precursor enhances their survival and promotes their differentiation into osteoclast precursor cells.[61] Hence, mice defective in production of functional M-CSF develop osteopetrosis due to a severe deficiency in mature osteoclasts.[62] Importantly, osteoclast precursor cells express the membrane bound receptor activator of nuclear factor kappa B (RANK) for RANKL, thus mediating the direct osteoblast-osteoclast communication via RANKL binding.[63] Consequently, osteoclasts terminally differentiate, fuse and polarize to become mature osteoclasts which actively resorb bone.[42] Growth factors including insulin-like growth factor-I (IGF-I) and transforming growth factor-ß (TGF-ß) are released from the degraded bone matrix which in turn are postulated to promote osteoblastogenesis.[12]

Regulation of the RANK-RANKL interaction is modulated within bone by osteoprotegerin (OPG), a soluble decoy receptor, as first demonstrated by Simonet et al. in 1997.[64, 65] Once produced by osteoblastic cells, OPG binds to RANKL and thus prevents the

binding of RANKL to RANK.[37] As a result, OPG protects the degradation of bone matrix by blunting RANKL-induced osteoclastogenesis.[64] Therefore, the RANKL/OPG ratio primarily determines the extent of bone resorption and bone remodelling. Hormones such as parathyroid hormone (PTH) and 1,25-dihydroxy-vitamin D3 have been shown to modify this ratio via alteration of RANKL and OPG synthesis. More recently, other inflammatory cytokines including interleukin-1, -6 and -11 and tumor necrosis factor (TNF) have been shown to stimulate RANKL synthesis directly or indirectly[37], thus participating in the close interaction between bone and the immune system, known as the discipline of osteoimmunology.[14]

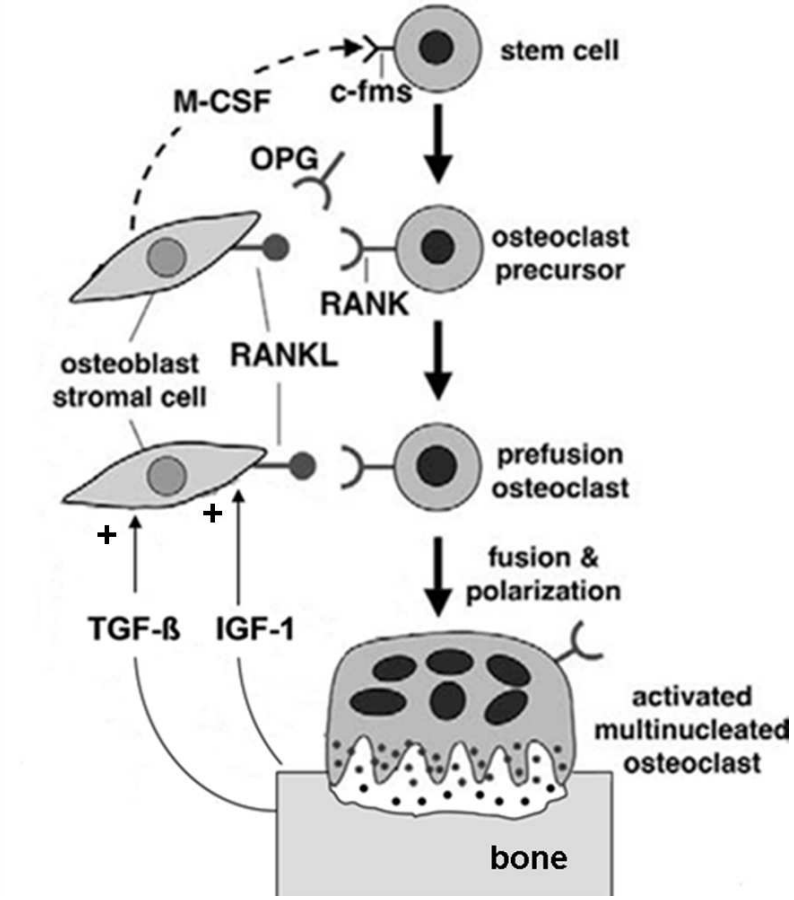

Figure 3: Osteoclast differentiation and coupling of osteoblasts and osteoclasts. RANK-receptor activator of nuclear factor kappa B, RANKL-receptor activator of nuclear factor kappa B ligand, OPG-osteoprotegerin, M-CSF-macrophage-colony stimulating factor, TGF-ß-transforming growth factor-ß, IGF-I-insulin-like growth factor I (picture adapted from Troen BR, Exp Gerontol, 2003[42]).

2.1.6 Osteoblast Differentiation

In contrast to the predominantly cytokine-regulated differentiation of osteoclasts, osteoblast differentiation is governed by a completely different set of regulatory mechanisms. This regulation is of particular importance to provide a reservoir of osteoblasts essential for bone

growth, remodelling and fracture healing. Osteoblasts are derived from mesenchymal stem cells (MSCs) primarily found in the bone marrow which also give rise to myocytes, adipocytes, chondrocytes and fibroblasts under the control of lineage-specific transcription factors (Figure 4).[12]

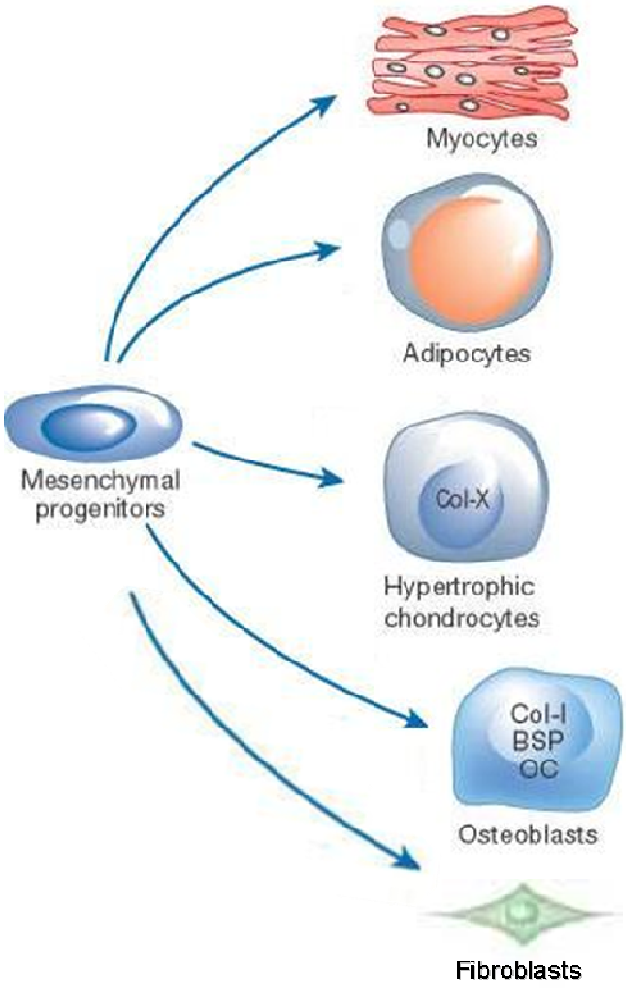

Figure 4: Mesenchymal stem cell differentiation (picture adapted from Harada S and Rodan GA, Nature, 2003[12]).

Recently, various *in vitro* studies reported on the plasticity of MSCs to differentiate into non-mesodermal cells including hepatocytes and neuronal cells.[66, 67] However, due to the lack of evidence of its physiological relevance *in vivo*, the concept of plasticity and trans-differentiation is currently being debated in stem cell biology. Generally more accepted is the inter-conversion of cells within the mesodermal lineage. For example, mature differentiated osteoblasts have been shown to undergo adipogenic differentiation under certain culture conditions.[68] On the other hand, *in vitro* culture studies also demonstrated the differentiation of mature adipocytes into bone-forming cells.[69] Osteoblasts and adipocytes are derived from a common mesenchymal cell

progenitor as supported by a reciprocal relationship between adipocytic and osteogenic cell differentiation in a rat bone marrow stromal cell culture system.[70, 71] A decrease in bone volume and increase in adipose tissue is also seen clinically in osteoporotic patients, during aging and after treatment with GC.[72-76] In 2005, Hong et al. proposed an underlying molecular mechanism hypothesizing that transcriptional co-activator with PDZ-binding motif (TAZ), represses the key gene transcription factor peroxisome proliferator-activator receptor γ (PPARγ) driving adipogenesis while coactivating runt-related transcription factor 2 (Runx2), the major transcription factor promoting osteoblastogenesis.[77]

Runx2 (also called core binding factorα-1 [Cbfa1]), a member of the runt-domain gene family, controls the initial step in osteoblastogenesis in conjunction with its subunit Cbfß: the commitment of mesenchymal progenitor cells and their subsequent differentiation into pre-osteoblasts (Figure 5).[78] This differentiation stage is marked by the expression of low levels of type I collagen (Col1a1). In the next step osterix (Osx), a zinc-finger-containing transcription factor leads to the differentiation into mature functional osteoblasts which then express higher concentrations of type I collagen.[18, 79] While extracellular matrix is produced, further late stage differentiation marker genes are expressed including osteocalcin, osteonectin, osteopontin and bone sialoprotein.[18]

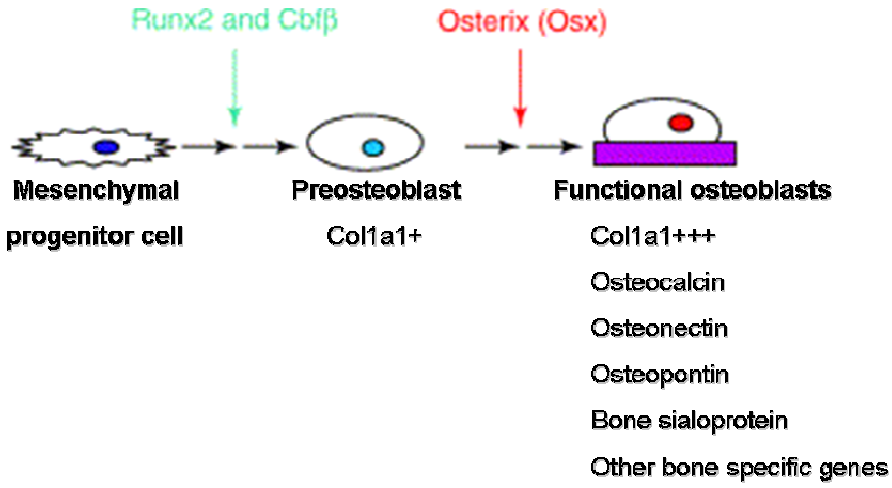

Figure 5: Osteoblast differentiation: transcription factors and differentiation stage-specific expression of osteoblast-marker genes; + low concentration, +++ high concentration, Col1a1-type I collagen (picture adapted from Nakashima K and de Crombrugghe B, Trends Genet, 2003[18]).

The importance of these two transcription factors as the “master genes” for osteoblast differentiation is demonstrated by the observations that Runx2- and Osx-null/deficient mice reveal a complete absence of osteoblasts and bone tissue. In addition, Osx-deficient mice

expressed Runx2 but Runx2-deficient mice in turn did not express Osx, further indicating that Osx acts downstream of Runx2.[18, 80-82]

In addition to transcriptional control, osteoblastogenesis is also governed by signalling pathways and their signalling molecules including bone morphogenetic proteins (BMPs), Hedgehogs and fibroblast growth factors (FGFs).[83] Of note are the Wnt signalling pathways which are not only known as key regulators during embryogenesis and organogenesis but have also been shown to play a crucial role in bone formation and tissue homeostasis.[84, 85] The Wnt signalling molecules are highly conserved secreted glycoproteins belonging to the family of growth factors, which were named after their isolation as the segment polarity gene wingless in drosophila melanogaster and their identification as the homolog of the mouse mammary oncogene int-1.[86, 87] When signalling through the canonical or Wnt/ß-catenin pathway, which has been demonstrated for Wnt1, Wnt3a and Wnt10b amongst others, Wnt proteins bind to frizzled receptors and their co-receptors, the low-density lipoprotein receptor-related proteins 5/6 (LRP5/6).[83, 88] Hence, a signalling cascade is activated which eventually leads to the stabilization of the key mediator ß-catenin in the cytosol and its translocation into the nucleus. There, ß-catenin interacts with lymphoid enhancer-binding factor 1/T cell-specific transcription factor (LEF/TCF) to trigger the transcription of target genes.[83-85]

Perturbations of this signalling cascade have been associated with tumorigenesis and human degenerative diseases.[83] For example, patients with a loss-of-function mutation in the LRP5 gene developed the osteoporosis pseudoglioma syndrome (OPPG) which is accompanied by eye abnormalities.[89] Several studies report controversial effects of Wnt signalling in the control of bone formation, which overall seem to depend on the stage of osteoblast differentiation. In early differentiation stages, activated Wnt signalling was found to stimulate osteoblast differentiation in many cases[90-94] whilst others demonstrated an inhibition of their differentiation at later stages.[95, 96] However, the canonical Wnt signalling pathway is regarded as the major mediator of osteoblastogenesis, osteoclastogenesis and their tight coupling, thus providing an attractive research field of pharmacological targets for anabolic drug intervention in the treatment of osteoporosis.[97]

Interestingly, our cooperation partner from the ANZAC Research Institute of the University of Sydney, recently identified Wnt signalling as a new mechanism in bone biology by which mature osteoblasts directly communicate with mesenchymal progenitor cells to control their lineage commitment.[6] This mechanism is proposed to be GC-dependent, further pointing at the important role of GC in osteoblast differentiation and function.

2.2 Fracture Healing

Fracture healing is a complex, specialized form of wound repair that involves the coordinated participation of several cell types and tissues to restore the bones pre-injury mechanical stability without the formation of scar tissue.[98, 99] Complex interactions of growth and differentiation factors, hormones, cytokines and matrix proteins are known to regulate this multistage process.[98] Histologically, there are two types of fracture healing: primary and secondary fracture healing.[8]

2.2.1 Primary Fracture Healing

Primary fracture healing, also known as direct bone healing, occurs in a rigid stable environment which does not allow any motion between the fracture ends.[99] Such conditions are achieved by the combination of anatomical reduction with internal fixation by interfragmentary compression, *e.g.* as in the classical plate osteosynthesis.[100, 101]

Primary bone healing is initiated by the formation of osteoclastic "cutting cones", discrete remodelling units tunnelling across the fracture line, parallel to the longitudinal axis of the cortical bone (Figure 8).[98, 100] Just as normal bone remodelling, bone resorption is followed by the replacement of new bone matrix synthesized by osteoblasts forming the "closing cone". As a result, the continuity of the Haversian systems of the fracture fragments is re-established. Throughout the process, bone is formed without a cartilage intermediate, known as desmal or intramembranous ossification.[100, 102]

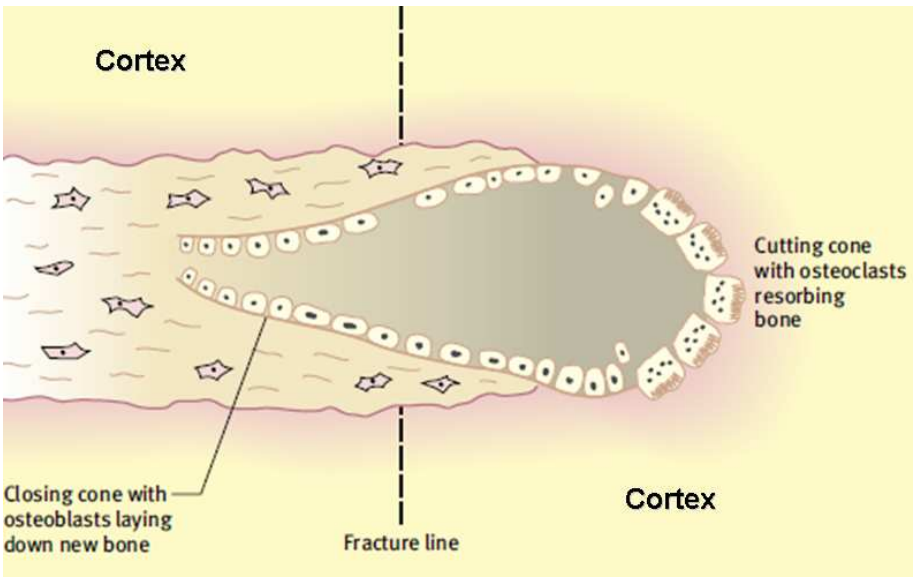

Figure 8: Primary fracture healing (picture adapted from Wraighte PJ and Scammell BE, Surgery, 2006[100]).

2.2.2 Secondary Fracture Healing

By contrast, secondary or indirect bone healing, the most common type of bone repair, occurs at a fracture site of mobility and interfragmentary space, as found in fractures treated in a plaster cast or by external fixation.[99-102] This type of bone healing involves both, intramembranous and endochondral bone repair. Analogous to embryological development, the latter process encompasses the formation of a cartilaginous matrix which is then gradually replaced by bone.[99,101]

Secondary fracture healing follows an ordered sequence of five overlapping phases, as originally described by McKibbin et al.: hematoma formation, inflammation, soft callus, hard callus and remodelling (Figure 9).[103]

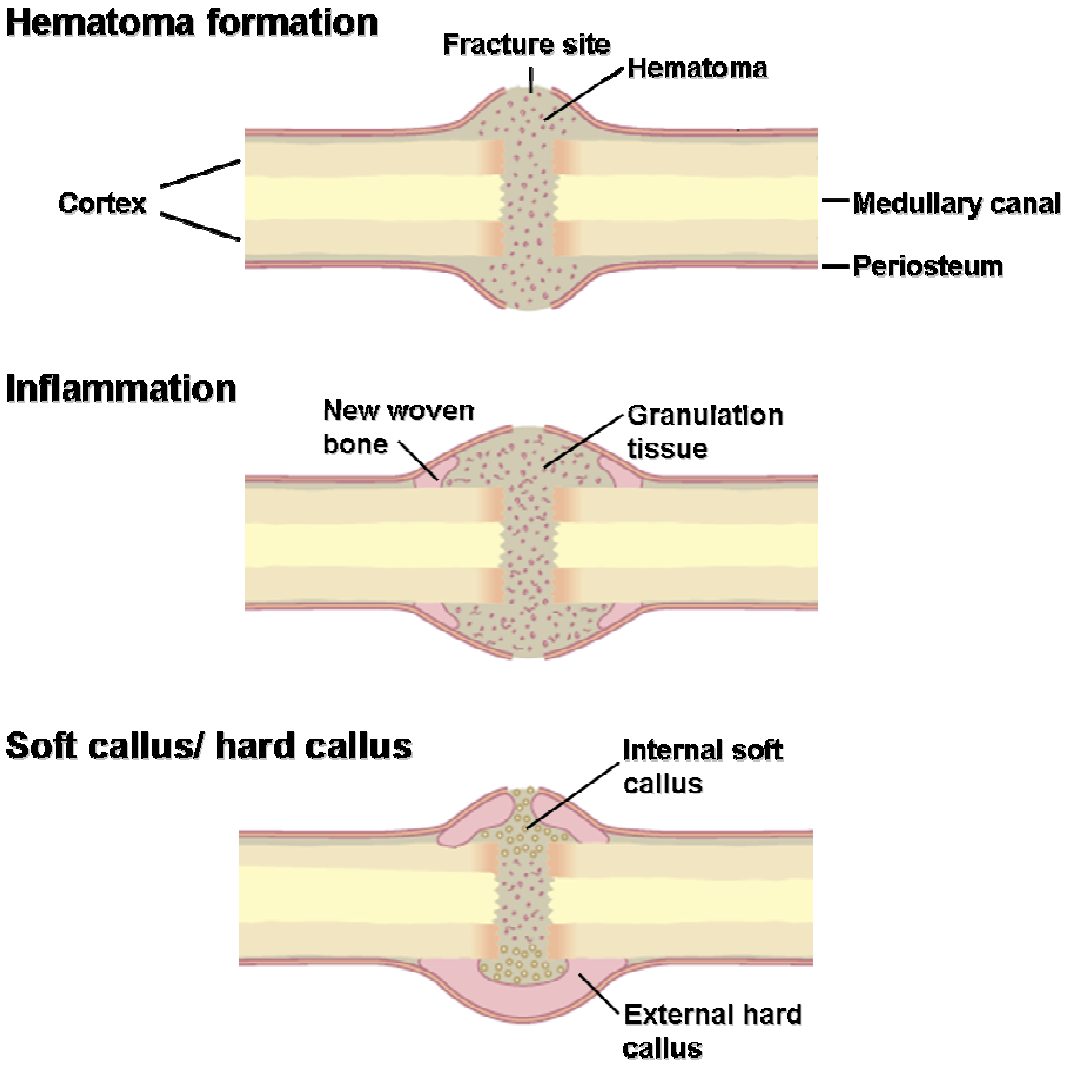

Figure 9: Secondary fracture healing (picture adapted from Wraighte PJ and Scammell BE, Surgery, 2006[100]).

Hematoma Formation:

Following injury, bleeding from soft tissues, periosteum and medullary cavity results in the formation of a hematoma.[100, 103] It contains hematopoietic cells and activated platelets which trigger the initiation of the inflammatory cascade by releasing growth factors.[101] Of those, PDGF and TGF-ß are the most important factors, both known for their role in angiogenesis, chemotaxis and mesenchymal cell regulation.[101, 104]

Inflammation:

The following inflammatory response involves the invasion of the inflammatory cells macrophages, lymphocytes, mast cells and monocytes.[99, 101] However, the most important cells of this phase are neutrophil granulocytes which release pro-inflammatory cytokines activating the migration, proliferation and differentiation of osteoprogenitor cells. The disruption of the blood supply and its consequential lowering of oxygen tension and pH further stimulates the cytokine release.[101]

Over time, the hematoma matures into granulation tissue consisting of fibroblasts, capillaries and type I collagen.[100] Osteoblasts begin with the deposition of woven bone beneath the periosteum through intramembranous bone formation.[99, 101]

Soft Callus/ Hard Callus:

In the next phase, woven bone formation progresses, forming a bridge between the fracture ends, the external hard callus. Another, internal soft callus is formed by the differentiation of pluripotent mesenchymal cells originating from the granulation tissue into chondrocytes. With their release of phosphatases and proteases, the cartilaginous matrix is prepared for the subsequent calcification. As chondroclasts then degrade the calcified matrix, blood vessels from the periosteum invade the callus tissue fracture site providing mesenchymal stem cells for the differentiation into osteoprogenitor cells and osteoblasts which begin to form woven bone through endochondral ossification.[99-101]

Remodelling:

Finally, the woven bone is remodelled into lamellar bone, mediated by the coordinated action of osteoblasts and osteoclasts.[100, 103]

2.3 Glucocorticoids and Bone

2.3.1 Glucocorticoids

Glucocorticoids are lipophilic steroid hormones, synthesized and released by the zona fasciculata and reticularis of the adrenal cortex.[105] They are known to regulate diverse physiological processes including sodium and water homeostasis, carbohydrate and lipid metabolism, immune function and stress responses.[106-108]

The circulating concentration of endogenous GC is controlled and maintained by the hypothalamo-pituitary-adrenal (HPA) axis: decreasing cortisol levels in the blood, stress or other triggers stimulate corticotropin releasing hormone (CRH) secretion in the hypothalamus activating adrenocorticotropic hormone (ACTH) production in the anterior pituitary which in turn activates adrenal cortisol production. An overproduction of cortisol is prevented through a negative feed-back regulation ensuring the inhibition of CRH and ACTH activation when cortisol levels are high.[109-111]

Clinically, therapy with exogenous GC was first introduced in 1948 by Philip Hench.[112] Since then, these synthetic compounds have been used in the management of a variety of conditions including asthma, rheumatoid arthritis, autoimmune disorders, neoplastic diseases and organ transplantation.[1, 113] Currently, up to 0.5% of the population worldwide take GC on a long-term basis highlighting their important role as effective immunosuppressive and anti-inflammatory agents.[114] However, GC-associated side effects are frequent and are reported to be dose- and duration-dependent. Moreover, the treatment of these effects produces high costs.[115] The variety of adverse effects includes weight gain, skin thinning, diabetes mellitus, muscle atrophy, eye disorders (glaucoma, cataract), onset of hypertension and osteoporosis.[112, 116]

2.3.2 Glucocorticoid-induced Osteoporosis

The major complication of long-term systemic GC excess is the detrimental effect on bone.[1, 117] Chronic hypercortisolism of both iatrogenic and endogenous origin (e.g. Cushing's syndrome) leads to bone loss in approximately 30-50% of affected patients and is associated with an increased fracture risk, especially at the hip and the spine.[117-119] Glucocorticoid-induced osteoporosis (GIO), the most common form of secondary osteoporosis, is marked by an early rapid phase of bone loss, up to 12% within the first year of therapeutic intervention, followed by a slower decline of bone mineral density approximately 3% annually.[1, 120, 121] Histomorphometric

analyses of bone biopsies of GIO patients helped to identify the underlying mechanism of these effects, demonstrating an increased bone resorption coupled with a reduced bone formation.[122-125] Moreover, mean trabecular wall thickness is reduced, reflecting a reduced bone turnover.[123] However, it is generally assumed that the impairment of bone formation is the cardinal feature in the pathomechanism of GIO as supported by a marked decrease of the bone formation markers osteocalcin and N-terminal propeptide of type I collagen (PINP).[126-128] In contrast to these direct effects of GC action on bone primarily targeting osteoblasts, indirect effects including altered gastrointestinal/renal calcium handling, reduction in endogenous sex steroid production and decreased muscle mass are proposed to play a secondary role in the pathogenesis of GIO.[113, 126]

Recently, Weinstein et al.[129] introduced a new concept regarding the pathogenesis of GIO, explaining the loss of bone strength and the frequent occurrence of fractures in GC-treated patients without a reduction in bone mineral density. The authors suggest that the interaction between the osteocyte-canalicular network and the vascular system is an important determinant of bone strength which is influenced by GC excess. In particular, it is postulated that early GC-induced apoptosis of osteoblasts and osteocytes leads to a decreased biosynthesis of angiogenic factors. Consequently, lacunar-canalicular circulation and blood vessel fluid volume are decreased. This in turn results in decreased bone water volume with diminished bone strength and an early increased fracture risk. At a later stage, decreased bone formation and increased osteoclast activity lead to the disruption of cancellous architecture and loss of bone mass with a further increased risk of fractures.[129]

2.3.3 Catabolic Effects of Glucocorticoids

Catabolic effects of high-dose, long-term GC treatment have also been demonstrated by *in vivo* studies. Using a mouse model of elevated GC through administration of high-dose prednisolone for 27 days, Weinstein et al. demonstrated a decreased bone mineral density accompanied by decreased serum osteocalcin levels. Moreover, histomorphometric analysis revealed a diminished bone formation rate and bone turnover.[130] Thus, altogether these observations *in vivo* clearly correlated with those changes seen in GIO patients.

Various *in vitro* and *ex vivo* culture studies using human and murine bone marrow derived osteoblast and stromal cell lines further investigated the inhibitory effects of GC and also showed that these effects are mediated directly via the osteoblast cell lineage.

Treatment of human and murine bone marrow derived cell cultures with high concentrations of GC analogues resulted in a direct impairment of osteoblast cell recruitment,

proliferation, differentiation and maturation, as assessed by the number and size of mineralized, alkaline phosphatase positive colonies formed, quantification of DNA synthesis by measuring 5-bromo-2'deoxyuridine (BrdU) or [^{3}H]-thymidine incorporation, amongst other parameters.[130-136] Underlying mechanisms accounting for the decreased osteoblastogenesis are proposed to be opposed Wnt-ß-catenin signalling and repression of BMP-2, both known for their anabolic properties in bone.[137, 138] In addition, a shift of differentiation of mesenchymal stromal cells from the osteoblastic lineage towards the adipocyte lineage along with an induction of nuclear factors of the CCAAT enhancer-binding protein family and the repression of cbfa-1-expression might be involved.[135]

Other studies report an enhanced apoptosis of mature osteoblasts and osteocytes in the presence of high-dose GC treatment, *in vivo* and *in vitro*, through activation of caspase 3, a key mediator of apoptosis.[130, 139, 140] Particularly, osteocytes' reduced life-span is thought to be of significance, leading to an accumulation of non-detected bone microdamage.[140] Taken together the impaired osteoblastogenesis and enhanced programmed cell-death leads to a reduced number of mature bone-forming cells. Furthermore, it has been shown that the function and metabolism of this reduced pool of osteoblasts is impaired by GC excess.

The biological effects of excess GC are varied. For example, GC decrease type I collagen synthesis via posttranscriptional and transcriptional mechanisms and increase the degradation of collagen matrix breakdown through enhanced expression of collagenase-3 (matrix metallo-proteinase-13 [mmp-13]) mRNA.[141-144] GC also affect osteoblasts indirectly through changes of their microenvironment. In particular, the synthesis of IGF-I and the expression of IGF-I mRNA transcripts are suppressed under GC treatment, which normally exert an anabolic effect on the skeleton through a decrease in collagenase 3 and increase of collagen type I synthesis.[145-148] Another important GC-induced change involves the shifting of TGF-ß1 binding from signal-transducing receptors to extracellular non-signalling binding proteins as demonstrated in osteoblast-enriched cultures from fetal rat bone. As a consequence, the synthesis of collagen and other matrix proteins is impaired.[149]

Despite the bone-forming cells, bone-resorbing cells are also affected by supra-physiological doses of GC. However, it seems that these changes are predominantly mediated indirectly by the osteoblasts as supported by the finding that mature osteoclasts appear to lack functional receptors for GC.[150] GC have been shown to enhance RANK-L and M-CSF expression while decreasing OPG expression in human and murine osteoblastic cells.[151, 152] Consequently, due to the coupling of bone formation and resorption, the shifted RANKL/OPG ratio results in an increased osteoclastogenesis and bone degradation. This mechanism is

proposed to account for the initial rapid phase of bone loss seen in GIO patients. However, osteoclastogenesis is eventually reduced at later stages due to a reversal of this mechanism. Moreover, the decreased osteoblastogenesis and reduced number of osteoblasts at later stages in GIO patients is associated with the reduction of the osteoblast signals M-CSF and RANK-L.

The effects of pharmacological levels of GC on osteoclast survival are contradictory. Induction and suppression of apoptosis have been demonstrated by *in vitro* studies.[153, 154] Altogether, GC at pharmacological doses *in vitro* exert deleterious direct effects on osteoblasts and these effects are consistent with the changes seen *in vivo* following GC excess administration.

2.3.4 Anabolic Effects of Glucocorticoids

In contrast to the deleterious effects on bone caused by pharmacological doses of GC, *in vitro* studies demonstrated anabolic effects of GC when administered at a dose considered to be within the physiological range (~10^{-8} M). Dexamethasone treatment of *in vitro* cell culture systems with cells obtained from chick embryo calvariae, fetal rat calvariae and human bone marrow resulted in an increased number and size of osteogenic nodules with a mineralized matrix.[4, 5, 155-157] These effects appeared to be dose-related, with a maximal response at a constant exposure to physiological dexamethasone concentrations. Moreover, the sensitivity to GC seemed to be more pronounced in marrow stromal cell cultures as compared to primary osteoblast cultures, implicating that dexamethasone induces the proliferation of early osteoprogenitor cells.

Other investigators showed a requirement of low-dose dexamethasone treatment for the induction and enhancement of osteoblast differentiation and matrix mineralization in various cell culture models including human and murine bone marrow derived cell cultures, calvarial cell cultures from fetal and adult murine species as well as the rat osteoblastic sarcoma cell line (ROS17/2.8).[3, 158-170] These studies used elevated alkaline phosphatase activity (ALP) amongst other parameters as a marker of the osteoblast phenotype and differentiation.

Interestingly, a recent study by Eijken et al. showed that dexamethasone needs to be present during early developmental stages in a specific time-window in order to trigger osteoblast differentiation.[3] However, the mechanisms by which dexamethasone promotes osteoblast differentiation *in vitro* are unknown. Studies by Igarashi and Mikami et al. suggest that dexamethasone induces the expression of the osteoblast-specific transcription factors Runx2 and/or osterix genes which may be followed by the activation of osteoblast-specific marker genes as demonstrated by cultured primary rat calvariae cells and ROS 17/2.8 cells.[170, 171]

Accordingly, GC treatment was found to up-regulate the expression of osteoblast specific marker genes including alkaline phospatase,[3, 158] osteopontin,[158, 172] osteonectin, osteocalcin[158, 164, 171, 173] and bone sialoprotein[158, 164, 171, 173] in various cell cultures derived from multiple species. Interestingly, dexamethasone does not consistently induce the entire set of genes associated with osteoblastic differentiation. For example, Eijken et al. found a GC-induced promotion of ALP expression which was accompanied by a down-regulation of osteocalcin and osteopontin in a pre-osteoblast model (SV-HFO). By contrast, Rickard et al. demonstrated an up-regulation of all typical genes in rat bone marrow stromal cell cultures following dexamethasone treatment.[158] These contradictive effects mark the limitation of *in vitro* studies: effects might rely on species, age of experimental animals, methodology, developmental stages of osteoblasts or osteoblast precursors and different culture conditions including type of GC used.

The effects of GC on collagen synthesis and protein expression are controversial. Physiological concentrations of GC have been shown to enhance collagen synthesis and collagen protein mRNA expression in rat calvariae and human cells.[3, 167, 174] However, others found a down-regulation of collagen synthesis by measuring a decreased production of PINP, a precursor type of collagen I, in human bone marrow stromal cells following low-dose dexamethasone treatment.[160]

Canalis et al. demonstrated both anabolic and catabolic action on collagen synthesis of GC in one culture system. 24 hour cortisol treatment of rat calvariae cells treated at 10^{-9} M increased type I collagen synthesis, whereas collagen synthesis was inhibited in cells treated at 10^{-6} M. Treatment for 96 hours also decreased collagen synthesis in cells treated at 10^{-9} M.[174] Thus, whether GC exert stimulatory or inhibitory effects on bone might be concentration- and time-dependent.

Taken together, these *in vitro* studies show an anabolic direct action of GC on bone when administered at a physiological dose. However, the informative value of *in vitro* studies is limited. Therefore, *in vivo* studies are necessary to show whether the anabolic stimulatory effects on osteoblasts seen *in vitro* are of physiological relevance *in vivo.* The generation of specific genetic manipulated *in vivo* mouse models in which the normal GC signalling pathway is particularly abrogated in osteoblasts offers an approach to further study the role of endogenous GC *in vivo*.

2.3.5 Glucocorticoid Signalling in Osteoblasts

Extracellular GC may mediate their effects in skeletal cells by signalling through the classical steroid-hormone receptor pathway. Once passed through the plasma membrane by diffusion, GC bind to the cytosolic glucocorticoid receptor alpha (cGRα), a member of the nuclear hormone receptor superfamily.[111, 175] However, GC also activate the mineralcorticoid receptor (MR) which has been shown to be expressed in osteoblasts.[176, 177] Following ligand-binding, a conformational change of the receptor is induced, including its release from a heat shock protein (HSP) 90-containing inactive protein complex and the unmasking of nuclear localization signals. Thus, the ligand-activated hormone receptor complex translocates into the nucleus where it binds to glucocorticoid response elements (GREs) to regulate the transcription of glucocorticoid target genes.[111, 178]

Despite these genotropic effects, GC are also proposed to induce rapid, non-genomic, transcription independent responses via non-specific interaction with cellular membranes or specific interaction with cytosolic GR (cGR) or membrane-bound GR (mGR).[179, 180]

Several investigators developed *in vivo* models in which the normal GC signalling pathway was abrogated on the receptor level as an approach to study GC action in bone. For example, Cole et al. generated global homozygous GR knockout (GR -/-) mice by gene targeting in embryonic stem cells. However, these GR-deficient mice demonstrated an impaired embryonic development and respiratory failure at birth leading to a high degree of perinatal lethality. In addition, the cortex of the adrenal glands was hypertrophic due to a severely impaired feedback regulation via the HPA axis.[181] Consequently, the utility of this approach is limited. In addition, global knockout of the GR gene does not allow the differentiation of osteoblast-specific effects from other effects mediated by other cells. Moreover, GC function is presumably not completely disrupted, as GC may signal through the intact MR pathway. The generation of double MR/GR knockout mice to block all pathways is likely not to be realizable due to the high perinatal lethality which also has been demonstrated for MR knockout mice.[182] Thus, an alternative strategy is required to further investigate the role of endogenous GC in bone.

2.4 The Col2.3-11ßHSD2 Transgenic Mouse Model

Kream and colleagues in 2001 described a novel and unique transgenic (tg) mouse model in which intracellular GC signalling had been abrogated on the pre-receptor level exclusively in osteoblasts and osteocytes through ligand metabolism via tg overexpression of the GC-

inactivating enzyme, 11ß-hydroxysteroid-dehydrogenase type 2 (11ßHSD2) under the control of the type I collagen promoter (Col2.3-11ßHSD2 tg mouse).[183, 184]

11ßHSD2 and its isoform, 11ß-hydroxysteroid-dehydrogenase type 1 (11ßHSD1), are members of the 11ß-hydroxysteroid-dehydrogenase family of enzymes which are known to modulate intracellular GC metabolism locally, at the pre-receptor level (Figure 6). The NADPH-dependent bi-directional reductase 11ßHSD1 predominantly converts hormonally inactive GC (cortisone in humans and 11-dehydrocorticosterone in rodents) to their biological active form (cortisol in humans and corticosterone in rodents) leading to an increased differentiation and possibly apoptosis. By contrast, the NAD-dependent dehydrogenase 11ßHSD2 uni-directionally catalyses the conversion of the active GC to their inactive metabolites.[108, 110, 185-187] This results in promotion of cell proliferation.[110] Interestingly, both isoenzymes share only 14% sequence homology and are derived from separate gene products.[188]

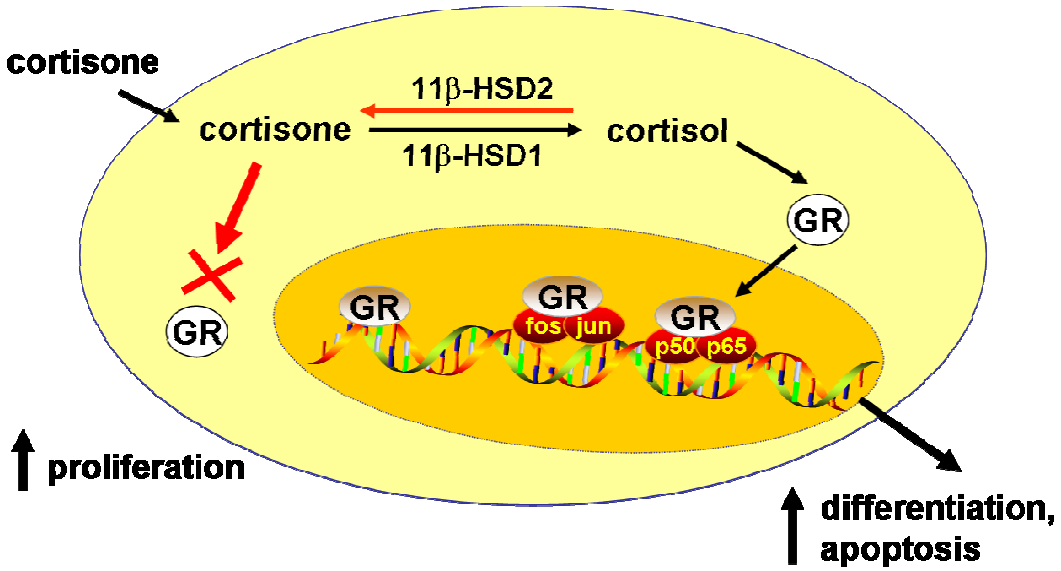

Figure 6: Pre-receptor regulation of the GR by 11beta-hydroxysteroid-dehydrogenases (picture adapted from Rabbitt EH et al., J Steroid Biochem Mol Biol, 2003[110]).

Even though 11ßHSD1 and 11ßHSD2 are exclusively localized to the endoplasmic reticulum membrane, their tissue distribution differs.[187] While 11ßHSD1 is expressed in a number of tissues including lung, liver, brain and adipose tissue, 11ßHSD2 is primarily found in mineralcorticoid target tissues such as the colon and kidney.[108, 186, 189-193] As the "kidney isoenzyme", 11ßHSD2 protects the MR from illicit GC binding as GC are present at much higher levels than aldosterone.[194, 195] Accordingly, 11ßHSD2 knockout (KO) mice exhibited phenotypic features of the human inherited form of hypertension, known as the syndrome of

"apparent mineralcorticoid excess" (AME) caused by a mutation in the 11ßHSD2 gene.[196-198] However, in the placenta, 11ßHSD2 modulates GC access to the GR to protect the fetus from high maternal GC concentrations.[194, 199] In bone, the expression of both HSD isoforms has been reported. While 11ßHSD1 is found in primary osteoblast cultures and osteoclasts, 11ßHSD2 is expressed in osteosarcoma cell lines and fetal bone.[200-203] However, in adult bone, 11ßHSD1 is the predominant isoform in osteoblasts while 11ßHSD2 is expressed at very low levels.[203]

Thus, the strategy of the Col2.3-11ßHSD2 tg mouse model used in this study was to overexpress 11ßHSD2 in bone which should abrogate GC signalling upstream of the GR and MR including the disruption of non-genomic and genomic signalling pathways. However, to specifically target osteoblasts and to avoid complications of global transgene expression, a specific promoter would be necessary which is selectively expressed in osteoblasts. Such a candidate is the collagen type I promoter which has been shown to target gene expression specifically to mature osteoblasts.[204, 205]

In the Col2.3-11ßHSD2 tg mouse model used in this study, the rat 11ßHSD2 complementary DNA (cDNA) was linked to a 2.3-kilobase fragment of the rat α1(I)-collagen (Col1a1) promoter to induce overexpression of 11ßHSD2 specifically to mature osteoblasts and osteocytes (Figure 7).[183, 184] Tg mice were generated in a CD-1 outbred background using pronuclear injection. The transgene was inherited in the mandalian ratio and litter sizes were normal.[184]

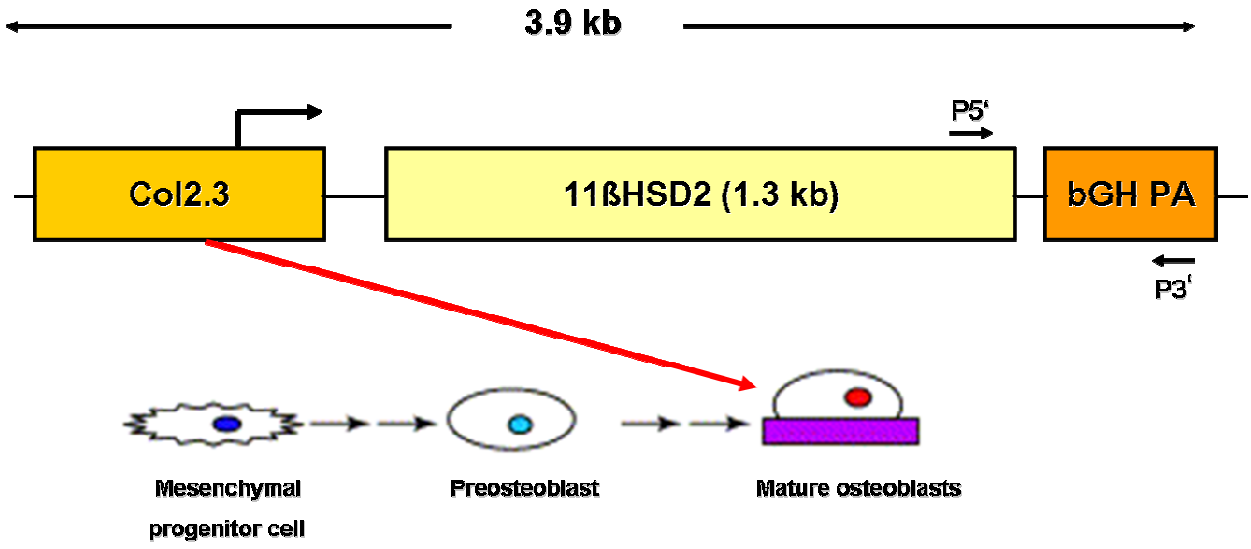

Figure 7: Col2.3-11ßHSD2 construct. The rat 11ßHSD2 cDNA was cloned downstream of the 2.3-kilobase fragment of the collagen type I (Col1a1) promoter and upstream of the bovine GH polyadenylation sequence (bGH PA) targeting mature osteoblasts (P5' forward primer; P3' reverse primer) (picture adapted from Woitge H et al., Endocrinology, 2001[183]).

Employing the Col2.3-11ßHSD2 tg mouse model, Zhou et al. demonstrated that endogenous GC regulate lineage commitment of mesenchymal progenitors towards the osteoblast lineage and control intramembranous bone development of calvariae in mice.[6, 7] Sher et al. further characterized the phenotype of tg mice and their WT littermates. Tg mice exhibited vertebral trabecular osteopenia in females and a reduction in femoral cortical bone parameters in males and females indicating that GC signalling in osteoblasts may play a role in bone mass maintenance and cortical bone mass acquisition.[184, 206] In addition, endogenous GC might be required to maintain normal bone structure and strength as suggested by Kalak et al. The comparison in bone volume parameters of long bones also revealed lower bone volume in long bones of tg mice when compared to their WT littermates as assessed by micro-CT. However, the difference in total between the two groups of mice was subtle.[207] Thus, challenged conditions as those occurring in fracture repair might be required to further investigate the role of endogenous GC.

2.5 Fracture Healing and Glucocorticoids

Despite the well-known complications of long-term systemic GC treatment on bone causing osteoporosis and leading to an increased fracture risk, the effects of GC on fracture repair have just begun to be understood. In recent years, only a few animal studies have been conducted investigating the effects of pharmacological and supra-pharmacological doses of GC on fracture healing.

Early studies by Blunt et al. and Sissons et al. reported a delay in the healing of closed femoral and tibial fractures in rabbits receiving supra-therapeutic, high-dose cortisone treatment (10-25 mg/kg/day) throughout the healing period. In particular, callus formation was found to be decreased and histological processes of repair including the development of granulation tissue were retarded when compared to untreated controls.[208, 209] More recent studies also support these findings in rabbits. For example, Waters et al. and Bostrom et al. used a non-critical sized ulna defect osteotomy model. Prolonged, systemic treatment with therapeutic concentrations of prednisone at 0.15 mg/kg/day administered before and post surgery was shown to impair bone healing as indicated by a higher rate of non-union, a smaller callus size and a fracture site with lower mineral content and strength than in the non-treated control group.[210, 211] Also using a similar osteotomy model, Luppen et al. additionally demonstrated an impairment of bone healing following prednisolone treatment (0.35 mg/kg/day).[212]

Murakami and colleagues created fractures in guinea pigs and administered cortisone at 5 mg/kg/day. Even though ossification, cartilage formation and osteoblastic cell numbers were decreased in the early phase of bone healing in cortisone-treated animals when compared to non-treated littermates, final bony union at the end of the study was comparable between the two groups.[213] Impairment solely in the initial phase of bone healing was also demonstrated by a study observing the effects of prednisolone (2.5 mg/kg/day) on the healing of defects in chicken. While early mineralization of the fracture callus was decreased in GC-treated animals, the ultimate mineralization was similar in the control and the experimental group.[214]

Studies observing the effects of GC on fracture healing in rats are contradictory. While some investigators reported no interference with fracture repair for GC including cortisone, prednisone, methylprednisolone at a high-dose for short-and long-term treatment[215-218], others did report a delay of the repair process by dexamethasone, cortisone and prednisolone.[219-221] Different factors are proposed to account for these differing results including species, fracture model and type, duration, dosage and type of GC. In addition, the rat is known to have a different active endogenous corticosteroid than humans and rabbits.[2]

Altogether, increasing evidence suggests that GC treatment at pharmacological and supra-pharmacological doses might interfere with fracture repair. However, the role of endogenous GC in bone healing has not been investigated.

2.6 Hypothesis

Mechanisms by which GC exert their effects on bone cells are poorly understood, particularly during fracture healing. While GC at pharmacological doses are known to interfere with fracture repair, the role of endogenous GC in bone healing is unclear. Based on previous observations made in the Col2.3-11ßHSD2 tg mouse model, we reasoned that endogenous GC not only play a role in bone mass maintenance and in the control of intramembranous bone development but also in osteoblastic repair mechanisms. We specifically hypothesized that osteoblastic repair of a bone defect would involve the cell-specific action of endogenous GC. Thus, osteoblast-targeted disruption of intracellular glucocorticoid signalling, as present in the Col2.3-11ßHSD2 tg mouse model, would adversely affect (i.e. delay) intramembranous bone healing in a model of fracture repair.

To test this hypothesis we aimed to:

(1) Establish a well-defined intramembranous fracture model in which bone formation is induced without an endochondral component which can be applied to Col2.3-11ßHSD2 tg mice and their WT littermates.

(2) Identify time-dependent structural and histological parameters of bone repair comparing Col2.3-11ßHSD2 tg mice and their WT littermates by using this particular fracture model.

3 Animals and Methods

3.1 Experimental Animals and Study Design

Col2.3-11ßHSD2 tg mice were generated as described in chapter 2.4 and were a gift from Dr Barbara Kream, Department of Medicine, University of Connecticut Health Center, Farmington, CT, USA. Mice were maintained at the animal facilities of the ANZAC Research Institute (Sydney, Australia) in accordance with Institutional Animal Welfare Guidelines and according to an approved protocol. Mice were allowed access to food and water ad libitum and were exposed to a 12-hour light/dark cycle.

Surgical procedures were performed on 7-week-old male Col2.3-11ßHSD2 tg mice (mean body weight 29.94 ±2.29 g) and their wild-type (WT) littermates (mean body weight 32.95 ±2.43 g). A total of 70 mice from the two groups were randomly assigned to three experimental groups to assess the early and late phase of defect repair at 1, 2 and 3 weeks post fracture (Figure 10).

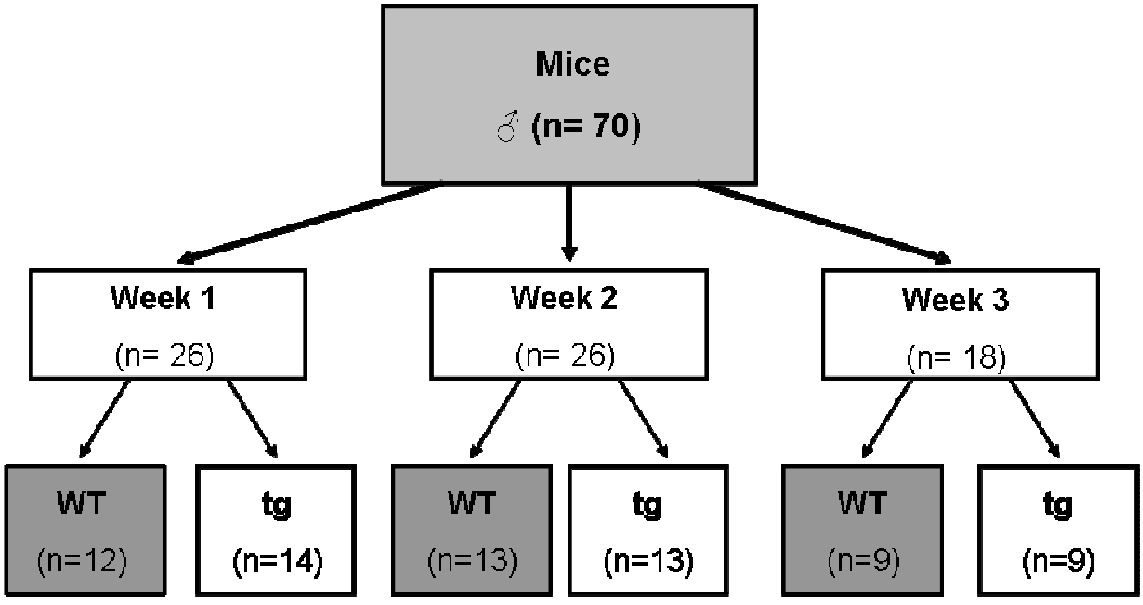

Figure 10: Study design.

3.2 Genotype Analysis

Since tg and WT mice do not differ in phenotypic appearance genotyping was carried out. Toes of all animals were collected between 7 and 12 days of age and their genomic DNA was isolated. Tissue samples were incubated with a lysis mixture containing 198.3 µL Milli-Q water, 25 µL

$MgCl_2$ (20 mM; Ajax Finechem Pty. Ltd., Taren Point, Australia), 25 µL DNA Polymerase 10x Reaction Buffer (Fisher Biotec Australia, Wembley, Australia) and 17 µL proteinase K (Roche Applied Sciences, Castle Hill, Australia) per sample at 55°C for 2 h. An incubation at 98°C for 15 min followed to deactivate proteinase K.

The lysed DNA samples were amplified by PCR (Eppendorf Mastercycler ep, Eppendorf AG, Hamburg, Germany). The PCR reaction mix contained:

- Milli-Q water (autoclaved): 13.75 µL
- 10x Reaction buffer (Bioline Pty Ltd., Alexandria, Australia): 2.5 µL
- $MgCl_2$ (50 mM; Bioline Pty Ltd., Alexandria, Australia): 1 µL
- Mango Taq DNA polymerase enzyme (1000 units; Bioline Pty Ltd., Alexandria, Australia): 0.75 µL
- dNTPs (desoxyribonucleoside triphosphates; 1 mM; Invitrogen Corp., Carlsbad, CA, USA): 1 µL
- HSD2 primers (10 mM): 1 µL
- 5 µL of lysed DNA

The selected forward oligonucleotide primer sequence 5'-ACC TTA GCC CCG TTG TAG-3' was part of the HSD2 gene and the reverse primer sequence was 5'-G AGG GGC AAA GAA GAA CAG ATG-3' within the bovine GH polyadenylation region (see chapter 2.4, Figure 7). The PCR was started with one cycle at 94°C for 5 min and was continued with 30 cycles (94°C 30 s, 60° 30 s, 72° 45 s). The reaction ended with a cycle at 72°C for 5 min.

3.3 Tibia Cortical Defect Repair Model

Preoperatively, general anaesthesia and analgesia was induced by injecting ketamine (75 mg/kg body weight; Cenvet Pty. Ltd., Kings Park, Australia) and xylazine (10 mg/kg body weight; Cenvet Pty. Ltd., Kings Park, Australia) intraperitoneally. The operating area was shaved and disinfected with 70% v/v ethanol. A 1 cm long skin incision was made over the dorsal aspect of the left knee and then the tibia was exposed by dividing the anterior tibial muscle. A uni-cortical, full-thickness standardized tibial bone defect was created 5 mm below the tibia patellar tendon insertion using a low-speed 0.8 mm diameter drill (Dremel Stylus Variable Speed Rotary Tool, Dremel, Mount Prospect, IL, USA) (Figure 11). The skin wound was then closed with interrupted stitches using 5-0 nylon suture (Ethicon Inc., Somerville, NJ, USA).

Subsequent to the operation, radiographs were obtained with a MX-20 digital Faxitron X-ray system (Faxitron X-ray Corp., Wheeling, IL, USA) to confirm the correct position of the defect. Animals were placed under heated lamps to maintain constant body temperature and observed until awake. Mice were allowed unrestricted cage activity and were closely monitored for pain-related behaviour until time-point of sacrifice. Body weight was assessed weekly.

Figure 11: Tibia cortical defect repair model: X-ray (Faxitron) showing the localisation of the drill-site at the left tibia.

3.4 Sample Preparation

Mice were sacrificed at the assigned time-points by cervical dislocation under anaesthesia. Tibiae were collected with some remaining soft tissue and fixed in 4% paraformaldehyde (PFA extra pure, Merck KGaA, Darmstadt, Germany) buffered with 0.1 mol/L phosphate buffer (AMRESCO Inc., Solon, OH, USA; pH 7.4) for 48 h at 4°C. Samples were then immersed in PBS solution until subjected to micro-CT. Following micro-CT scanning, samples were decalcified in 10% ethylene diamine tetraacetic acid (EDTA; Fronine Laboratory Supplies, Taren Point, Australia; pH 7.0) for 3 weeks at 4°C with twice weekly change of the solution.

Tibiae were then processed for paraffin embedding with an automated tissue processing machine (Leica TP 1020, Leica Microsystems GmbH, Wetzlar, Germany) in which sections were dehydrated in a series of ascending concentrations of ethanol (50% v/v 4 h, 70% v/v 4 h, 95% v/v 4 h, 95% v/v 4 h, 100% 2 h, 100% 2 h, 100% vacuum 2 h) and cleared in xylene (2 h

vacuum, 2 h, 2 h vacuum). Samples were then embedded in paraffin wax (Paraplast Tissue Embedding Medium, Tyco Healthcare Group, Mansfield, MA, USA).

Serial longitudinal 5 µm-thick sections were obtained using a Leica microtome (Leica Microsystems GmbH, Wetzlar, Germany) and mounted onto slides coated with 3-aminopropyltriethoxysilane (AES; Sigma-Aldrich Inc., St. Louis, MO, USA).

3.5 Staining Procedures

Sections displaying the defect gap were prepared for staining by deparaffinization and rehydration with xylene (two changes, each for 5 min) and graded ethanol concentrations (100% 3 min, 100% 3 min, 100% 3 min, 95% v/v 3 min, 70% v/v 2 min). Sections were then rinsed in double-distilled water.

3.5.1 Hematoxylin and Eosin (H&E)

For general histology of the defect site and identification of osteoblasts, sections were stained with hematoxylin (Lillie-Mayer's hematoxylin, Fronine Laboratory Supplies, Taren Point, Australia) and eosin (Eosin Y, Fronine Laboratory Supplies, Taren Point, Australia) following a standard protocol. Hematoxylin in its oxidised active form hematein stains basophilic structures such as nuclei purple-blue and eosin colours eosinophilic structures such as cytoplasm pink-red. The incubation time in hematoxylin was 4 min and in eosin 10 min.

3.5.2 Tartrate Resistant Acid Phosphatase (TRAP)

To identify osteoclasts, sections were stained for the presence of TRAP, a metallophosphoesterase highly expressed in osteoclasts within the ruffled border area, lysosomes and in Golgi cisternae and vesicles.[222] Sections were incubated in TRAP solution containing TRAP buffer (sodium acetate anhydrous [50 mM, Fluka Chemie AG, Basel, Switzerland], potassium sodium tartrate [40 mM, Sigma-Aldrich Inc., St. Louis, MO, USA] pH 5.0), naphthol AS-BI phosphate (Sigma-Aldrich Inc., St. Louis, MO, USA) dissolved in N,N-dimethylformamide (Sigma-Aldrich Inc., St. Louis, MO, USA) as a substrate and fast red violet Luria-Bertani salt (Sigma-Aldrich Inc., St. Louis, MO, USA) as detection agent for the reaction product.[223] The incubation was done at 37ºC for 0.5-2 h until colour was developed and the reaction was stopped by rinsing the sections in tap water. Sections were counterstained by treatment with a 1:10 v/v solution of Gills no.3 hematoxylin (Fronine Laboratory Supplies, Taren

Point, Australia) for 30 s. Slides were dried at 37°C overnight, mounted in DEPEX medium (BDH Ltd., Poole, UK) and coverslipped.

3.5.3 Toluidine Blue

For cartilage matrix detection, slides were stained with toluidine blue (0.1%) for 3 min, rinsed in tap water and dried in a 37°C oven overnight. While structures including nuclei and cytoplasm are stained blue, cartilage matrix with its proteoglycan content appears purple/dark blue.

3.6 Analyses of Defect Repair

3.6.1 Microcomputed Tomography (micro-CT) Analysis

Micro-CT images of all tibia samples were obtained for morphological quantification of newly formed mineralized bone at the drill site. As a technique commonly employed in bone biology, micro-CT allows the generation of high resolution 3-dimensional visualisation of bone microarchitecture generated by X-rays. In the present study, a Skyscan 1172 X-ray microtomograph (SkyScan, Kontich, Belgium) was used consisting of an X-ray source, a specimen holder and a CCD camera for X-ray detection. The equipment was connected to a computer with tomographic reconstruction software (Figure 12).

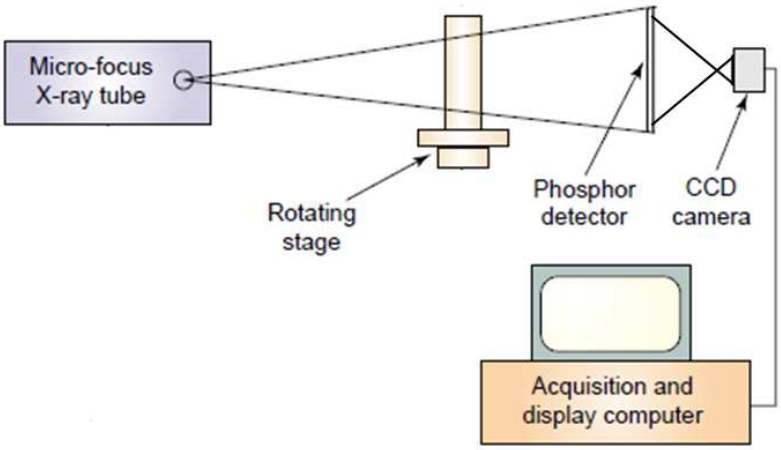

Figure 12: Micro-CT setup (picture adapted from Holdsworth DW and Thornton MM, Trends in Biotechnology, 2002[224]).

Tibia samples were placed in the specimen holder, immersed in PBS solution to prevent them from drying out. Scanning was carried out at 100 kV, 100 µA with an exposure set to 590 ms. A 1 mm aluminium filter was used to reduce the phenomenon of beam hardening which would lead to artefacts in the processed tomogram. A set of 1800 X-ray projections was collected at multiple viewing angles around the sample at a resolution of 6.93 µm/pixel. The projection data was then reconstructed using a modified Feldkamp cone-beam algorithm with beam hardening correction set to 50%.

The defect gap was represented over approximately 100 2-dimensional cross sections per sample and 'CTAnalyser' software (version 1.02, SkyScan, Kontich, Belgium) was employed to analyse the defect repair. This analysis of all sections of the defect gap was done for two different regions of interest (ROI) to prevent bias of results due to selected area and to establish a convenient measurement method for this defect repair model (Figure 13).

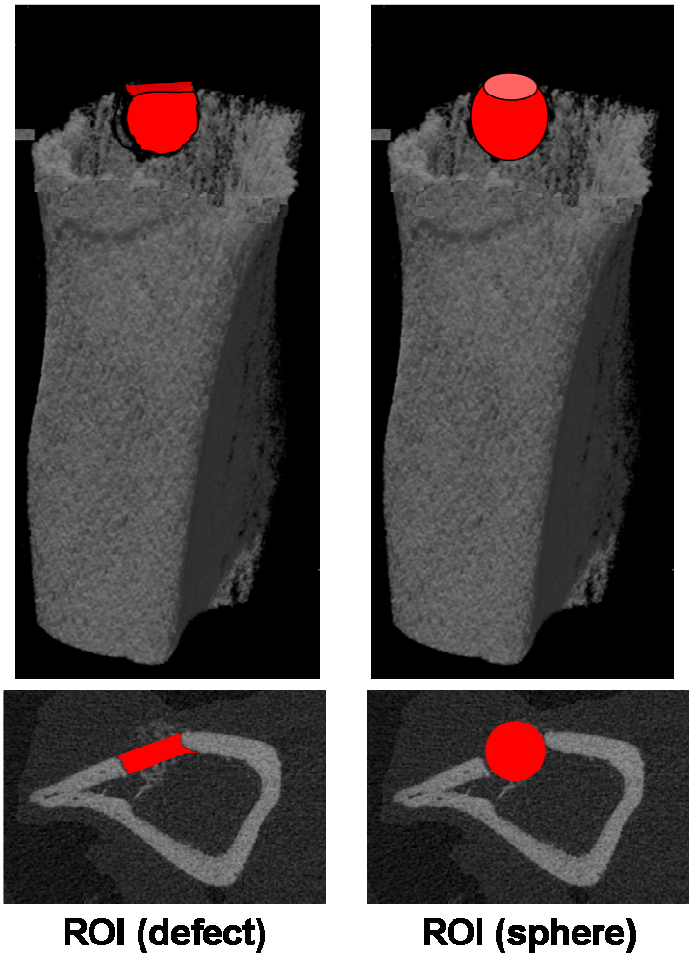

Figure 13: Region of Interests (ROIs) for micro-CT analysis with CTAnalyser` software. ROI (defect) comprised the entire volume of the immediate defect site in the cortical bone area. ROI (sphere) was cylindrical-shaped, additionally covering newly formed bone volume on the outer and inner region of the defect site.

One ROI comprised the entire volume of the immediate defect site in the cortical bone area and was termed ROI (defect). This ROI was free-hand drawn using a mouse.

The other ROI was cylindrical-shaped, additionally covering newly formed bone volume on the outer and inner region of the defect site and was defined as ROI (sphere). This ROI was delineated using the round shape form from the file menu. The centre of the cylinder was located in the middle of the defect gap.

Following the selection of ROI, pictures were viewed in the binary images viewing mode (Figure 14). This mode applies only to the ROI while the non-selected part of the image shows the usual window background colour (green). In this mode, the histogram shows indexed grey levels ranging from 0 (black) to 255 (white). A binary threshold selection was set between grey scale index 70 and 250 to separate bone tissue from other soft tissue, muscles and bone marrow. White colour in these images represents areas with brightness within the range of the binary threshold selection (bone), and the areas outside this selection are black (representing soft tissue, muscles and bone marrow).

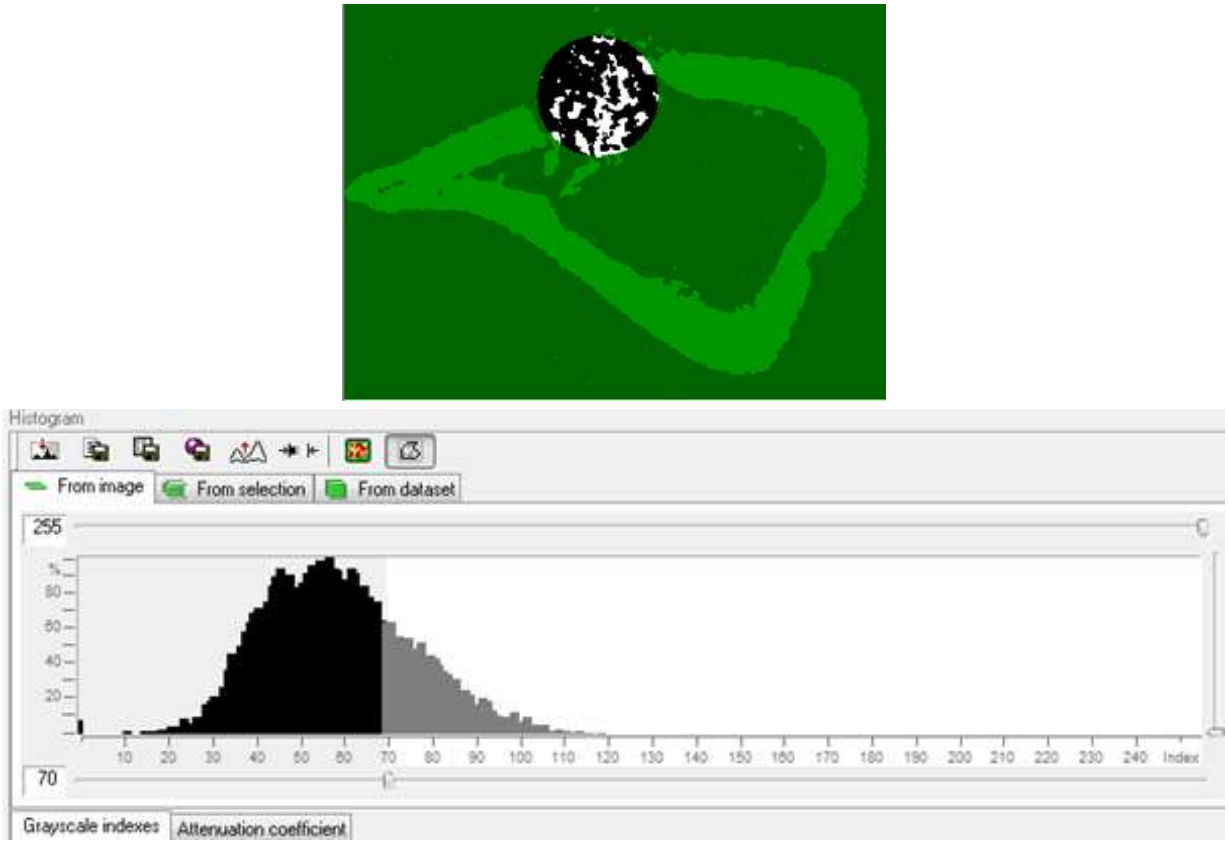

Figure 14: Binary images viewing mode (CTAnalyser' software) with histogram demonstrating indexed grey levels from 0 to 255 for the ROI. The binary threshold selection was set between grey scale index 70 and 255 to separate bone tissue (white colour) from other soft tissue, muscles and bone marrow (black colour).

The following morphological parameters were then measured for the two ROI:

- **BV**: bone volume (grey scale index 70-255)
- **TV**: tissue volume
- **BV/TV**: bone volume/tissue volume (%)
  Percentage of newly formed mineralized bone volume of the immediate cortical defect site
- **Mean density BV/TV**: mean density bone volume/tissue volume
  mean density of newly formed mineralized bone of the immediate cortical defect site, measured as the mean value of grey in the selected threshold selection for bone tissue 70-255)

Three-dimensional images for a general overview of the defect site were created with VGStudio MAX imaging software (Version 1.2, Volume Graphics, Germany). Images representative of n=70 samples.

3.6.2 Histomorphometric Analysis

Histomorphometric characterization of defect calluses was performed on all defect tibiae using Bioquant Osteo II System, (version 8; Bioquant Image Analysis Corp., Nashville, TN, USA). Three representative levels of H&E and TRAP stained sections within the centre of the cortical defect, each approximately 15 micrometers apart, were examined with a light microscope (Leica Microsystems GmbH, Wetzlar, Germany) at 200-fold magnification. All samples were analysed in a blind fashion and results were averaged.

The selected ROI for quantitative analysis of defect area was a rectangle, with a standard height of 350 μm and a width adjusted to the defect dimension with a gap of 30 μm to each side of the original cortical bone (Figure 15).

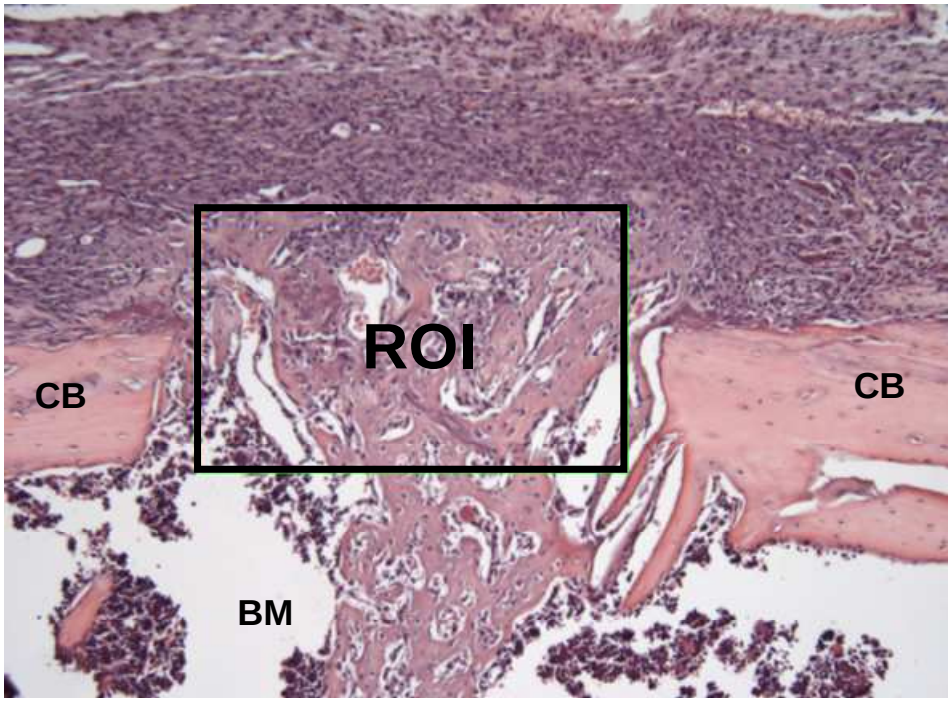

Figure 15: Region of interest (ROI) for histomorphometric analysis of defect callus at drill site. CB-cortical bone, BM-bone marrow. Image representative of n=70 samples.

The following standard static histomorphometric parameters of volumes and surfaces as recommended by the ASBMR Histomorphometric Nomenclature Committee[225] were then measured manually by tracing around the respective areas on the screen with a mouse and calculated by the software:

- **BV**: newly formed bone volume (mm^2)
- **TV**: tissue volume (mm^2)
- **BV/TV**: bone volume/tissue volume (%)
  Percentage of newly formed bone volume of tissue volume at defect site
- **BS/BV**: bone surface/bone volume (%)
  Percentage of bone surface of newly formed bone volume
- **Ob.S/BS**: osteoblast surface/bone surface (%)
  Percentage of bone surface covered with osteoblasts
- **N.Oc/BS**: number of osteoclasts/bone surface (per mm)
  Mean number of osteoclasts per mm bone surface
- **Oc.S/BS**: osteoclast surface/bone surface (%)
  Percentage of bone surface covered with osteoclasts

The identification of the defect site with newly formed woven and lamellar bone of week 3 post-fracture samples was facilitated by the use of polarized light microscopy.

For a general overview of the fracture site at all time points of repair assessment, pictures were created at 100-fold magnification using QCapture Software (Quantitative Imaging Corp., Surrey, Canada).

3.6.3 Second-harmonic Imaging Microscopy (SHIM)

The orientation and organization of collagen fibre structure of newly formed defect calluses of respective week 1 WT and Col2.3-11ßHSD2 tg animals were observed by second-harmonic imaging microscopy. This relatively new microscopy technique is based on the ability of highly polarisable material to produce a nonlinear optical effect known as second-harmonic generation (SHG). Once intensive laser light passes through the material, second harmonic light with half the wavelength of the entering light emerges from it. This optical phenomenon is due to annihilation of two photons and creation of one single photon at double frequency.[226]

The SHG effect was first demonstrated in 1961 by Franken et al.[227] on polarisable crystalline quartz but it was not until 1986 when Freund et al. performed the first biological SHG imaging experiments to study the orientation of collagen fibres in rat tail tendon. Only recently, SHIM has been developed as a high resolution 3-dimensional technique for imaging live cells and tissues and is about to gain importance in research and clinical pathology. In order to produce SHG, structures are required to be noncentrosymmetric such as microtubules, muscle myosin and collagen. Especially type I collagen, abundant in fracture calluses, is known as a strong mediator of SHG signals due to its high degree of crystallinity and arrangement in a triple helix.

In the present work, SHIM images were combined with two-photon excited fluorescence (TPEF) images to additionally demonstrate cell structures at the defect site. While SHIM involves nonlinear scattering, TPEF is based on nonlinear absorption resulting in fluorescence.
For the SHIM procedure, representative 5 µm-thick sections of defect calluses of week 1 defect samples were dewaxed in xylene for 20 min, mounted on slides with DEPEX medium and coverslipped.

The general experimental setup consisted of a pulsed infra-red femtosecond laser coupled to a confocal scanning system (Leica TCS SP2, Leica Microsystems GmbH, Wetzlar, Germany) and an inverted microscope (Leica DM IRBE, Leica Microsystems GmbH, Wetzlar, Germany) (Figure 16).

In detail, an infra-red, femtosecond titanium-sapphire (Ti-S) laser (Tsunami, Spectra Physics, Mountain View, CA, USA) synchronously pumped by a 5 W diode laser (Millenia, Spectra Physics, Mountain View, CA, USA) provided the excitation beam with a wavelength of 870 nm (red). This beam was focused and scanned across the sample. SHG is emitted in the forward scattered direction, along the path of the excitation laser (blue). Second harmonic light was collected by a high numerical aperture oil immersion condenser and detected with photomultiplier tube 1 (PMT1). An infra-red blocking filter with a cut-off at 700 nm was fitted in a filter cube to remove direct laser light from the optical path. A barrier filter with a window of 395-440 nm ensured the passing through and detection of SHG photons at a wavelength of 433 nm only, whereas autofluorescence with longer wavelengths was effectively blocked.

In contrast to SHG, TPEF is emitted in all directions and thus can be collected by the objective lens in the backscattered direction (green). Photomultiplier tube 2 (PMT2) detected autofluorescence with an adjusted wavelength range set to 500-600 nm. Leica Confocal Software (Leica Microsystems GmbH, Wetzlar, Germany) was used to control the microscope, acquire and analyse scans.

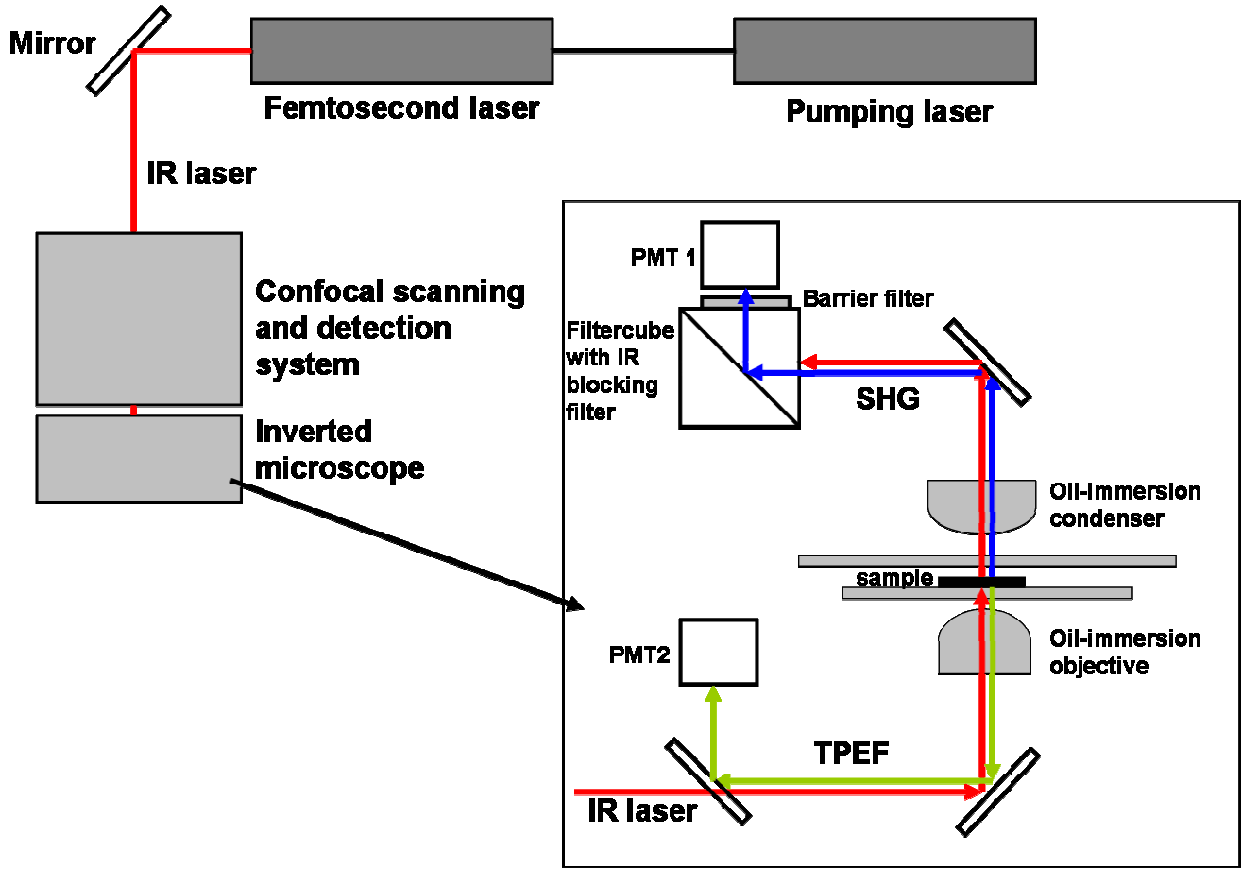

Figure 16: Second-Harmonic Generation (SHG) Microscopy: experimental setup; see text for explanation. IR laser-infra-laser, SHG-second-harmonic generation, PMT-photomultiplier tube, TPEF-two-photon fluorescence.

3.7 Immunohistochemistry

Immunohistochemical assessment of HSD2 transgene expression at the defect site was performed by using the avidin-biotin complex (ABC) technique. This method is based upon avidin, a 68,000 molecular weight glycoprotein which can be labelled with a peroxidase. Avidin binds irreversibly and rapidly with a high affinity (dissociation constant 10^{-15} M) to the vitamin biotin, thus allowing for a high sensitivity of this method.[228]

Three layers of antibodies are involved (Figure 17): an unlabelled primary antibody binds directly to the HSD2 antigen which is followed by the binding of a biotinylated secondary antibody to the primary antibody. The third layer consists of a preformed avidin and biotinylated horseradish peroxidase complex. The peroxidase is finally developed by 3,3'-diaminobenzidine (DAB) substrate-chromogen resulting in a brown stain.

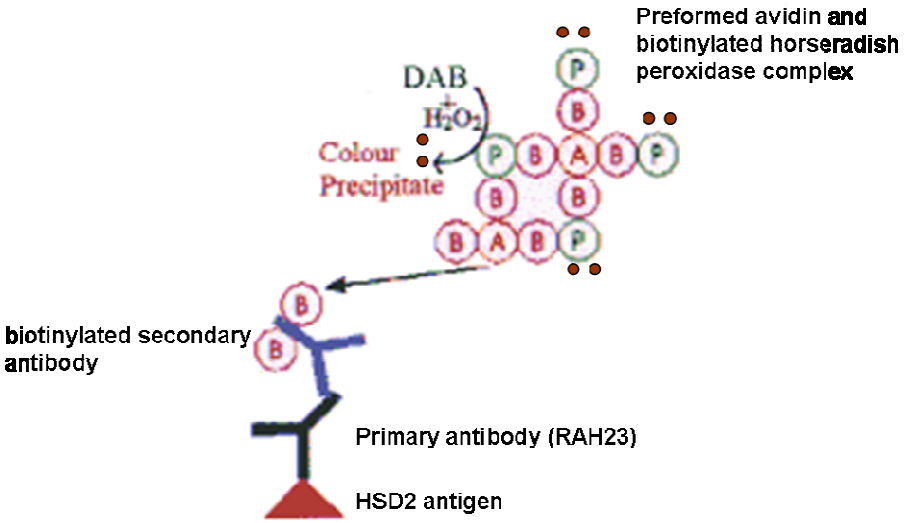

Figure 17: Avidin-biotin complex (ABC) technique for immunohistochemical assessment of HSD2 transgene expression at defect site using RAH23 antibody. A-avidin; B-biotin, DAB-3,3'-diaminobenzidine (picture adapted from www.hmds.org.uk/histology.html).

In detail, 5 µm-thick tibia sections of representative Col2.3-11ßHSD2 tg and WT samples of all time points of repair assessment showing the defect site were used for the procedure. Sections were deparaffinized in xylene (two times for 5 min), hydrated in a series of graded ethanol solutions (100%, 95% v/v, 70% v/v; each for 3 min) and washed in Milli-Q water. Endogenous peroxidase activity was quenched by 3% v/v hydrogen peroxide (Riedel-deHaën, Seelze, Germany) diluted in Milli-Q water for 10 min. Slides were then rinsed in PBS/BSA

Triton buffer (1 L PBS with 0.15% BSA (bovine serum albumin; Sigma-Aldrich Inc., St. Louis, MO, USA) and 0.1% Triton X-100 (Sigma- Aldrich Inc., St. Louis, MO, USA); two times for 5 min).

To prevent potential binding of antibodies to nonspecific antigens, slides were incubated in blocking solution containing normal goat serum (150 µL) made up in PBS/BSA Triton Buffer (10 mL) for 30 min. Sections were encircled with a PAP pen (The Binding Site Ltd, Birmingham, UK) and the blocking solution was removed. Sections were incubated with a primary antibody, the purified polyclonal rabbit anti-rat 11ßHSD2 antibody RAH23[229] diluted at a concentration of 1:1000 v/v in the blocking solution in a humidified chamber at 4°C overnight. Samples were rinsed in PBS/BSA Triton buffer (3 changes for 3 min, 10 min, 5 min) and incubated with the biotinylated anti-rabbit IgG secondary antibody (Vectastatin ABC kit, Vector Laboratories, Burlingame, CA, USA) diluted in the blocking solution at 1:200 v/v for 1 h in a humidified chamber. The antibody was tipped off and sections were washed with PBS/BSA Triton buffer (3 changes for 5 min each) and avidin-biotinylated horseradish peroxidase complex reagent (Vectastatin ABC kit, Vector Laboratories, Burlingame, CA, USA) was added for 30 min.

A DAB substrate kit for peroxidase (Vector Laboratories, Burlingame, CA, USA) was used for chromagen development. Following an incubation time of 4 min, the reaction was stopped by dipping the slides in Milli-Q water. Samples were washed in Milli-Q water for 5 min and counterstained with Gill's no.3 hematoxylin (Fronine Laboratory Supplies, Taren Point, Australia) at a dilution of 1:20 v/v for 1-2 min. Slides were then washed in tap water for 5 min, dehydrated in ethanol (95% v/v for 5 min, 100% 2 changes for 5 min each), cleared in xylene (2 changes for 10 min each) and coverslipped with DEPEX permanent mounting medium (BDH Ltd, Poole, UK).

3.8 Statistical Analysis

Data are represented as the means ± standard error of the mean (SEM). Statistical analysis was performed with Student's t-test, 2-way ANOVA and 2-way ANCOVA using SPSS statistics program (SPSS ver. 15, SPSS Inc. Chicago, USA). A p-value of less than 0.05 was considered statistically significant.

4 Results

4.1 Tibia Defect Repair Model

Surgical procedures were well-tolerated by all animals and there were no procedure-related deaths. After recovering from anaesthesia, mice displayed normal behaviour and started to move around the cages with full weight bearing. Post-operative X-rays confirmed successful surgical outcomes in all animals. Tibia defects were created in a reproducible manner at the designated location on the medial aspect of the left tibia, 5 mm below the knee joint. Thus, no animals had to be excluded from the study post-operatively.

Throughout the post-operative monitoring period mice showed no preference in the use of their legs as assessed daily. The healing of defects occurred without complications. No wound infections were developed and no suture insufficiency was noted.

4.2 Body Weight

Pre-surgery mean body weight, measured two days prior to operation, was significantly lower in Col2.3-11ßHSD2 tg mice when compared to their respective WT littermates in all experimental groups of fracture healing assessment at weeks 1, 2 and 3 (Figure 18; $p<0.05$). However, mean body weight gain during the fracture-healing period was similar between WT and tg mice for all analysed time-points (Figure 19; $p>0.05$).

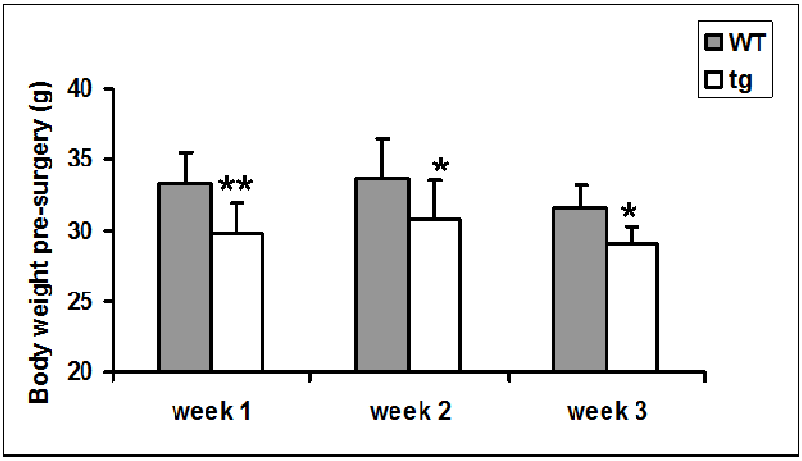

Figure 18: Body weight pre-surgery. A total of 70 WT and tg mice were randomly assigned to three experimental groups. The first group was sacrificed after 1 week, the second after 2 weeks and the third after 3 weeks. Data are shown as means ± SEM. *$p<0.05$; **$p<0.001$ versus WT. WT-wild-type, tg-transgenic.

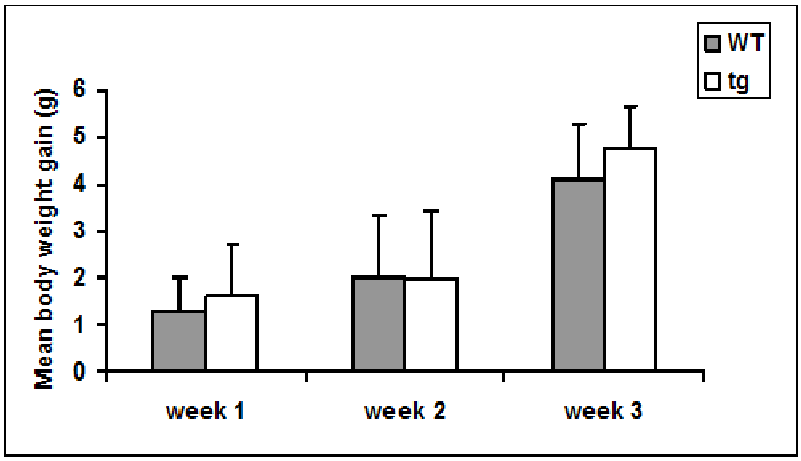

Figure 19: Mean body weight gain during fracture healing monitoring period. Mean body weight gain was not significantly different between WT and tg mice for all study groups (weeks 1, 2 and 3) ($p>0.05$). Data are shown as means ± SEM. WT-wild-type, tg-transgenic.

4.3 The Sequence of Defect Repair

The progression of defect repair was examined in all tibia defects at 1, 2 and 3 weeks following surgical procedure. Three-dimensional micro-CT images of the tibia and two-dimensional cross-sections of the site of bony repair illustrated newly formed mineralized bone. H&E and TRAP stained sections provided insight into the morphology of cellular mechanisms occurring in healing process (Figure 20).

Over time, defects were restored to their original architecture via intramembranous bone formation as revealed by light microscopy. No cartilage was detected in the drilled cortical area or in the marrow cavity at any time-point. Several WT and tg samples showed cartilage formation on the outer bone surface, but this was strictly limited to bone surface adjacent to the fracture site, as a result of periosteal reaction (Figure 21). No morphological difference was detected between WT and tg animals at any time-point monitored.

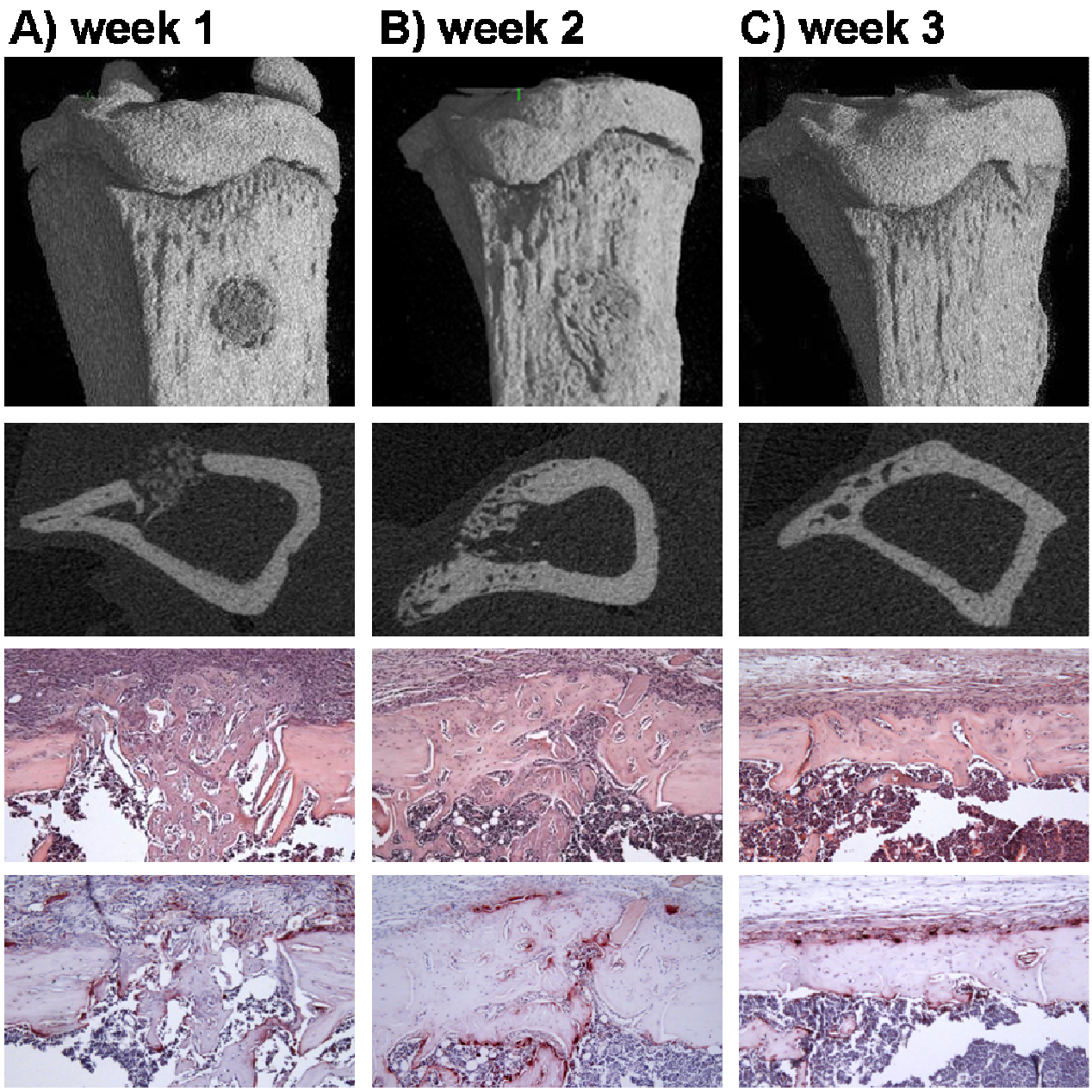

Figure 20: Micro-CT images (3-D first panel; cross sections second panel) and histology (H&E third panel; TRAP fourth panel; original magnification x100) of unicortical diaphyseal defects in the proximal tibia of WT animals at weeks 1, 2 and 3 post fracture. Morphological comparison of the defect site revealed no difference between WT and tg mice at respective time-points. At week 1 (A) mineralized woven bone was formed at the defect site, which increased in volume and density by week 2 (B). At week 3 (C) healing of defect was nearly completed in all WT and tg animals. WT-wild-type, tg-transgenic; images representative of n=70 samples.

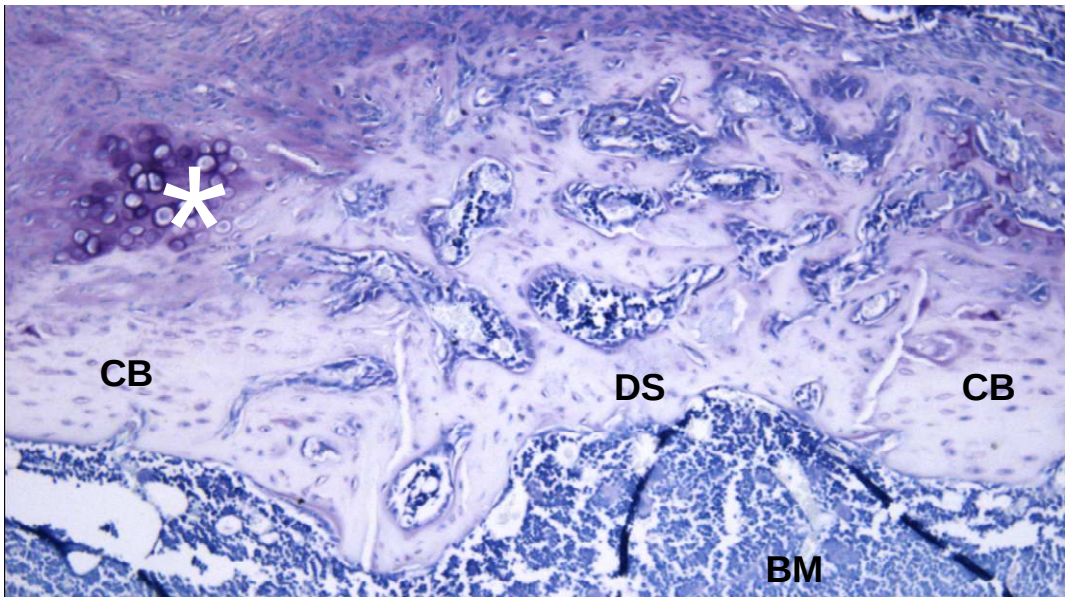

Figure 21: Representative histological image of cartilage formation, restricted to the periosteum; intramembranous bone formation at defect site (Toluidine Blue staining, original magnification x100). Asterisk-cartilage, DS-defect site, BM-bone marrow, CB-cortical bone.

At week 1, micro-CT imaging demonstrated formation of poorly mineralized bone at the drill site and bone marrow cavity (Figure 20A), while histology revealed active woven bone formation. This early, fine, disorganized, cancellous repair tissue was invaded by blood capillaries along with undifferentiated mesenchymal tissue and was predominantly deposited towards the centre of the defect, extending into the medullary cavity and onto the outer surface. Bone trabeculae contained large oval osteocytes and their surface was densely lined with cuboidal osteoblasts. First multinucleated osteoclasts appeared at the wound site at that time-point (Figure 20A).

Throughout week 2, deposition of newly formed bone continued particularly in the periphery of the defect, forming a bony bridge at the drill site joining both ends of the original cortex (Figure 20B). The mineral density of the newly formed bone matrix was increased as demonstrated by micro-CT. Histology demonstrated the diminishing of capillaries and the increase in osteoclast number.

At week 3, bone healing was nearly complete. Thus, the defect was no longer apparent on micro-CT imaging, as it was filled with tissue indistinguishable from the surrounding cortical bone (Figure 20C). However, original lamellar and newly formed woven bone was clearly discernable by polarized light microscopy of histological sections, again demonstrating that the defect was nearly completely filled with new bone (Figure 22) which was beginning to be

compacted and replaced with mature lamellar bone. Accordingly, TRAP-stained sections revealed the advanced healing stage by numerous osteoclasts (Figure 20C).

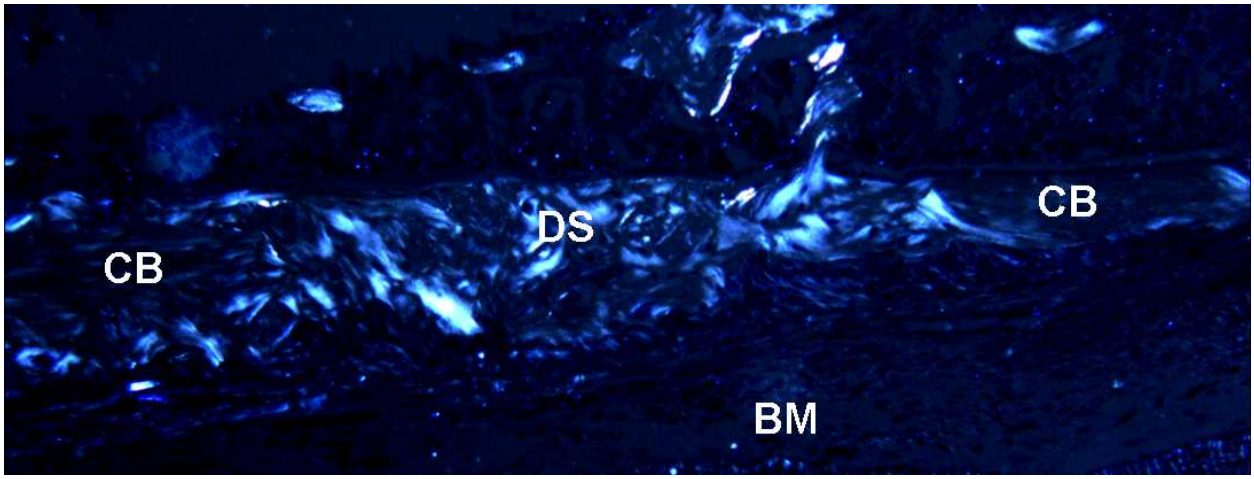

Figure 22: Polarized light microscopy of H&E stained section (original magnification x100) distinguishing original lamellar and newly formed woven bone; DS-defect site, BM-bone marrow, CB-cortical bone.

4.4 Analyses of Defect Repair

4.4.1 Microcomputed Tomography

Micro-CT analysis was performed on all tibia samples at week 1 and 2 post fracture to characterize and quantify the newly formed bone (week 1: WT n=12, tg n=14; week 2: WT n=13, tg n=13). Week 3 samples (WT n=9, tg n=9) were not analysed due to inaccurate detection of fracture site caused by progressed tissue repair.

Corresponding with the morphological observations of three-dimensional micro-CT images, the percentage of newly formed bone volume (BV/TV) in the defect area and its mean density increased from week 1 to week 2 post fracture in WT and tg animals (Figure 23A, B) as determined by the analysis of a region of interest covering the immediate defect site (ROI defect site). The comparison of percentage of newly formed bone volume (BV/TV) and its mean density between WT and tg mice revealed no statistical difference at either time-point ($p>0.05$; Figure 23A, B; ROI defect) indicating a similar osteogenesis regarding the rate of bone healing and its mineralisation.

The analysis of the wider sphere-shaped region of interest of cortical defect area (ROI sphere) demonstrated similar results for both assessed parameters of bone healing and likewise

did not detect a statistical difference between the two groups of mice at week 1 and 2 ($p>0.05$; Figure 23C, D). The high Pearson correlation coefficients between the two ROIs (Table 1) indicate that both methods give reproducible results and are convenient to measure repair tissue in this defect repair model. However, ROI sphere might be recommended for future studies as it is less time-consuming and more effective.

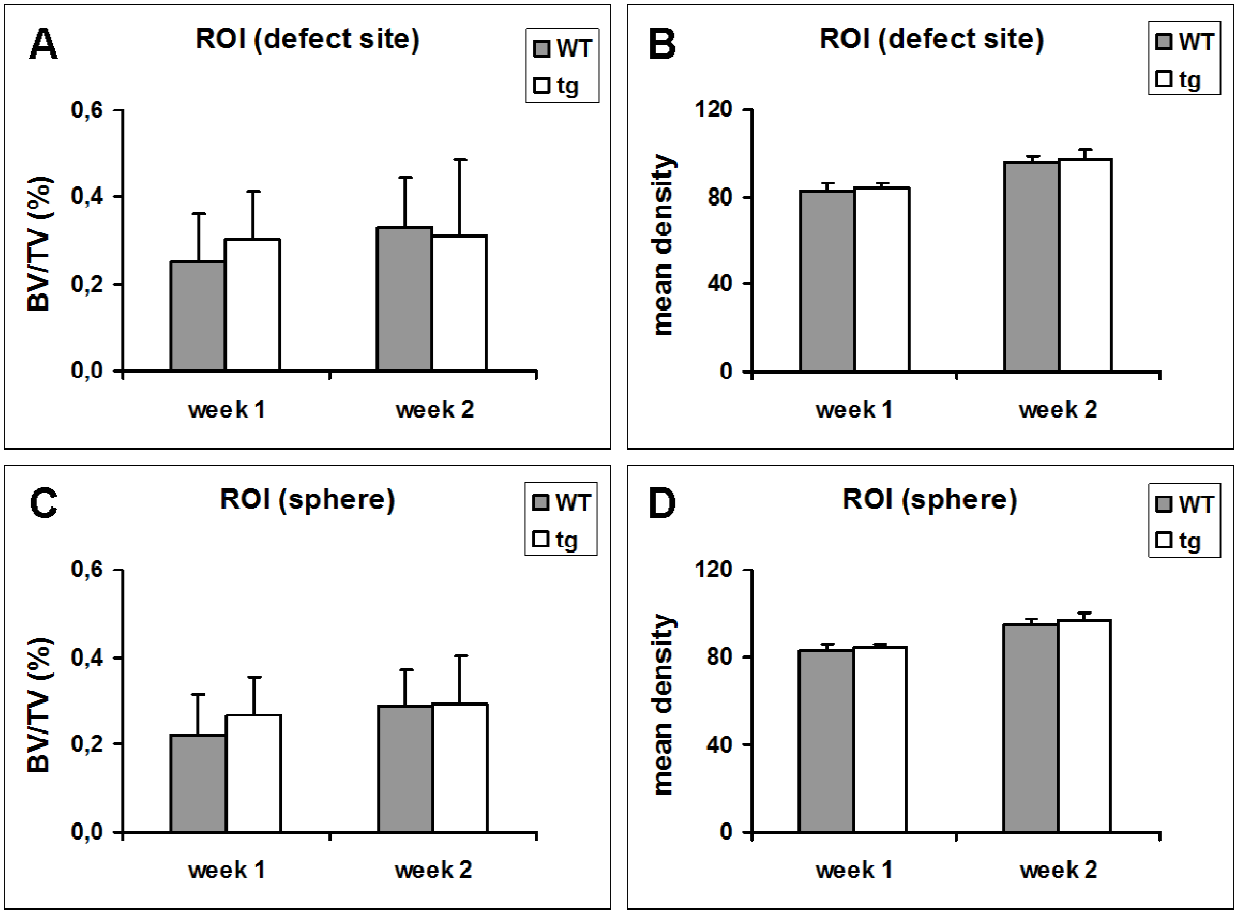

Figure 23: Micro-CT analysis of defect site (approximately 100 2-dimensional cross sections per sample (n=52)), excluding cortical bone for ROI (defect site) (A; B) and ROI (sphere) (C; D).
Comparison of WT and tg animals at week 1 and 2 post-surgery, revealed similar results for % of newly formed bone volume (BV/TV) (A; C) and mean density of bone volume (B; D) ($p>0.05$) for both ROI. At week 3, an accurate ROI was not detectable, due to progressed tissue repair. Data shown are means ± SEM. ROI-region of interest, WT-wild-type, tg-transgenic, BV/TV-bone volume/tissue volume.

	BV/TV		mean density	
	week 1	week 2	week 1	week 2
WT	.929 (n=12)	.836 (n=13)	.980 (n=12)	.879 (n=13)
tg	.924 (n=14)	1 (n=13)	.812 (n=14)	1 (n=13)

Table 1: Correlation for parameters of micro-CT analysis (BV/TV) and mean density of ROI (defect site) and ROI (sphere), separated for WT and tg animals for study groups week 1 and 2 post fracture. Shown are Pearson correlation coefficients. BV/TV-bone volume/tissue volume, ROI-region of interest, WT-wild-type, tg-transgenic.

4.4.2 Histomorphometry

Histomorphometric measurements were performed to characterize bony repair on the cellular level. Tibia samples (week1: WT n=12, tg n=14; week2: WT n=13, tg n=13, week3: WT n= 9, tg n=9) taken at all time-points were analysed. Eleven samples (week1: WT n=4, tg n=2, week 2: wt n=3, tg n=2) were excluded from the analysis due to difficulties in finding the correct orientation layer of the defect.

In accordance with micro-CT analysis and histology, the percentage of bone volume (BV/TV) formed increased throughout the 3-week healing period in WT and tg animals (Figure 24A). This was consequently accompanied by a time-dependent decrease in the percentage of bone surface per bone volume (BS/BV; Figure 24B). The percentage of bone surface covered with osteoblasts (Ob.S/BS) decreased from week 1 to week 3, whereas the number of osteoclasts per bone surface (N.Oc/BS) and the percentage of bone surface covered with osteoclasts (Oc.S/BS) increased by week 2 (Figure 24C- E).

The comparison of WT and tg mice for the proportion of bone surface covered with osteoblasts (Ob.S/BS) and osteoclasts (Oc.S/BS), and osteoclast number per bone surface (N.Oc/BS) did not differ between tg and WT mice at any time-point ($p>0.05$, Figure 24C- E). Furthermore, percentage of bone volume (BV/TV) and percentage of bone surface per bone volume (BS/BV) were similar between the two groups at all time-points ($p>0.05$; Figure 24A, B).

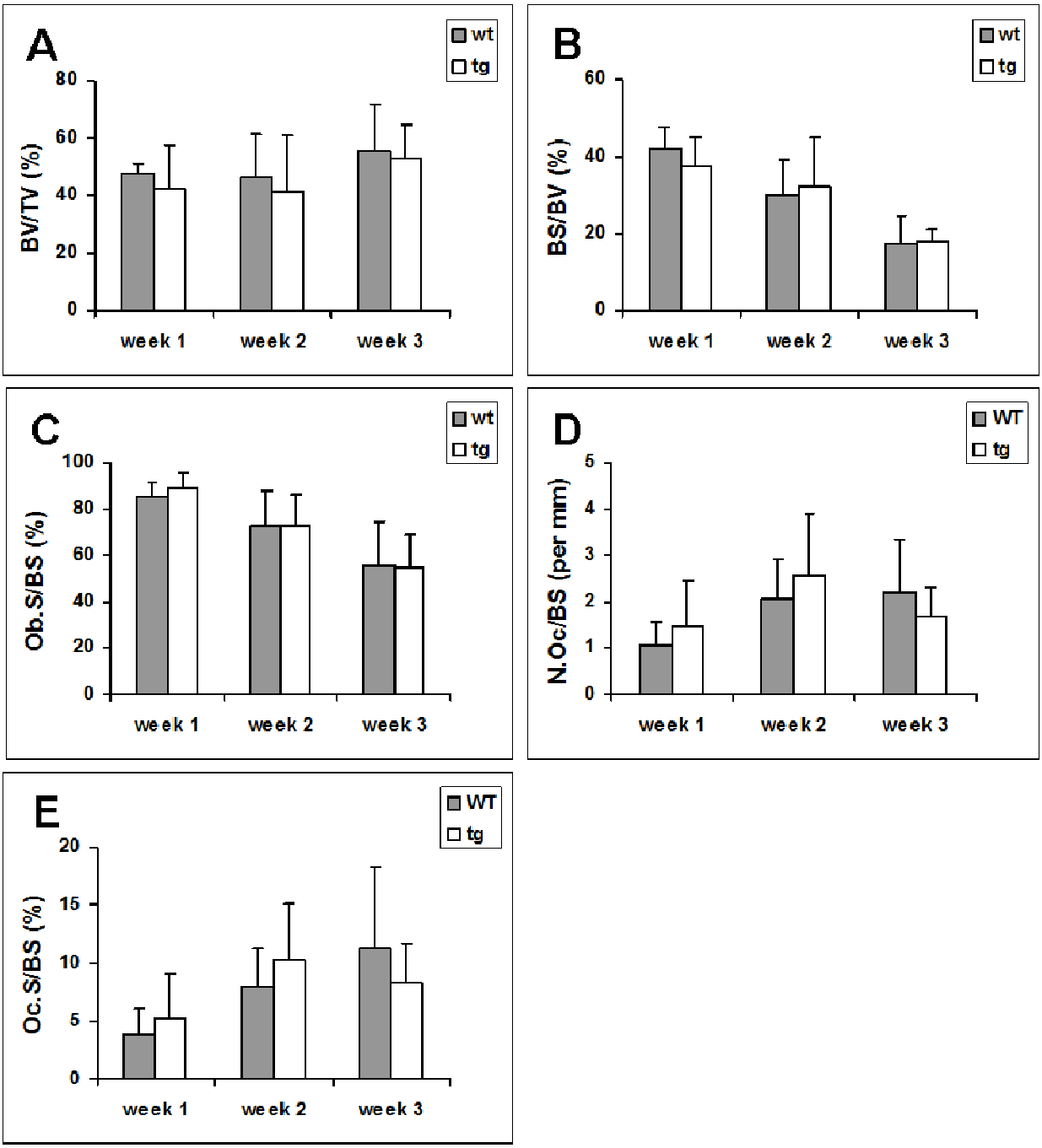

Figure 24: Histomorphometry analysis of H&E and TRAP stained tibia samples (three representative levels within the centre of the cortical defect, each approximately 15 micrometers apart, per sample (n=59) at 1, 2 and 3 weeks post fracture.

No difference between WT and tg animals was observed in A) % bone volume (BV/TV), B) % bone surface (BS/BV), C) % osteoblast surface (Ob.S/BS), D) number of osteoclasts/mm (N.Oc/BS) and E) % of osteoclast surface (Oc.S/BS) ($p>0.05$). Shown are means ± SEM. WT-wild-type, tg-transgenic.

Two-way ANOVA showed no interaction between time-point and genotype for any of the analysed parameters (Table 2). In addition, no interaction was found for time-point and genotype with body weight as a covariate using ANCOVA analysis.

		2-way ANOVA Interaction time-point x genotype	**2- way ANCOVA Interaction time-point x genotype (correction for body weight)**
Micro-CT			
- ROI defect	BV/TV (%)	0.367	0.386
	Mean density	0.880	0.910
- ROI sphere	BV/TV (%)	0.465	0.491
	Mean density	0.792	0.759
Histology			
	BV/TV (%)	0.777	0.666
	BS/BV (%)	0.547	0.670
	Ob.S/BS (%)	0.874	0.866
	N.Oc/BS (/mm)	0.201	0.238
	Oc.S/BS (%)	0.149	0.174

Table 2: Two-way ANOVA analysis for time-point x genotype interaction and its correction by body weight using two-way ANCOVA analysis. Shown are p-values with $p<0.05$ considered statistically significant.

4.4.3 Second-harmonic Imaging Microscopy

Second-harmonic imaging microscopy demonstrated the orientation and organization of collagen fibrils of newly formed defect calluses of respective WT and Col2.3-11ßHSD2 tg animals at week 1 post fracture. An impression of the entire fracture site was achieved by overlapping scans (Figure 25A). SHG images (Figure 25C) of the bony repair site were then combined with TPEF images (Figure 25B) to provide a contrast between the extracellular matrix and cells (Figure 25D). In these images, the golden, bright colour represents the SHG signal arising from the collagen, whilst the green colour represents two-photon excited auto fluorescence from various tissue components including osteoblasts, mesenchymal cells and capillaries filled with erythrocytes (Figure 25D). Essentially no background signals are produced with this method.

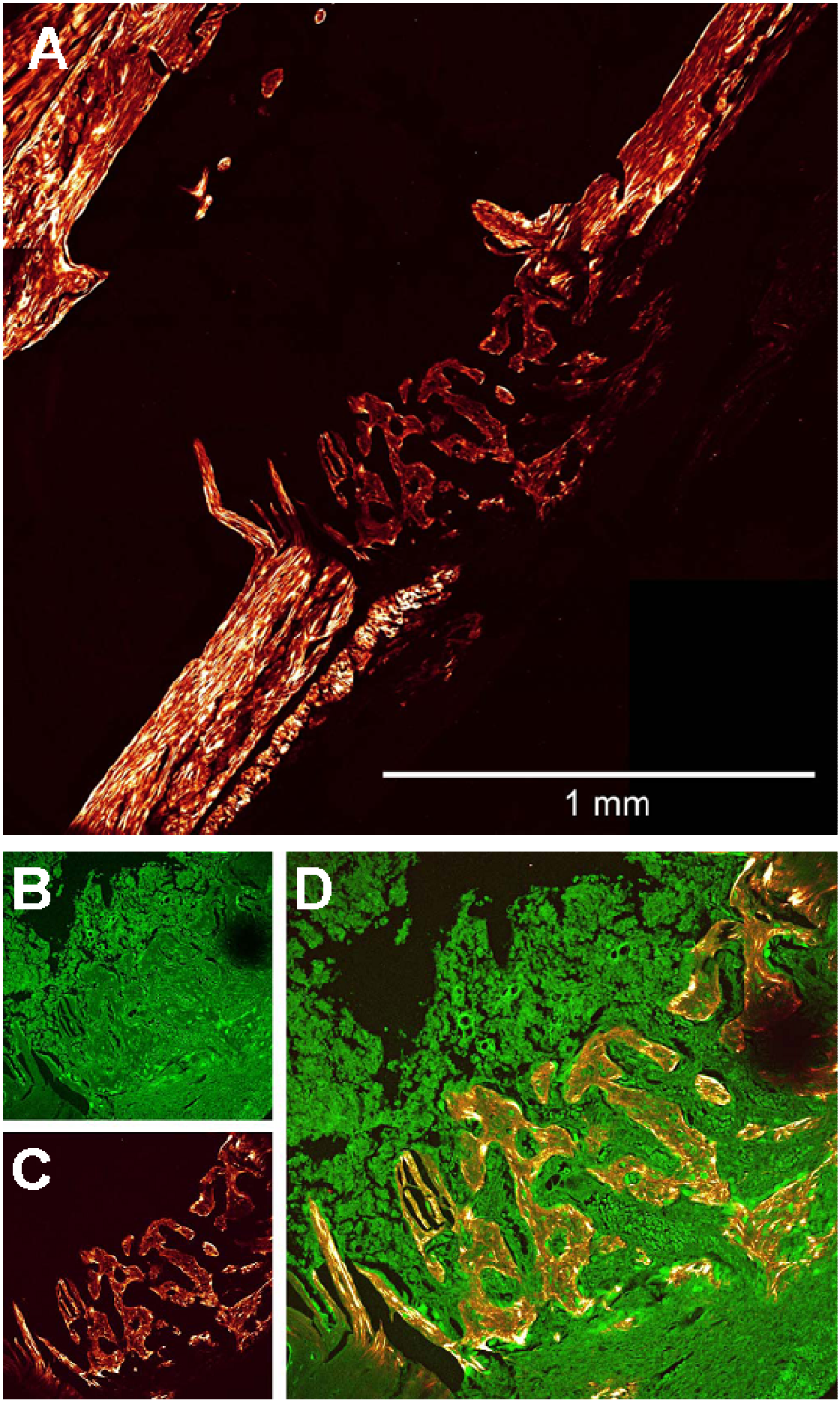
A
1 mm
B
C
D

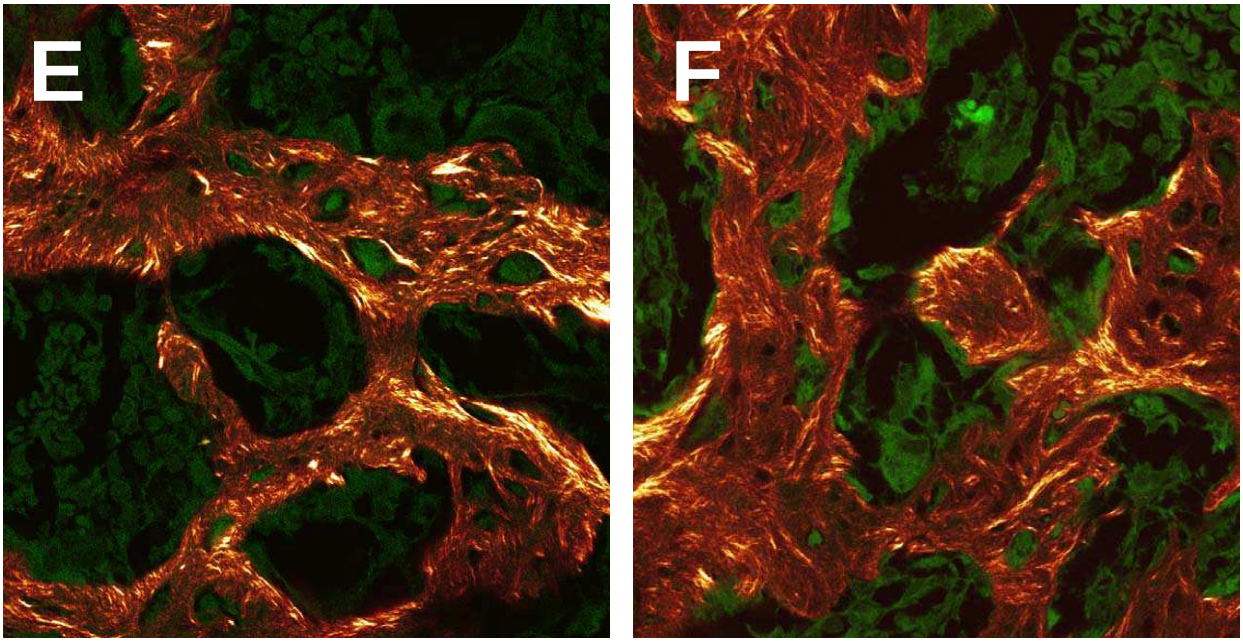

Figure 25: Second-harmonic generation images of defect site at week 1 post fracture.
A) Overview of defect site and surrounding area (picture is composed of eight overlapping scans, using 20x objective); two-photon fluorescence (B) was combined with SHG (C); D) combined SHG and two-photon fluorescence image (20x oil immersion objective);
Comparison of representative WT (E) and tg (F) samples revealed no difference in collagen fibre orientation at defect site (100x oil immersion objective). Golden colour-SHG from collagen, green colour-two-photon fluorescence, WT-wild-type, tg-transgenic.

The morphological comparison of collagen fibre arrangement comprising the woven bone matrix in the regenerating tissue area at a high magnification (x100) revealed no difference between WT and tg mice (Figure 25E, F).

4.4.4 Summary of Analyses of Defect Repair

Taken together, the repair of cortical defects in tibiae of WT and tg mice was similar in terms of structural and histological parameters of bone repair as demonstrated by histology and three-dimensional micro-CT- and SHG imaging and analysis of parameters of bone healing. In particular, the amount of newly formed bone volume and its mean density was similar indicating that disruption of endogenous GC did not effect bone formation and its mineralization process in this repair model.

4.5 Immunohistochemistry

Throughout the repair process, immunohistochemistry confirmed transgene expression of 11ß-HSD2 in osteoblasts and osteocytes of Col2.3-11ßHSD2 tg mice (Figure 26A). Transgene expression was not detected in WT animals (Figure 26B).

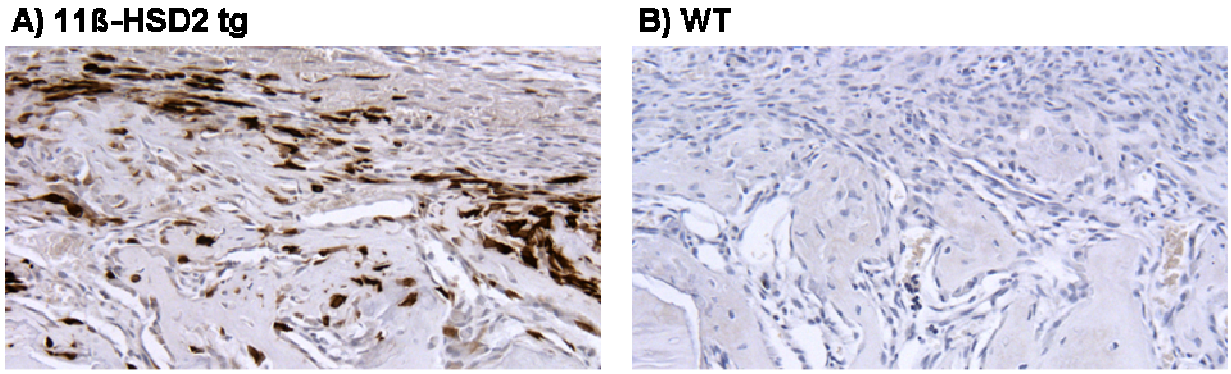

Figure 26: Expression of 11ß-HSD2 at drill-site of tg samples (n=36) (A). Transgene activity was not detected in WT samples (n=34) (B) (Original magnification x200); WT-wild-type, tg-transgenic.

5 Discussion

5.1 Discussion of Methods

The Col2.3-11ßHSD2 tg mouse model is characterised by complete disruption of GC signalling in mature osteoblasts and osteocytes. This cell-targeted pre-receptor disconnect allows to investigate the physiological role of endogenous GC specifically in osteoblast differentiation and function during fracture repair. As the sequence of fracture repair is well documented, studying fracture healing in mice allows for the identification of specific temporal stages when delayed under certain experimental conditions.

In the present study, an intramembranous cortical defect ("fracture") healing model was chosen, since bone formation and remodelling occurs without an endochondral intermediate and thus, effects can be determined in a short time frame. In addition, both the level of communication between mesenchymal stem cells and mature osteoblasts, and the magnitude of effects on osteoblast function are likely to be greater due to accelerated bone metabolism occurring in fracture repair. Hence, cortical defects as a model of intramembranous fracture repair were created in the surgically easyly accessible tibiae of Col2.3-11ßHSD tg mice and their WT littermates.

Mice are frequently used as experimental animals in skeletal research and their advantages over larger species include their short gestation period, low-cost, easy handling and the availability of reagents for cellular and molecular analyses. However, this species has limitations as a result of its small size, e.g. the extraction of sufficient RNA material for molecular biological analyses often requires the pooling of samples[230] and biomechanical conditions comparable to those of humans are not existent. In recent years, the comprehensive understanding of the mouse genome compared to other species and its amenability allowed for the introduction of a great number of genetically engineered tg mouse models to investigate pathological skeletal conditions and the role of specific proteins.[231] Corresponding to other animal species, also the mouse has demonstrated gender-specific differences including their skeletal size with a larger bone size in males.[207, 232] Consequently, in the present study only male mice were used to avoid these effects.

The tibia cortical defect repair model requires a technically relatively simple operating procedure, which was well-tolerated by all animals as indicated by the lack of pain-related

behaviour throughout the post-operative monitoring period. Moreover, defects were created in a reproducible manner.

Several studies have employed cortical defect models of differing sizes at different skeletal locations as experimental models of intramembranous bone repair in a variety of species including rats, chicken, rabbits, dogs, sheep and mice.[233-251] In particular, mice studies involving the creation of cortical defects in the tibia similarly observed advantages as seen in the present study such as reduced pain, lack of infections[239], reproducibility of defects and unproblematic toleration of the procedure by the animals.[238] However, these studies differ in details of experimental design, including the strain of mice used, the size of the defect produced and the duration of the monitoring period.

Providing a stable mechanical environment, bone repair in the present cortical bone drill-hole model occurred via intramembranous bone formation and permitted its characterization and analysis by standard techniques including histology and non-invasive micro-CT. Moreover, the progression of fracture repair over time followed the usual sequence and was comparable to similar tibial and femoral cortical drill-hole models in mice. These studies likewise demonstrated the early deposition of woven bone around week 1 and a well advanced repair process with active bone remodelling by week 3 in control groups.[238-240, 248] In addition, cartilage formation was strictly limited to the outer bone surface adjacent to the defect site consistent with a periosteal reaction that has been reported by several other investigators.[230, 238, 239] This chondrogenic response is proposed to result from an altered mechanical strain environment at the injury site.[230]

In contrast to the tibia defect model, others established osteotomy models to study intramembranous bone formation in the murine species.[252, 253] For example, Thompson et al. created closed tibial fractures by three-point bending in mice and rigidly stabilized the fracture segments with an external fixation device. However, in this type of stabilization micro-motion may occur which is proposed to induce bone formation.[252] Aronson et al. employed a model of distraction osteogenesis which involved the attachment of an external ring fixator to the tibiae of rats. Following the generation of transverse fractures tibial lengthening was ensured by a daily distraction rate of 0.5-2.0 mm. Even though fracture repair occurred predominantly via intramembranous bone formation in this alternative model, the production of cartilage islands making up to 3-5% of the intercortical gap was noted.[253]

Taken together, the tibial defect repair model applied in the Col2.3-11ßHSD2 tg mouse provides a unique and highly informative methodological combination that allows for the study of the effects of endogenous GC on intramembranous bone healing over a short period of time.

5.2 Discussion of Results

The analysis of the repair callus by histomorphometry, micro-CT and SHIM revealed no difference between tg animals and their WT littermates in regards to their cellular and structural characteristics of bone healing. These results suggest that endogenous GC signalling does not affect intramembranous fracture repair in this model and mouse strain. This is somewhat unexpected as previous *in vivo* studies employing the same Col2.3-11ßHSD2 tg mouse model demonstrated that endogenous GC are required for osteoblast differentiation and function in intramembranous and endochondral bone.

Sher et al. initially characterized the endochondral bone phenotype of mature, 7- and 24-week-old female and male Col2.3-11ßHSD2 tg mice by micro-CT and histology. While female mice exhibited vertebral trabecular osteopenia with an increased osteoid surface as an indicator of impaired mineralization, no changes were seen in trabecular bone volume in femurs of respective female tg mice or in the femurs and vertebrae of male tg mice when compared to WT littermates. Thus, these observations suggested that endogenous GC signalling is required for normal trabecular bone mass maintenance and architecture in mature mice with an effect depending on skeletal site and possibly gender.[184] Northern blot analysis revealed no statistically significant difference in transgene expression between sexes or among skeletal sites between tg and WT animals. A subsequent study by Sher et al. additionally demonstrated the role of endogenous GC in cortical bone mass acquisition as indicated by a lower femoral cortical bone area and thickness in 7-week-old tg mice than in their WT littermates. By contrast to the initial study, this effect was independent of gender as both male and female mice were affected.[206]

Also, a recent study by Kalak et al. demonstrated the requirement of endogenous GC signalling to maintain normal bone structure and strength. 7-week-old sexually mature tg mice had lower trabecular and cortical tibial bone volume and consequently a reduced mechanical bone strength and stiffness than WT littermates as assessed by micro-CT and mechanical testing. These transgene-induced changes were also seen in the tibiae of skeletally immature 3-week-old mice. However, in vertebrae, significant differences in trabecular bone volume parameters between WT and tg, mature and immature mice were restricted to the mature animals. This might indicate that the effects of the transgene in vertebrae may be modulated by changes in circulating sex hormone levels and/or age. In this study, no effect of gender was seen for any of the analysed parameters.[207]

Taken together, these previous studies employing the Col2.3-11ßHSD2 tg mouse model clearly indicate an effect of endogenous GC on osteoblast differentiation and function in

endochondral bone, modulated by factors including skeletal site and sexual maturity, but not gender.

In vivo effects of GC on endochondral bone were also studied by O'Brien and co-workers who introduced a similar tg mouse model in which 11ßHSD2 overexpression was driven by a 1.3 kb murine osteoblast- and osteocyte-specific osteocalcin gene 2 promoter (OG2) fragment to produce OG2-11ßHSD2 tg mice in a C57BL/6 background. Interestingly, by contrast to Col2.3-11ßHSD2 tg mice, OG2-11ßHSD2 tg mice displayed a normal bone development and turnover when compared to WT littermates. However, OG2-11ßHSD2 tg mice were protected from excess GC-induced osteoblast and osteocytes apoptosis.[254] These differences in findings between the two tg mouse models might be explained by their different genetic background and/or by the level of transgene expression which has been shown to be stronger in Col2.3-11ßHSD2 tg mice. However, in light of the fact that the osteocalcin promoter is expressed at a later stage than the collagen type Ia1 promoter when osteoblasts and osteocytes are fully differentiated, the results from the two mice models might indicate that osteoblast differentiation requires endogenous GC at an earlier stage, in a specific time-window.

The effect of endogenous GC signalling at a skeletal site of intramembranous bone has also been demonstrated previously. *In vitro*, primary calvarial cell cultures generated from 1-day old Col2.3-11ßHSD2 tg mice and their WT littermates clearly indicate that GC direct lineage commitment and differentiation of mesenchymal progenitor cells via a canonical Wnt signalling pathway originating in mature osteoblasts.[6] Furthermore, *in vivo* experiments demonstrate that endogenous GC signalling in osteoblasts is essential during early intramembranous skeletal development of calvarial bones in mice. Thus, newborn Col2.3-11ßHDSD2 tg mice exhibit a distinct calvarial phenotype, which includes delayed calvarial bone formation and reduced calvarial thickness.[7] It is generally accepted that fracture healing reflects the same formation patterns as in bone development, demonstrating the same array of structural proteins and various regulators of differentiation, chemotaxis and mitosis. However, the specific mechanism of bone repair is also determined by the biomechanical environment provided by the fracture site. In addition, fracture repair occurs in a compressed time frame at a precise location.[102]

The Col2.3-11ßHSD2 tg mouse model and its construct have been well characterized in previous studies. Osteoblastic ROS 17/2.8 cells transfected with the Col2.3-HSD2 construct demonstrated reduced GC-dependent induction of a mouse mammary tumor virus (MMTV) promoter-reporter construct, regulation of cell growth and expression of osteoblastic messenger RNA markers.[183] Enzymatic activity of the 11ßHSD2 transgene was additionally confirmed by

measuring the conversion of (^{3}H) corticosterone to (^{3}H) 11-dehydrocorticosterone in ROS 17/2.8 cells and primary calvarial cell cultures by thin layer chromatography (TLC). Moreover, tg calvariae showed lower collagen synthesis rates when compared to their WT littermates and were protected from 300 nM hydrocortisone-induced impairment of collagen synthesis.[184]

Immunohistochemical analyses performed in previous studies demonstrate that tg protein expression is specifically localized to osteoblasts and osteocytes of cortical and trabecular bone (long bone, vertebrae, calvariae) in tg animals. Transgene expression was not found in tissues of WT mice or in non-skeletal tissues (brain, lung, liver, kidney, skin) of tg mice.[184] In the tibia cortical defect model described here, immunohistochemistry confirmed the expression of 11ßHSD2 transgene in osteoblasts and osteocytes in the repairing bone defect site. Transgene activity was not detected in WT animals. Therefore, in the present study, 11ßHSD2 overexpression likely disrupted endogenous GC signalling during the cortical bone repair in tg mice.

A specific characteristic of the Col2.3-11ßHSD2 tg mice seems to be their lower body weight when compared to WT littermates which has also been demonstrated by previous studies employing the Col2.3-11ßHSD2 tg mouse model.[184, 207] At present, it is unclear whether the lower body weight results from a lower bone mass only or is also due to a lower muscle, water and fat content of the animals. A reduction of bone formation might lead to smaller bones leading to a smaller body in total with a lower body weight. However, as osteoblasts make up a small proportion of the total body mass, the question remains whether these cells might produce such an effect. Nevertheless, the difference in body weight between tg and WT mice did not affect intramembranous fracture repair in the present study as assessed by 2-way ANOVA and ANCOVA analysis although in some cases the low number of animals employed may have impacted on the analysis.

The observations of the present work raise a number of possibilities in regards to the underlying physiological mechanisms. Thus, endogenous GC signalling in mature osteoblasts may not possess a non-redundant role in intramembranous bone repair, and their function in regards to new bone formation or bone repair may be shared by other signalling molecules or pathways.

During the intramembranous bone repair, osteoblasts differentiate directly from mesenchymal cells, whereas endochondral bone repair involves a cartilage intermediate. However, since this intramembranous bone was created in an endochondral bone environment,

the process of intramembranous bone formation may differ from that occurring in the calvaria. Further studies are required to investigate whether GC affect intramembranous bone repair in an intramembranous environment, e.g. the calvariae.

As with all tg mouse models, there is the possibility that adaptation to the impaired GC signalling in mature osteoblasts and osteocytes occurred in the adult tissue. However, as intramembranous fracture healing is initiated by mesenchymal stem cells recruited and completing differentiated into osteoblasts over a very short (2 weeks) time frame, the observations are unlikely to be related to adaptation.

Finally, as defect healing in both animal groups was complete at 3 weeks post fracture, it is possible that a defect of only 0.8 mm in diameter was too small to produce detectable defects in a short time frame. Even though a number of studies have employed cortical drill-hole defect models in mice involving different defect diameters, these studies do not allow direct conclusions to be drawn regarding the ideal defect size for this tg mouse model, since fracture healing is known to depend on a number of factors including the age of animals, their strain and the fracture site.[255] Thus, only future experiments involving the generation of larger defects to produce tougher conditions would provide further insight.

Other future approaches might include the utilization of different closed and open fracture healing models of long bones for WT and Col2.3-11ßHSD2 tg mice which would also make it possible to study the role of endogenous GC in endochondral fracture repair. A well-established closed fracture model by Manigrasso and O`Connor involves the insertion of a stainless steel wire into the intramedullary canal and the subsequent creation of standardized diaphyseal fractures by a 3-point bending device.[256] This model might be further modified. For example, post fracture, the intramedullary wire might be used as a guide wire to insert an intramedullary locking nail to achieve rotational stability.[257] Alternatively, the insertion of an intramedullary compression screw would additionally provide axial stability.[258] While these closed fracture models are generally associated with minor soft tissue damage, open fracture models are known to lead to a major soft tissue trauma with a preserved endosteum and bone marrow.[259] Using a lateral approach, the open surgical procedure generally involves the splitting of the entire lateral muscle layer and the creation of a midshaft osteotomy of the exposed bone. Stable fracture fixation might be then achieved by the application of an external fixator, a locking plate or a pin-clip device as described by several authors.[260-264] These osteosynthesis techniques might also be used to stabilize bone segmental defects or to compare fracture repair in a model of rigid versus loose fracture fixation. The introduction of a bone lengthening model,

e.g. by utilizing an external ring fixator, would make it possible to assess intramembranous and endochondral ossification simultaneously.

Other future approaches might include the modification of the tg mouse model. For example, a different promoter might be used to drive the expression of the HSD2 transgene at a different time of the osteoblastic lineage. In addition, different genetic loss-of-function mouse models abrogating endogenous GC signalling in osteoblastic cells might be generated, e.g. by the conditional disruption of the GR gene (Grl1) via Cre/loxP technology to avoid effects of global transgene expression including perinatal lethality as seen in GR knockout mice.

In conclusion, the present work demonstrated that endogenous GC signalling in mature osteoblasts is not essential for fracture healing in this model of defect repair. However, this study provided a valuable basis for future experiments to gain insight into mechanisms governing osteoblast differentiation and function during fracture healing.

6 Summary

Mechanisms by which GC exert their effects on bone cells, particularly in the fracture healing process, are poorly understood. While GC at pharmacological doses have been shown to interfere with fracture repair, the role of endogenous GC in bone repair is poorly understood.

Thus, the aim of the present study was to examine whether endogenous GC affect bone healing in an *in vivo* model of cortical defect repair.

A well-established tg mouse model was employed in which intracellular GC signalling was abrogated exclusively in mature osteoblasts and osteocytes through tg overexpression of 11ß-hydroxysteroid-dehydrogenase type 2 (11ßHSD2) under the control of a collagen type Ia1 promoter (Col2.3-11ßHSD2). Unicortical bone defects (Ø 0.8 mm) were created in 7-week-old tg mice (n=36) and their WT littermates (n=34) using a drill on the anteromedial aspect of the left tibia. Fracture repair was assessed by histomorphometry, immunohistochemistry, second-harmonic imaging microscopy (SHIM) and microcomputed tomography (micro-CT) analysis at one, two and three weeks after defect initiation.

Micro-CT images demonstrated the progression of fracture repair. At week 1 post-surgery, mineralized, intramembranous bone was present which increased in volume and density throughout week 2. At week 3, healing of the defect was nearly complete with the fracture site no longer distinguishable from the surrounding cortical bone. Micro-CT analyses comparing WT and tg animals revealed similar amounts of newly formed bone (BV/TV) with comparable mean densities for the analyzable time-points at week 1 and 2 post fracture ($p>0.05$). Moreover, histomorphometric analyses performed for all time-points demonstrated similar newly formed bone volume (BV/TV) in WT and tg animals ($p>0.05$). Accordingly, no statistical differences where found between the two groups of mice for the proportion of bone surface covered by osteoblasts (Ob.S/BS), osteoclast surfaces (Oc.S/BS) and osteoclast numbers (N.Oc/BS) at any post-surgical time-point. Moreover, second-harmonic imaging microscopy for week 1 samples demonstrated a similar orientation and organization of collagen fibrils of newly formed bone between WT and tg animals. The activity of the transgene at the defect site of Col2.3-11ßHSD2 tg animals was confirmed by immunohistochemistry.

Altogether these results suggest that disruption of endogenous GC signalling in mature osteoblasts and osteocytes does not affect intramembranous fracture healing in a tibia defect repair model. However, previous studies employing the same Col2.3-11ßHSD2 tg mouse model clearly indicated a role of endogenous GC signalling in osteoblast differentiation and function in bone. In particular, endogenous GC signalling might be required for bone mass maintenance,

structure and strength of endochondral bone. In intramembranous bone, GC signalling in osteoblasts is essential during early skeletal development of calvariae and directs lineage commitment and differentiation of mesenchymal progenitor cells via a canonical Wnt signalling pathway *in vitro*.

The unexpected observations of the present study raise a number of possibilities in regards to the underlying physiological mechanisms. Firstly, endogenous GC signalling in mature osteoblasts may not posses a non-redundant role in intramembranous bone repair and their function in regards to new bone formation may be shared by other signalling molecules or pathways. In addition, the process of intramembranous bone formation in the present tibia defect repair model may differ from that occurring in the calvariae, as bone healing was induced in an endochondral bone environment. Finally, the well-progressed fracture repair at 3 weeks post-fracture may indicate that the generation of larger defects is necessary to produce an effect.

It remains to be shown whether GC signalling has a role in intramembranous bone healing in an intramembranous environment and in endochondral fracture repair.

7 Zusammenfassung

Es ist bisher noch nicht gelungen, die Mechanismen der Glucocorticoidwirkungen auf Knochenzellen insbesondere während der Frakturheilung vollständig zu erklären. Während Glucocorticoide (GC) in pharmakologischer Dosierung bei der Frakturheilung interferieren, ist die Rolle der endogenen GC in der Knochenheilung nur ungenügend verstanden.

Ziel der vorliegenden Arbeit war es, den Einfluss endogener GC auf die Frakturheilung in einem *in vivo* Modell von kortikaler Defektheilung zu untersuchen.

Für die Durchführung der Experimente wurde ein etabliertes Mausmodell verwendet. Der intrazelluläre GC-Signalweg wurde spezifisch in ausgereiften Osteoblasten und Osteozyten durch transgene Überexpression des 11ß-hydroxysteroid-dehydrogenase type 2 (11ßHSD2) Enzyms unter der Kontrolle des Kollagen Typ Ia1 Promoters (Col2.3-11ßHSD2) blockiert. Kortikale Knochendefekte (Ø 0,8 mm) wurden auf der anteromedialen Seite der Tibiae von sieben Wochen alten männlichen transgenen (n=36) und Wildtyp-Mäusen (n=34) mit Hilfe eines Bohrers generiert. Die Auswertung der Frakturheilung erfolgte nach ein, zwei und drei Wochen der Defektinitiierung durch Histomorphometrie, Immunhistochemie, Second-harmonic imaging Mikroskopie (SHIM) und Mikro-Computertomographie (Mikro-CT) Analyse.

Nach Woche 1 der Frakturheilung zeigte sich mineralisierter, intramembranöser Knochen, welcher an Volumen und Densität bis Woche 2 zunahm. Woche 3 des Heilungsprozesses war durch die fast abgeschlossene Defektheilung gekennzeichnet. Die Mikro-CT-Analyse, welche das Fortschreiten des Frakturheilungsprozesses in Wildtyp- und transgenen Mäusen verglich, zeigte eine gleichartige Menge an neu gebildetem Knochen (BV/TV) mit vergleichbarer durchschnittlicher Densität ($p>0,05$). Darüber hinaus zeigte die histomorphometrische Analyse gleichartiges neu gebildetes Knochenvolumen (BV/TV) in Wildtyp- und transgenen Tieren ($p>0,05$). Es konnte kein statistisch signifikanter Unterschied zwischen dem Anteil der mit Osteoblasten bedeckten Knochenoberfläche (Ob.S/BS), Osteoklastenoberfläche (Oc.S/BS) und Osteoklastenanzahl (N.Oc/BS) festgestellt werden. Auch in der Second-harmonic imaging Mikroskopie für Proben der Woche 1 konnte kein Unterschied in Orientierung und Organisation der Kollagenfibrillen des neu gebildeten Knochens festgestellt werden. Immunhistochemisch wurde die Aktivität des Transgens im Knochendefekt von Col2.3-11ßHSD2 transgenen Tieren bestätigt.

Insgesamt weisen die vorliegenden Ergebnisse daraufhin, dass die Blockade des intrazellulären Signalwegs endogener GC in ausgereiften Osteoblasten und Osteozyten die intramembranöse Frakturheilung in einem Tibia-Defekt-Reparaturmodell nicht beeinflusst.

Vorausgehende Studien, welche dasselbe Col2.3-11ßHSD2 transgene Mausmodell verwendeten, zeigten hingegen, dass endogene GC in Osteoblastendifferenzierung und Funktion des Knochens von Bedeutung sein könnten. Insbesondere könnten endogene GC zur Aufrechterhaltung der Knochenmasse, Struktur und Festigkeit in endochondralem Knochen erforderlich sein. In intramembranösem Knochen sind endogene GC während der frühen Skelettentwicklung von Calvaria essentiell und bewirken *in vitro* die Zelldifferenzierung mesenchymaler Vorläuferzellen durch den kanonischen Wnt-Signalweg.

Diese unerwarteten Beobachtungen der vorliegenden Studie eröffnen eine Vielzahl von Möglichkeiten in Bezug auf die zugrundeliegenden pathophysiologischen Mechanismen. So könnte der Signalweg endogener GC in ausgereiften Osteoblasten über eine redundante Funktion in der intramembranösen Knochenheilung verfügen. Diese Funktion könnte wiederum zusammen mit anderen Signalmolekülen oder Signalwegen erfolgen. Des Weiteren könnte der Prozess der intramembranösen Knochenbildung im vorliegenden Tibia-Defekt-Reparaturmodell von dem in der Calvaria vorkommenden differieren, da die Knochenheilung in einer endochondralen Umgebung erzeugt wurde. Letztendlich könnte die schon nach drei Wochen rasch fortgeschrittene Frakturreparatur indizieren, dass die Generierung von größeren Defekten notwendig wäre um einen Effekt herbeizuführen.

Es bleibt zu zeigen, ob endogene GC eine Rolle in intramembranöser Knochenheilung in einer intramembranösen Umgebung oder in endochondraler Frakturheilung spielen.

8 References

1. Canalis E, Mazziotti G, Giustina A, Bilezikian JP. Glucocorticoid-induced osteoporosis: pathophysiology and therapy. Osteoporos Int 2007;18(10):1319-28.
2. Aspenberg P. Drugs and fracture repair. Acta Orthop 2005;76(6):741-8.
3. Eijken M, Koedam M, van Driel M, Buurman CJ, Pols HA, van Leeuwen JP. The essential role of glucocorticoids for proper human osteoblast differentiation and matrix mineralization. Mol Cell Endocrinol 2006;248(1-2):87-93.
4. Bellows CG, Aubin JE, Heersche JN. Physiological concentrations of glucocorticoids stimulate formation of bone nodules from isolated rat calvaria cells in vitro. Endocrinology 1987;121(6):1985-92.
5. Cheng SL, Yang JW, Rifas L, Zhang SF, Avioli LV. Differentiation of human bone marrow osteogenic stromal cells in vitro: induction of the osteoblast phenotype by dexamethasone. Endocrinology 1994;134(1):277-86.
6. Zhou H, Mak W, Zheng Y, Dunstan CR, Seibel MJ. Osteoblasts directly control lineage commitment of mesenchymal progenitor cells through Wnt signaling. J Biol Chem 2008;283(4):1936-45.
7. Zhou H, Mak W, Kalak R, et al. Glucocorticoid-dependent Wnt signaling by mature osteoblasts is a key regulator of cranial skeletal development in mice. Development (Cambridge, England) 2009;136(3):427-36.
8. Einhorn TA. The cell and molecular biology of fracture healing. Clin Orthop Relat Res 1998;(355 Suppl):S7-21.
9. Axelrad TW, Kakar S, Einhorn TA. New technologies for the enhancement of skeletal repair. Injury 2007;38 Suppl 1:S49-62.
10. Boyle WJ, Simonet WS, Lacey DL. Osteoclast differentiation and activation. Nature 2003;423(6937):337-42.
11. Frost HM. Bone dynamics in metabolic bone disease. J Bone Joint Surg Am 1966; 48(6):1192-203.
12. Harada S, Rodan GA. Control of osteoblast function and regulation of bone mass. Nature 2003;423(6937):349-55.
13. Lemaire V, Tobin FL, Greller LD, Cho CR, Suva LJ. Modeling the interactions between osteoblast and osteoclast activities in bone remodeling. J Theor Biol 2004;229(3):293-309.
14. Cohen MM, Jr. The new bone biology: pathologic, molecular, and clinical correlates. Am J Med Genet A 2006;140(23):2646-706.
15. Downey PA, Siegel MI. Bone biology and the clinical implications for osteoporosis. Phys Ther 2006;86(1):77-91.
16. Baron R. Anatomy and ultrastructure of bone. In: Favus MJ, ed. Primer on the Metabolic Bone Diseases and Disorders of Mineral Metabolism. Philadelphia: Lippincott-Raven, 1996:3-10.
17. Kronenberg HM. Developmental regulation of the growth plate. Nature 2003;423(6937): 332-6.
18. Nakashima K, de Crombrugghe B. Transcriptional mechanisms in osteoblast differentiation and bone formation. Trends Genet 2003;19(8):458-66.
19. Wolff J. Das Gesetz der Transformation der Knochen. Berlin: Hirschwald, Germany, 1892.
20. Burger EH, Klein-Nulen J. Responses of bone cells to biomechanical forces in vitro. Adv Dent Res 1999;13:93-8.
21. Seeman E, Delmas PD. Bone quality-the material and structural basis of bone strength and fragility. N Engl J Med 2006;354(21):2250-61.

22. Webster SJ. The skeletal tissues. In: Weiss L, ed. Histology, cell and tissue biology. New York: Elsevier Biomedical, 1983.
23. Seeman E. Bone quality: the material and structural basis of bone strength. J Bone Miner Met 2008;26(1):1-8.
24. Teitelbaum SL. Bone resorption by osteoclasts. Science 2000;289(5484):1504-8.
25. Kassem M, Abdallah BM, Saeed H. Osteoblastic cells: differentiation and trans-differentiation. Arch Biochem Biophys 2008;473(2):183-7.
26. Scheven BA, Visser JW, Nijweide PJ. In vitro osteoclast generation from different bone marrow fractions, including a highly enriched haematopoietic stem cell population. Nature 1986;321(6065):79-81.
27. Fujikawa Y, Quinn JM, Sabokbar A, McGee JO, Athanasou NA. The human osteoclast precursor circulates in the monocyte fraction. Endocrinology 1996;137(9):4058-60.
28. Mostov K, Werb Z. Journey across the osteoclast. Science 1997;276(5310):219-20.
29. Vaananen HK, Zhao H, Mulari M, Halleen JM. The cell biology of osteoclast function. J Cell Sci 2000;113 (Pt 3):377-81.
30. Baron R, Neff L, Louvard D, Courtoy PJ. Cell-mediated extracellular acidification and bone resorption: evidence for a low pH in resorbing lacunae and localization of a 100-kD lysosomal membrane protein at the osteoclast ruffled border. J Cell Biol 1985;101(6):2210-22.
31. Ducy P, Schinke T, Karsenty G. The osteoblast: a sophisticated fibroblast under central surveillance. Science 2000;289(5484):1501-4.
32. Aubin JE, Triffitt JT. Mesenchymal stem cells and osteoblast differentiation. In: Bilezikian JP, Raisz LG, Rodan GA, eds. Principles of Bone Biology. San Diego, CA: Academic Press, 2002.
33. Marks SC, Hermey DC. The structure and development of bone. In: Bilezikian JP, Raisz LG, Rodan GA, eds. Principles of Bone Biology. San Diego, CA: Academic Press, 1996:3-14.
34. Cheng B, Zhao S, Luo J, Sprague E, Bonewald LF, Jiang JX. Expression of functional gap junctions and regulation by fluid flow in osteocyte-like MLO-Y4 cells. J Bone Miner Res 2001;16(2):249-59.
35. Frost HM. The Bone Dynamics in Osteoporosis and Osteomalacia. Springfield, IL: Thomas 1966.
36. Frost HM. Tetracycline-based histological analysis of bone remodeling. Calcif Tissue Res 1969;3(3):211-37.
37. Jilka RL. Biology of the basic multicellular unit and the pathophysiology of osteoporosis. Med Pediatr Oncol 2003;41(3):182-5.
38. Parfitt AM. Targeted and nontargeted bone remodeling: relationship to basic multicellular unit origination and progression. Bone 2002;30(1):5-7.
39. Hazenberg JG, Freeley M, Foran E, Lee TC, Taylor D. Microdamage: a cell transducing mechanism based on ruptured osteocyte processes. J Biomech 2006;39(11):2096-103.
40. Martin TJ, Seeman E. Bone remodelling: its local regulation and the emergence of bone fragility. Best Pract Res Clin Endocrinol Metab 2008;22(5):701-22.
41. Canalis E, Giustina A, Bilezikian JP. Mechanisms of anabolic therapies for osteoporosis. N Engl J Med 2007;357(9):905-16.
42. Troen BR. Molecular mechanisms underlying osteoclast formation and activation. Exp Gerontol 2003;38(6):605-14.
43. Lips P. Vitamin D physiology. Prog Biophys Mol Biol 2006;92(1):4-8.
44. Eisman JA. Osteomalacia. Bailliere's Clin Endocrinol Metab 1988;2(1):125-55.
45. Manolagas SC, Kousteni S, Jilka RL. Sex steroids and bone. Recent Prog Horm Res 2002;57:385-409.

46. Weitzmann MN, Pacifici R. Estrogen deficiency and bone loss: an inflammatory tale. J Clin Invest 2006;116(5):1186-94.
47. Riggs BL, Khosla S, Melton LJ, 3rd. A unitary model for involutional osteoporosis: estrogen deficiency causes both type I and type II osteoporosis in postmenopausal women and contributes to bone loss in aging men. J Bone Miner Res 1998;13(5):763-73.
48. Albright F, Smith PH, Richardson AM. Postmenopausal osteoporosis. JAMA 1941(116): 2465-74.
49. Ducy P, Amling M, Takeda S, et al. Leptin inhibits bone formation through a hypothalamic relay: a central control of bone mass. Cell 2000;100(2):197-207.
50. Yadav VK, Oury F, Suda N, et al. A serotonin-dependent mechanism explains the leptin regulation of bone mass, appetite, and energy expenditure. Cell 2009;138(5):976-89.
51. Yadav VK, Ryu JH, Suda N, et al. Lrp5 controls bone formation by inhibiting serotonin synthesis in the duodenum. Cell 2008;135(5):825-37.
52. Yadav VK, Balaji S, Suresh PS, et al. Pharmacological inhibition of gut-derived serotonin synthesis is a potential bone anabolic treatment for osteoporosis. Nat Med;16(3):308-12.
53. Baldock PA, Sainsbury A, Couzens M, et al. Hypothalamic Y2 receptors regulate bone formation. J Clin Invest 2002;109(7):915-21.
54. Elefteriou F, Ahn JD, Takeda S, et al. Leptin regulation of bone resorption by the sympathetic nervous system and CART. Nature 2005;434(7032):514-20.
55. Sato S, Hanada R, Kimura A, et al. Central control of bone remodeling by neuromedin U. Nat Med 2007;13(10):1234-40.
56. Rodan GA, Martin TJ. Role of osteoblasts in hormonal control of bone resorption-a hypothesis. Calcif Tissue Int 1981;33(4):349-51.
57. Lacey DL, Timms E, Tan HL, et al. Osteoprotegerin ligand is a cytokine that regulates osteoclast differentiation and activation. Cell 1998;93(2):165-76.
58. Kodama H, Nose M, Niida S, Yamasaki A. Essential role of macrophage colony-stimulating factor in the osteoclast differentiation supported by stromal cells. J Exp Med 1991;173(5):1291-4.
59. Quinn JM, Elliott J, Gillespie MT, Martin TJ. A combination of osteoclast differentiation factor and macrophage-colony stimulating factor is sufficient for both human and mouse osteoclast formation in vitro. Endocrinology 1998;139(10):4424-7.
60. Ross FP, Christiano AM. Nothing but skin and bone. J Clin Invest 2006;116(5):1140-9.
61. Pixley FJ, Stanley ER. CSF-1 regulation of the wandering macrophage: complexity in action. Trends Cell Biol 2004;14(11):628-38.
62. Yoshida H, Hayashi S, Kunisada T, et al. The murine mutation osteopetrosis is in the coding region of the macrophage colony stimulating factor gene. Nature 1990;345(6274): 442-4.
63. Hsu H, Lacey DL, Dunstan CR, et al. Tumor necrosis factor receptor family member RANK mediates osteoclast differentiation and activation induced by osteoprotegerin ligand. Proc Natl Acad Sci USA 1999;96(7):3540-5.
64. Simonet WS, Lacey DL, Dunstan CR, et al. Osteoprotegerin: a novel secreted protein involved in the regulation of bone density. Cell 1997;89(2):309-19.
65. Zaidi M. Skeletal remodeling in health and disease. Nat Med 2007;13(7):791-801.
66. Luk JM, Wang PP, Lee CK, Wang JH, Fan ST. Hepatic potential of bone marrow stromal cells: development of in vitro co-culture and intra-portal transplantation models. J Immunol Methods 2005;305(1):39-47.
67. Dezawa M, Kanno H, Hoshino M, et al. Specific induction of neuronal cells from bone marrow stromal cells and application for autologous transplantation. J Clin Invest 2004; 113(12):1701-10.

68. Nuttall ME, Patton AJ, Olivera DL, Nadeau DP, Gowen M. Human trabecular bone cells are able to express both osteoblastic and adipocytic phenotype: implications for osteopenic disorders. J Bone Miner Res 1998;13(3):371-82.
69. Justesen J, Pedersen SB, Stenderup K, Kassem M. Subcutaneous adipocytes can differentiate into bone-forming cells in vitro and in vivo. Tissue Eng 2004;10(3-4):381-91.
70. Beresford JN, Bennett JH, Devlin C, Leboy PS, Owen ME. Evidence for an inverse relationship between the differentiation of adipocytic and osteogenic cells in rat marrow stromal cell cultures. J Cell Sci 1992;102 (Pt 2):341-51.
71. Bellows CG, Heersche JN. The frequency of common progenitors for adipocytes and osteoblasts and of committed and restricted adipocyte and osteoblast progenitors in fetal rat calvaria cell populations. J Bone Miner Res 2001;16(11):1983-93.
72. Meunier P, Aaron J, Edouard C, Vignon G. Osteoporosis and the replacement of cell populations of the marrow by adipose tissue. A quantitative study of 84 iliac bone biopsies. Clin Orthop Relat Res 1971;80:147-54.
73. Burkhardt R, Kettner G, Bohm W, et al. Changes in trabecular bone, hematopoiesis and bone marrow vessels in aplastic anemia, primary osteoporosis, and old age: a comparative histomorphometric study. Bone 1987;8(3):157-64.
74. Justesen J, Stenderup K, Ebbesen EN, Mosekilde L, Steiniche T, Kassem M. Adipocyte tissue volume in bone marrow is increased with aging and in patients with osteoporosis. Biogerontology 2001;2(3):165-71.
75. Verma S, Rajaratnam JH, Denton J, Hoyland JA, Byers RJ. Adipocytic proportion of bone marrow is inversely related to bone formation in osteoporosis. J Clin Pathol 2002;55(9): 693-8.
76. Wang GJ, Sweet DE, Reger SI, Thompson RC. Fat-cell changes as a mechanism of avascular necrosis of the femoral head in cortisone-treated rabbits. J Bone Joint Surg Am 1977;59(6):729-35.
77. Hong JH, Hwang ES, McManus MT, et al. TAZ, a transcriptional modulator of mesenchymal stem cell differentiation. Science 2005;309(5737):1074-8.
78. Marie PJ. Transcription factors controlling osteoblastogenesis. Arch Biochem Biophys 2008;473(2):98-105.
79. Maes C, Kobayashi T, Kronenberg HM. A novel transgenic mouse model to study the osteoblast lineage in vivo. Ann NY Acad Sci 2007;1116:149-64.
80. Komori T, Yagi H, Nomura S, et al. Targeted disruption of Cbfa1 results in a complete lack of bone formation owing to maturational arrest of osteoblasts. Cell 1997;89(5):755-64.
81. Otto F, Thornell AP, Crompton T, et al. Cbfa1, a candidate gene for cleidocranial dysplasia syndrome, is essential for osteoblast differentiation and bone development. Cell 1997; 89(5):765-71.
82. Nakashima K, Zhou X, Kunkel G, et al. The novel zinc finger-containing transcription factor osterix is required for osteoblast differentiation and bone formation. Cell 2002; 108(1):17-29.
83. Logan CY, Nusse R. The Wnt signaling pathway in development and disease. Annu Rev Cell Dev Biol 2004;20:781-810.
84. Piters E, Boudin E, Van Hul W. Wnt signaling: a win for bone. Arch Biochem Biophys 2008;473(2):112-6.
85. Gaur T, Lengner CJ, Hovhannisyan H, et al. Canonical WNT signaling promotes osteogenesis by directly stimulating Runx2 gene expression. J Biol Chem 2005;280(39): 33132-40.
86. Bodine PV, Komm BS. Wnt signaling and osteoblastogenesis. Rev Endocr Metab Disord 2006;7(1-2):33-9.

87. Rijsewijk F, Schuermann M, Wagenaar E, Parren P, Weigel D, Nusse R. The Drosophila homolog of the mouse mammary oncogene int-1 is identical to the segment polarity gene wingless. Cell 1987;50(4):649-57.
88. Kennell JA, MacDougald OA. Wnt signaling inhibits adipogenesis through beta-catenin-dependent and -independent mechanisms. J Biol Chem 2005;280(25):24004-10.
89. Gong Y, Slee RB, Fukai N, et al. LDL receptor-related protein 5 (LRP5) affects bone accrual and eye development. Cell 2001;107(4):513-23.
90. Bennett CN, Longo KA, Wright WS, et al. Regulation of osteoblastogenesis and bone mass by Wnt10b. Proc Natl Acad Sci USA 2005;102(9):3324-9.
91. Rawadi G, Vayssiere B, Dunn F, Baron R, Roman-Roman S. BMP-2 controls alkaline phosphatase expression and osteoblast mineralization by a Wnt autocrine loop. J Bone Miner Res 2003;18(10):1842-53.
92. Day TF, Guo X, Garrett-Beal L, Yang Y. Wnt/beta-catenin signaling in mesenchymal progenitors controls osteoblast and chondrocyte differentiation during vertebrate skeletogenesis. Dev Cell 2005;8(5):739-50.
93. Bain G, Muller T, Wang X, Papkoff J. Activated beta-catenin induces osteoblast differentiation of C3H10T1/2 cells and participates in BMP2 mediated signal transduction. Biochem Biophys Res Commun 2003;301(1):84-91.
94. Hill TP, Spater D, Taketo MM, Birchmeier W, Hartmann C. Canonical Wnt/beta-catenin signaling prevents osteoblasts from differentiating into chondrocytes. Dev Cell 2005;8(5): 727-38.
95. van der Horst G, van der Werf SM, Farih-Sips H, van Bezooijen RL, Lowik CW, Karperien M. Downregulation of Wnt signaling by increased expression of Dickkopf-1 and -2 is a prerequisite for late-stage osteoblast differentiation of KS483 cells. J Bone Miner Res 2005;20(10):1867-77.
96. de Boer J, Siddappa R, Gaspar C, van Apeldoorn A, Fodde R, van Blitterswijk C. Wnt signaling inhibits osteogenic differentiation of human mesenchymal stem cells. Bone 2004; 34(5):818-26.
97. Yavropoulou MP, Yovos JG. The role of the Wnt signaling pathway in osteoblast commitment and differentiation. Hormones (Athens, Greece) 2007;6(4):279-94.
98. Dimitriou R, Tsiridis E, Giannoudis PV. Current concepts of molecular aspects of bone healing. Injury 2005;36(12):1392-404.
99. Einhorn TA. The science of fracture healing. J Orthop Trauma 2005;19(10 Suppl):S4-6.
100. Wraighte PJ, Scammell BE. Principles of fracture healing. Surgery 2006;24(6):198-207.
101. Webb JCJ. A review of fracture healing. Current Orthopaedics 2000;14:457-63.
102. Shapiro F. Bone development and its relation to fracture repair. The role of mesenchymal osteoblasts and surface osteoblasts. Eur Cell Mater 2008;15:53-76.
103. McKibbin B. The biology of fracture healing in long bones. J Bone Joint Surg Br 1978;60-B(2):150-62.
104. Bolander ME. Regulation of fracture repair by growth factors. Proc Soc Exp Biol Med 1992;200(2):165-70.
105. Orth DN, Kovacs WJ. Williams textbook of endocrinology. In: Foster DW, Kronenberg HM, Larsen PR, eds. 9th ed. Philadelphia: W.B. Saunders, 1998.
106. Harrison JR, Woitge HW, Kream BE. Genetic approaches to determine the role of glucocorticoid signaling in osteoblasts. Endocrine 2002;17(1):37-42.
107. Munck A, Mendel DB, Smith LI, Orti E. Glucocorticoid receptors and actions. Am Rev Respir Dis 1990;141(2 Pt 2):S2-10.
108. Draper N, Stewart PM. 11beta-hydroxysteroid dehydrogenase and the pre-receptor regulation of corticosteroid hormone action. J Endocrinol 2005;186(2):251-71.

109. Stewart PM. Tissue-specific Cushing's syndrome, 11beta-hydroxysteroid dehydrogenases and the redefinition of corticosteroid hormone action. Eur J Endocrinol 2003;149(3):163-8.
110. Rabbitt EH, Gittoes NJ, Stewart PM, Hewison M. 11beta-hydroxysteroid dehydrogenases, cell proliferation and malignancy. J Steroid Biochem Mol Biol 2003;85(2-5):415-21.
111. Vegiopoulos A, Herzig S. Glucocorticoids, metabolism and metabolic diseases. Mol Cell Endocrinol 2007;275(1-2):43-61.
112. McDonough AK, Curtis JR, Saag KG. The epidemiology of glucocorticoid-associated adverse events. Curr Opin Rheumatol 2008;20(2):131-7.
113. Pierotti S, Gandini L, Lenzi A, Isidori AM. Pre-receptorial regulation of steroid hormones in bone cells: insights on glucocorticoid-induced osteoporosis. J Steroid Biochem Mol Biol 2008;108(3-5):292-9.
114. Shaker JL, Lukert BP. Osteoporosis associated with excess glucocorticoids. Endocrinol Metab Clin North Am 2005;34(2):341-56, viii-ix.
115. Pisu M, James N, Sampsel S, Saag KG. The cost of glucocorticoid-associated adverse events in rheumatoid arthritis. Rheumatology (Oxford, England) 2005;44(6):781-8.
116. Schacke H, Docke WD, Asadullah K. Mechanisms involved in the side effects of glucocorticoids. Pharmacol Ther 2002;96(1):23-43.
117. Alesci S, De Martino MU, Ilias I, Gold PW, Chrousos GP. Glucocorticoid-induced osteoporosis: from basic mechanisms to clinical aspects. Neuroimmunomodulation 2005; 12(1):1-19.
118. Van Staa TP, Leufkens HG, Abenhaim L, Zhang B, Cooper C. Use of oral corticosteroids and risk of fractures. J Bone Miner Res 2000;15(6):993-1000.
119. Lukert BP, Raisz LG. Glucocorticoid-induced osteoporosis: pathogenesis and management. Ann Intern Med 1990;112(5):352-64.
120. Weinstein RS. Glucocorticoid-induced osteoporosis. Rev Endocr Metab Disord 2001;2(1): 65-73.
121. Mazziotti G, Angeli A, Bilezikian JP, Canalis E, Giustina A. Glucocorticoid-induced osteoporosis: an update. Trends Endocrinol Metab 2006;17(4):144-9.
122. Dempster DW. Bone histomorphometry in glucocorticoid-induced osteoporosis. J Bone Miner Res 1989;4(2):137-41.
123. Dempster DW, Arlot MA, Meunier PJ. Mean wall thickness and formation periods of trabecular bone packets in corticosteroid-induced osteoporosis. Calcif Tissue Int 1983;35 (4-5):410-7.
124. Carbonare LD, Arlot ME, Chavassieux PM. Comparison of trabecular bone microarchitecture and remodeling in glucocortiociod-induced and post-menopausal osteoporosis. J Bone Miner Res 2001(16):97-103.
125. Hahn TJ, Halstead LR, Teitelbaum SL, Hahn BH. Altered mineral metabolism in glucocorticoid-induced osteopenia. Effect of 25-hydroxyvitamin D administration. J Clin Invest 1979;64(2):655-65.
126. Canalis E. Clinical review 83: Mechanisms of glucocorticoid action in bone: implications to glucocorticoid-induced osteoporosis. J Clin Endocrinol Metab 1996;81(10):3441-7.
127. Peretz A, Praet JP, Bosson D, Rozenberg S, Bourdoux P. Serum osteocalcin in the assessment of corticosteroid induced osteoporosis. Effect of long and short term corticosteroid treatment. J Rheumatol 1989;16(3):363-7.
128. Cooper MS, Blumsohn A, Goddard PE, et al. 11beta-hydroxysteroid dehydrogenase type 1 activity predicts the effects of glucocorticoids on bone. J Clin Endocrinol Metab 2003; 88(8):3874-7.
129. Weinstein RS. Glucocorticoids, osteocytes, and skeletal fragility: the role of bone vascularity. Bone 2010;46(3):564-70.

130. Weinstein RS, Jilka RL, Parfitt AM, Manolagas SC. Inhibition of osteoblastogenesis and promotion of apoptosis of osteoblasts and osteocytes by glucocorticoids. Potential mechanisms of their deleterious effects on bone. J Clin Invest 1998;102(2):274-82.
131. Chen TL. Inhibition of growth and differentiation of osteoprogenitors in mouse bone marrow stromal cell cultures by increased donor age and glucocorticoid treatment. Bone 2004;35(1):83-95.
132. Engelbrecht Y, de Wet H, Horsch K, Langeveldt CR, Hough FS, Hulley PA. Glucocorticoids induce rapid up-regulation of mitogen-activated protein kinase phosphatase-1 and dephosphorylation of extracellular signal-regulated kinase and impair proliferation in human and mouse osteoblast cell lines. Endocrinology 2003;144(2):412-22.
133. Pereira RM, Delany AM, Canalis E. Cortisol inhibits the differentiation and apoptosis of osteoblasts in culture. Bone 2001;28(5):484-90.
134. Song LN. Effects of retinoic acid and dexamethasone on proliferation, differentiation, and glucocorticoid receptor expression in cultured human osteosarcoma cells. Oncol Res 1994; 6(3):111-8.
135. Pereira RC, Delany AM, Canalis E. Effects of cortisol and bone morphogenetic protein-2 on stromal cell differentiation: correlation with CCAAT-enhancer binding protein expression. Bone 2002;30(5):685-91.
136. Lian JB, Shalhoub V, Aslam F, et al. Species-specific glucocorticoid and 1,25-dihydroxyvitamin D responsiveness in mouse MC3T3-E1 osteoblasts: dexamethasone inhibits osteoblast differentiation and vitamin D down-regulates osteocalcin gene expression. Endocrinology 1997;138(5):2117-27.
137. Ohnaka K, Tanabe M, Kawate H, Nawata H, Takayanagi R. Glucocorticoid suppresses the canonical Wnt signal in cultured human osteoblasts. Biochem Biophys Res Commun 2005;329(1):177-81.
138. Luppen CA, Smith E, Spevak L, Boskey AL, Frenkel B. Bone morphogenetic protein-2 restores mineralization in glucocorticoid-inhibited MC3T3-E1 osteoblast cultures. J Bone Miner Res 2003;18(7):1186-97.
139. Gohel A, McCarthy MB, Gronowicz G. Estrogen prevents glucocorticoid-induced apoptosis in osteoblasts in vivo and in vitro. Endocrinology 1999;140(11):5339-47.
140. Liu Y, Porta A, Peng X, et al. Prevention of glucocorticoid-induced apoptosis in osteocytes and osteoblasts by calbindin-D28k. J Bone Miner Res 2004;19(3):479-90.
141. Delany AM, Jeffrey JJ, Rydziel S, Canalis E. Cortisol increases interstitial collagenase expression in osteoblasts by post-transcriptional mechanisms. J Biol Chem 1995;270(44): 26607-12.
142. Lukert B, Mador A, Raisz LG, Kream BE. The role of DNA synthesis in the responses of fetal rat calvariae to cortisol. J Bone Miner Res 1991;6(5):453-60.
143. Advani S, LaFrancis D, Bogdanovic E, Taxel P, Raisz LG, Kream BE. Dexamethasone suppresses in vivo levels of bone collagen synthesis in neonatal mice. Bone 1997;20(1):41-6.
144. Delany AM, Gabbitas BY, Canalis E. Cortisol downregulates osteoblast alpha 1 (I) procollagen mRNA by transcriptional and posttranscriptional mechanisms. J Cell Biochem 1995;57(3):488-94.
145. Chen TL, Chang LY, Bates RL, Perlman AJ. Dexamethasone and 1,25-dihydroxyvitamin D3 modulation of insulin-like growth factor-binding proteins in rat osteoblast-like cell cultures. Endocrinology 1991;128(1):73-80.
146. McCarthy TL, Centrella M, Canalis E. Cortisol inhibits the synthesis of insulin-like growth factor-I in skeletal cells. Endocrinology 1990;126(3):1569-75.
147. Delany AM, Canalis E. Transcriptional repression of insulin-like growth factor I by glucocorticoids in rat bone cells. Endocrinology 1995;136(11):4776-81.

148. Swolin D, Brantsing C, Matejka G, Ohlsson C. Cortisol decreases IGF-I mRNA levels in human osteoblast-like cells. J Endocrinol 1996;149(3):397-403.
149. Centrella M, McCarthy TL, Canalis E. Glucocorticoid regulation of transforming growth factor beta 1 activity and binding in osteoblast-enriched cultures from fetal rat bone. Mol Cell Biol 1991;11(9):4490-6.
150. Beavan S, Horner A, Bord S, Ireland D, Compston J. Colocalization of glucocorticoid and mineralocorticoid receptors in human bone. J Bone Miner Res 2001;16(8):1496-504.
151. Rubin J, Biskobing DM, Jadhav L, et al. Dexamethasone promotes expression of membrane-bound macrophage colony-stimulating factor in murine osteoblast-like cells. Endocrinology 1998;139(3):1006-12.
152. Hofbauer LC, Gori F, Riggs BL, et al. Stimulation of osteoprotegerin ligand and inhibition of osteoprotegerin production by glucocorticoids in human osteoblastic lineage cells: potential paracrine mechanisms of glucocorticoid-induced osteoporosis. Endocrinology 1999;140(10):4382-9.
153. Dempster DW, Moonga BS, Stein LS, Horbert WR, Antakly T. Glucocorticoids inhibit bone resorption by isolated rat osteoclasts by enhancing apoptosis. J Endocrinol 1997;154(3):397-406.
154. Weinstein RS, Chen JR, Powers CC, et al. Promotion of osteoclast survival and antagonism of bisphosphonate-induced osteoclast apoptosis by glucocorticoids. J Clin Invest 2002; 109(8):1041-8.
155. Tenenbaum HC, Heersche JN. Dexamethasone stimulates osteogenesis in chick periosteum in vitro. Endocrinology 1985;117(5):2211-7.
156. Bellows CG, Heersche JN, Aubin JE. Determination of the capacity for proliferation and differentiation of osteoprogenitor cells in the presence and absence of dexamethasone. Dev Biol 1990;140(1):132-8.
157. Bellows CG, Aubin JE. Determination of numbers of osteoprogenitors present in isolated fetal rat calvaria cells in vitro. Dev Biol 1989;133(1):8-13.
158. Rickard DJ, Sullivan TA, Shenker BJ, Leboy PS, Kazhdan I. Induction of rapid osteoblast differentiation in rat bone marrow stromal cell cultures by dexamethasone and BMP-2. Dev Biol 1994;161(1):218-28.
159. Maniatopoulos C, Sodek J, Melcher AH. Bone formation in vitro by stromal cells obtained from bone marrow of young adult rats. Cell Tssue Res 1988;254(2):317-30.
160. Jorgensen NR, Henriksen Z, Sorensen OH, Civitelli R. Dexamethasone, BMP-2, and 1,25-dihydroxyvitamin D enhance a more differentiated osteoblast phenotype: validation of an in vitro model for human bone marrow-derived primary osteoblasts. Steroids 2004;69(4): 219-26.
161. Herbertson A, Aubin JE. Dexamethasone alters the subpopulation make-up of rat bone marrow stromal cell cultures. J Bone Miner Res 1995;10(2):285-94.
162. Cheng SL, Zhang SF, Avioli LV. Expression of bone matrix proteins during dexamethasone-induced mineralization of human bone marrow stromal cells. J Cell Biochem 1996;61(2):182-93.
163. Iba K, Chiba H, Sawada N, Hirota S, Ishii S, Mori M. Glucocorticoids induce mineralization coupled with bone protein expression without influence on growth of a human osteoblastic cell line. Cell Struct Funct 1995;20(5):319-30.
164. Atmani H, Chappard D, Basle MF. Proliferation and differentiation of osteoblasts and adipocytes in rat bone marrow stromal cell cultures: effects of dexamethasone and calcitriol. J Cell Biochem 2003;89(2):364-72.
165. Milne M, Quail JM, Baran DT. Dexamethasone stimulates osteogenic differentiation in vertebral and femoral bone marrow cell cultures: comparison of IGF-I gene expression. J Cell Biochem 1998;71(3):382-91.

166. McCulloch CA, Tenenbaum HC. Dexamethasone induces proliferation and terminal differentiation of osteogenic cells in tissue culture. Anat Rec 1986;215(4):397-402.
167. Shalhoub V, Conlon D, Tassinari M, et al. Glucocorticoids promote development of the osteoblast phenotype by selectively modulating expression of cell growth and differentiation associated genes. J Cell Biochem 1992;50(4):425-40.
168. Jaiswal N, Haynesworth SE, Caplan AI, Bruder SP. Osteogenic differentiation of purified, culture-expanded human mesenchymal stem cells in vitro. J Cell Biochem 1997;64(2):295-312.
169. Beresford JN, Joyner CJ, Devlin C, Triffitt JT. The effects of dexamethasone and 1,25-dihydroxyvitamin D3 on osteogenic differentiation of human marrow stromal cells in vitro. Arch Oral Biol 1994;39(11):941-7.
170. Mikami Y, Omoteyama K, Kato S, Takagi M. Inductive effects of dexamethasone on the mineralization and the osteoblastic gene expressions in mature osteoblast-like ROS17/2.8 cells. Biochem Biophys Res Commun 2007;362(2):368-73.
171. Igarashi M, Kamiya N, Hasegawa M, Kasuya T, Takahashi T, Takagi M. Inductive effects of dexamethasone on the gene expression of Cbfa1, Osterix and bone matrix proteins during differentiation of cultured primary rat osteoblasts. J Mol Histol 2004;35(1):3-10.
172. Pockwinse SM, Stein JL, Lian JB, Stein GS. Developmental stage-specific cellular responses to vitamin D and glucocorticoids during differentiation of the osteoblast phenotype: interrelationship of morphology and gene expression by in situ hybridization. Exp Cell Res 1995;216(1):244-60.
173. Kasugai S, Todescan R, Jr., Nagata T, Yao KL, Butler WT, Sodek J. Expression of bone matrix proteins associated with mineralized tissue formation by adult rat bone marrow cells in vitro: inductive effects of dexamethasone on the osteoblastic phenotype. J Cell Physiol 1991;147(1):111-20.
174. Canalis E. Effect of glucocorticoids on type I collagen synthesis, alkaline phosphatase activity, and deoxyribonucleic acid content in cultured rat calvariae. Endocrinology 1983; 112(3):931-9.
175. Hong D, Chen HX, Ge RS, Li JC. The biological roles of extracellular and intracytoplasmic glucocorticoids in skeletal cells. J Steroid Biochem Mol Biol 2008;111(3-5):164-70.
176. Boivin G, Anthoine-Terrier C, Morel G. Ultrastructural localization of endogenous hormones and receptors in bone tissue: an immunocytological approach in frozen samples. Micron 1994;25(1):15-27.
177. Liesegang P, Romalo G, Sudmann M, Wolf L, Schweikert HU. Human osteoblast-like cells contain specific, saturable, high-affinity glucocorticoid, androgen, estrogen, and 1 alpha,25-dihydroxycholecalciferol receptors. J Androl 1994;15(3):194-9.
178. Necela BM, Cidlowski JA. Mechanisms of glucocorticoid receptor action in noninflammatory and inflammatory cells. Proc Am Thorac Soc 2004;1(3):239-46.
179. Buttgereit F, Scheffold A. Rapid glucocorticoid effects on immune cells. Steroids 2002; 67(6):529-34.
180. Stahn C, Lowenberg M, Hommes DW, Buttgereit F. Molecular mechanisms of glucocorticoid action and selective glucocorticoid receptor agonists. Mol Cell Endocrinol 2007;275(1-2):71-8.
181. Cole TJ, Blendy JA, Monaghan AP, et al. Targeted disruption of the glucocorticoid receptor gene blocks adrenergic chromaffin cell development and severely retards lung maturation. Genes Dev 1995;9(13):1608-21.
182. Berger S, Bleich M, Schmid W, et al. Mineralocorticoid receptor knockout mice: pathophysiology of Na+ metabolism. Proc Natl Acad Sci USA 1998;95(16):9424-9.

183. Woitge H, Harrison J, Ivkosic A, Krozowski Z, Kream B. Cloning and in vitro characterization of alpha 1(I)-collagen 11 beta-hydroxysteroid dehydrogenase type 2 transgenes as models for osteoblast-selective inactivation of natural glucocorticoids. Endocrinology 2001;142(3):1341-8.
184. Sher LB, Woitge HW, Adams DJ, et al. Transgenic expression of 11beta-hydroxysteroid dehydrogenase type 2 in osteoblasts reveals an anabolic role for endogenous glucocorticoids in bone. Endocrinology 2004;145(2):922-9.
185. Agarwal AK, Monder C, Eckstein B, White PC. Cloning and expression of rat cDNA encoding corticosteroid 11 beta-dehydrogenase. J Biol Chem 1989;264(32):18939-43.
186. Stewart PM, Murry BA, Mason JI. Human kidney 11 beta-hydroxysteroid dehydrogenase is a high affinity nicotinamide adenine dinucleotide-dependent enzyme and differs from the cloned type I isoform. J Clin Endocrinol Metab 1994;79(2):480-4.
187. Odermatt A, Arnold P, Stauffer A, Frey BM, Frey FJ. The N-terminal anchor sequences of 11beta-hydroxysteroid dehydrogenases determine their orientation in the endoplasmic reticulum membrane. J Biol Chem 1999;274(40):28762-70.
188. Stewart PM, Krozowski ZS. 11 beta-Hydroxysteroid dehydrogenase. Vitam Horm 1999;57: 249-324.
189. Edwards CR, Stewart PM, Burt D, et al. Localisation of 11 beta-hydroxysteroid dehydrogenase--tissue specific protector of the mineralocorticoid receptor. Lancet 1988; 2(8618):986-9.
190. Whorwood CB, Ricketts ML, Stewart PM. Epithelial cell localization of type 2 11 beta-hydroxysteroid dehydrogenase in rat and human colon. Endocrinology 1994;135(6):2533-41.
191. Albiston AL, Obeyesekere VR, Smith RE, Krozowski ZS. Cloning and tissue distribution of the human 11 beta-hydroxysteroid dehydrogenase type 2 enzyme. Mol Cell Endocrinol 1994;105(2):R11-7.
192. Monder C, White PC. 11 beta-hydroxysteroid dehydrogenase. Vitam Horm 1993;47:187-271.
193. Ricketts ML, Verhaeg JM, Bujalska I, Howie AJ, Rainey WE, Stewart PM. Immunohistochemical localization of type 1 11beta-hydroxysteroid dehydrogenase in human tissues. J Clin Endocrinol Metab 1998;83(4):1325-35.
194. Krozowski Z, MaGuire JA, Stein-Oakley AN, Dowling J, Smith RE, Andrews RK. Immunohistochemical localization of the 11 beta-hydroxysteroid dehydrogenase type II enzyme in human kidney and placenta. J Clin Endocrinol Metab 1995;80(7):2203-9.
195. Krozowski Z. The 11beta-hydroxysteroid dehydrogenases: functions and physiological effects. Mol Cell Endocrinol 1999;151(1-2):121-7.
196. Stewart PM, Krozowski ZS, Gupta A, et al. Hypertension in the syndrome of apparent mineralocorticoid excess due to mutation of the 11 beta-hydroxysteroid dehydrogenase type 2 gene. Lancet 1996;347(8994):88-91.
197. White PC, Mune T, Agarwal AK. 11 beta-Hydroxysteroid dehydrogenase and the syndrome of apparent mineralocorticoid excess. Endocr Rev 1997;18(1):135-56.
198. Kotelevtsev Y, Brown RW, Fleming S, et al. Hypertension in mice lacking 11beta-hydroxysteroid dehydrogenase type 2. J Clin Invest 1999;103(5):683-9.
199. Thompson A, Han VK, Yang K. Spatial and temporal patterns of expression of 11beta-hydroxysteroid dehydrogenase types 1 and 2 messenger RNA and glucocorticoid receptor protein in the murine placenta and uterus during late pregnancy. Biol Reprod 2002;67(6): 1708-18.
200. Condon J, Gosden C, Gardener D, et al. Expression of type 2 11beta-hydroxysteroid dehydrogenase and corticosteroid hormone receptors in early human fetal life. J Clin Endocrinol Metab 1998; 83(12):4490-7.

201. Bland R, Worker CA, Noble BS, et al. Characterization of 11beta-hydroxysteroid dehydrogenase activity and corticosteroid receptor expression in human osteosarcoma cell lines. J Endocrinol 1999;161(3):455-64.
202. Eyre LJ, Rabbitt EH, Bland R, et al. Expression of 11 beta-hydroxysteroid dehydrogenase in rat osteoblastic cells: pre-receptor regulation of glucocorticoid responses in bone. J Cell Biochem 2001;81(3):453-62.
203. Cooper MS, Walker EA, Bland R, Fraser WD, Hewison M, Stewart PM. Expression and functional consequences of 11beta-hydroxysteroid dehydrogenase activity in human bone. Bone 2000;27(3):375-81.
204. Kalajzic I, Kalajzic Z, Kaliterna M, et al. Use of type I collagen green fluorescent protein transgenes to identify subpopulations of cells at different stages of the osteoblast lineage. J Bone Miner Res 2002;17(1):15-25.
205. Kalajzic I, Staal A, Yang WP, et al. Expression profile of osteoblast lineage at defined stages of differentiation. J Biol Chem 2005;280(26):24618-26.
206. Sher LB, Harrison JR, Adams DJ, Kream BE. Impaired cortical bone acquisition and osteoblast differentiation in mice with osteoblast-targeted disruption of glucocorticoid signaling. Calcif Tissue Int 2006;79(2):118-25.
207. Kalak R, Zhou H, Street J, et al. Endogenous glucocorticoid signalling in osteoblasts is necessary to maintain normal bone structure in mice. Bone 2009.
208. Blunt JW, Jr., Plotz CM, Lattes R, Howes EL, Meyer K, Ragan C. Effect of cortisone on experimental fractures in the rabbit. Proc Soc Exp Biol Med 1950;73(4):678-81.
209. Sissons HA, Hadfield GJ. The influence of cortisone on the repair of experimental fractures in the rabbit. Br J Surg 1951;39(154):172-8.
210. Waters RV, Gamradt SC, Asnis P, et al. Systemic corticosteroids inhibit bone healing in a rabbit ulnar osteotomy model. Acta Orthop Scand 2000;71(3):316-21.
211. Bostrom MP, Gamradt SC, Asnis P, et al. Parathyroid hormone-related protein analog RS-66271 is an effective therapy for impaired bone healing in rabbits on corticosteroid therapy. Bone 2000;26(5):437-42.
212. Luppen CA, Blake CA, Ammirati KM, et al. Recombinant human bone morphogenetic protein-2 enhances osteotomy healing in glucocorticoid-treated rabbits. J Bone Miner Res 2002;17(2):301-10.
213. Murakami H, Kowalewski K. Effects of cortisone and an anabolic androgen on the fractured humerus in guinea pigs: clinical and histological study over a six-week period of fracture healing. Can J Surg 1966;9(4):425-34.
214. Hellewell AB, Beljan JR, Goldman M. Effect of chronic administration of glucocorticoid (prednisolone) on the rate of healing of experimental osseous defects. Clin Orthop Relat Res 1974(100):349-55.
215. Key JA, Odell RT, Taylor LW. Failure of cortisone to delay or to prevent the healing of fractures in rats. J Bone Joint Surg Am 1952;24-A-3:665-75.
216. Weiss R, Ickowicz M. The Influence of Cortisone on the Healing of Experimental Fractures in Rats. Acta Anat 1964;59:163-81.
217. Aslan M, Simsek G, Yildirim U. Effects of short-term treatment with systemic prednisone on bone healing: an experimental study in rats. Dent Traumatol 2005;21(4):222-5.
218. Hogevold HE, Grogaard B, Reikeras O. Effects of short-term treatment with corticosteroids and indomethacin on bone healing. A mechanical study of osteotomies in rats. Acta Orthop Scand 1992;63(6):607-11.
219. Sato S, Kim T, Arai T, Maruyama S, Tajima M, Utsumi N. Comparison between the effects of dexamethasone and indomethacin on bone wound healing. Jpn J Pharmacol 1986;42(1):71-8.

220. Wiancko KB, Kowalewski K. Strength of callus in fractured humerus of rat treated with anti-anabolic and anabolic compounds. Acta Endocrinol 1961;36:310-8.
221. Gilley RS, Wallace LJ, Bourgeault CA, Kidder LS, Bechtold JE. OP-1 Augments Glucocorticoid-inhibited Fracture Healing in a Rat Fracture Model. Clin Orthop Relat Res 2009.
222. Ljusberg J, Wang Y, Lang P, et al. Proteolytic excision of a repressive loop domain in tartrate-resistant acid phosphatase by cathepsin K in osteoclasts. J Biol Chem 2005; 280(31):28370-81.
223. Zheng Y, Zhou H, Modzelewski JR, et al. Accelerated bone resorption, due to dietary calcium deficiency, promotes breast cancer tumor growth in bone. Cancer Res 2007; 67(19):9542-8.
224. Holdsworth D, Thornton M. Micro-CT in small animal and specimen imaging. Trends Biotechnol 2002;20(8):S34-9.
225. Parfitt AM, Drezner MK, Glorieux FH, et al. Bone histomorphometry: standardization of nomenclature, symbols, and units. Report of the ASBMR Histomorphometry Nomenclature Committee. J Bone Miner Res 1987;2(6):595-610.
226. Theodossiou TA, Thrasivoulou C, Ekwobi C, Becker DL. Second Harmonic Generation Confocal Microscopy of Collagen Type 1 from Rat Tendon Cryosections. Biophys J 2006; 91:4665-77.
227. Franken PA, Hill AE, Peters CW, Weinreich G. Generation of optical harmonics. Phys Rev Lett 1961(7):118-9.
228. Hsu SM, Raine L, Fanger H. Use of avidin-biotin-peroxidase complex (ABC) in immunoperoxidase techniques: a comparison between ABC and unlabeled antibody (PAP) procedures. J Histochem Cytochem 1981;29(4):577-80.
229. Smith RE, Li KX, Andrews RK, Krozowski Z. Immunohistochemical and molecular characterization of the rat 11 beta-hydroxysteroid dehydrogenase type II enzyme. Endocrinology 1997;138(2):540-7.
230. Uusitalo H, Rantakokko J, Ahonen M, et al. A metaphyseal defect model of the femur for studies of murine bone healing. Bone 2001;28(4):423-9.
231. Hiltunen A, Aro HT, Vuorio E. Regulation of extracellular matrix genes during fracture healing in mice. Clin Orthop Relat Res 1993;297:23-7.
232. Schindeler A, Morse A, Harry L, et al. Models of tibial fracture healing in normal and Nf1-deficient mice. J Orthop Res 2008;26(8):1053-60.
233. Virolainen P, Vuorio E, Aro HT. Gene expression at graft-host interfaces of cortical bone allografts and autografts. Clin Orthop Relat Res 1993;297:144-9.
234. Shapiro F. Cortical bone repair. The relationship of the lacunar-canalicular system and intercellular gap junctions to the repair process. J Bone Joint Surg Am 1988;70(7):1067-81.
235. Glimcher MJ, Shapiro F, Ellis RD, Eyre DR. Changes in tissue morphology and collagen composition during the repair of cortical bone in the adult chicken. J Bone Joint Surg 1980;62(6):964-73.
236. Meadows TH, Bronk JT, Chao YS, Kelly PJ. Effect of weight-bearing on healing of cortical defects in the canine tibia. J Bone Joint Surg 1990;72(7):1074-80.
237. Draenert Y, Draenert K. Gap healing of compact bone. Scan Electron Microsc 1980(4): 103-11.
238. Campbell TM, Wong WT, Mackie EJ. Establishment of a model of cortical bone repair in mice. Calcif Tissue Int 2003;73(1):49-55.
239. Kim JB, Leucht P, Lam K, et al. Bone regeneration is regulated by wnt signaling. J Bone Miner Res 2007;22(12):1913-23.

240. Street J, Bao M, deGuzman L, et al. Vascular endothelial growth factor stimulates bone repair by promoting angiogenesis and bone turnover. Proc Natl Acad Sci USA 2002; 99(15):9656-61.
241. Pereira AC, Fernandes RG, Carvalho YR, Balducci I, Faig-Leite H. Bone healing in drill hole defects in spontaneously hypertensive male and female rats' femurs. A histological and histometric study. Arq Bras Cardiol 2007;88(1):104-9.
242. Wang J, Zhou HY, Salih E, et al. Site-specific in vivo calcification and osteogenesis stimulated by bone sialoprotein. Calcif Tissue Int 2006;79(3):179-89.
243. He H, Huang J, Chen G, Dong Y. Application of a new bioresorbable film to guided bone regeneration in tibia defect model of the rabbits. J Biomed Mater Res A 2007;82(1):256-62.
244. Kusuzaki K, Kageyama N, Shinjo H, et al. Development of bone canaliculi during bone repair. Bone 2000;27(5):655-9.
245. Uchida S, Sakai A, Kudo H, et al. Vascular endothelial growth factor is expressed along with its receptors during the healing process of bone and bone marrow after drill-hole injury in rats. Bone 2003;32(5):491-501.
246. Tanaka M, Sakai A, Uchida S, et al. Prostaglandin E2 receptor (EP4) selective agonist (ONO-4819.CD) accelerates bone repair of femoral cortex after drill-hole injury associated with local upregulation of bone turnover in mature rats. Bone 2004;34(6):940-8.
247. Schilling T, Muller M, Minne HW, Ziegler R. Influence of inflammation-mediated osteopenia on the regional acceleratory phenomenon and the systemic acceleratory phenomenon during healing of a bone defect in the rat. Calcif Tissue Int 1998;63(2):160-6.
248. Nagashima M, Sakai A, Uchida S, Tanaka S, Tanaka M, Nakamura T. Bisphosphonate (YM529) delays the repair of cortical bone defect after drill-hole injury by reducing terminal differentiation of osteoblasts in the mouse femur. Bone 2005;36(3):502-11.
249. Petrizzi L, Mariscoli M, Valbonetti L, Varasano V, Langhoff JD, von Rechenberg B. Preliminary study on the effect of parenteral naloxone, alone and in association with calcium gluconate, on bone healing in an ovine "drill hole" model system. BMC Musculoskelet Disord 2007;8:43.
250. Wang J. Spatial orientation of the microscopic elements of cortical repair bone. Clin Orthop Relat Res 2000(374):265-77.
251. Honma T, Itagaki T, Nakamura M, et al. Bone formation in rat calvaria ceases within a limited period regardless of completion of defect repair. Oral Dis 2008;14(5):457-64.
252. Thompson Z, Miclau T, Hu D, Helms JA. A model for intramembranous ossification during fracture healing. J Orthop Res 2002;20(5):1091-8.
253. Aronson J, Shen XC, Skinner RA, Hogue WR, Badger TM, Lumpkin CK, Jr. Rat model of distraction osteogenesis. J Orthop Res 1997;15(2):221-6.
254. O'Brien CA, Jia D, Plotkin LI, et al. Glucocorticoids act directly on osteoblasts and osteocytes to induce their apoptosis and reduce bone formation and strength. Endocrinology 2004;145(4):1835-41.
255. Li X, Gu W, Masinde G, et al. Genetic variation in bone-regenerative capacity among inbred strains of mice. Bone 2001;29(2):134-40.
256. Manigrasso MB, O'Connor JP. Characterization of a closed femur fracture model in mice. J Orthop Trauma 2004;18(10):687-95.
257. Holstein JH, Menger MD, Culemann U, Meier C, Pohlemann T. Development of a locking femur nail for mice. J Biomech 2007;40(1):215-9.
258. Holstein JH, Matthys R, Histing T, et al. Development of a stable closed femoral fracture model in mice. J Surg Res 2009;153(1):71-5.

259. Holstein JH, Garcia P, Histing T, et al. Advances in the establishment of defined mouse models for the study of fracture healing and bone regeneration. J Orthop Trauma 2009;23(5 Suppl):S31-8.
260. Cheung KM, Kaluarachi K, Andrew G, Lu W, Chan D, Cheah KS. An externally fixed femoral fracture model for mice. J Orthop Res 2003;21(4):685-90.
261. Garcia P, Holstein JH, Histing T, et al. A new technique for internal fixation of femoral fractures in mice: impact of stability on fracture healing. J Biomech 2008;41(8):1689-96.
262. Garcia P, Holstein JH, Maier S, et al. Development of a reliable non-union model in mice. J Surg Res 2008;147(1):84-91.
263. Grongroft I, Heil P, Matthys R, et al. Fixation compliance in a mouse osteotomy model induces two different processes of bone healing but does not lead to delayed union. J Biomech 2009;42(13):2089-96.
264. Histing T, Garcia P, Matthys R, et al. An internal locking plate to study intramembranous bone healing in a mouse femur fracture model. J Orthop Res 2010;28(3):397-402.

9 Appendix

9.1 Publications and Presentations

Full-length original report (peer-reviewed):

Weber AJ, Li G, Kalak R, Street J, Buttgereit F, Dunstan CR, Seibel MJ, Zhou H. Osteoblast-targeted disruption of glucocorticoid signalling does not delay intramembranous bone healing. **Steroids** 2010;75(3):282-6

URL:http://www.ncbi.nlm.nih.gov/pubmed/20096296?itool=EntrezSystem2.PEntrez.Pubmed.Pubmed_ResultsPanel.Pubmed_RVDocSum&ordinalpos=1

Abstracts:

Weber AJ, Li G, Kalak R, Street J, Dunstan CR, Buttgereit F, Zhou H, Seibel MJ. Osteoblast-targeted disruption of glucocorticoid signalling: normal fracture healing during the early stages of intramembranous bone repair. The 18th Annual Scientific Meeting of the Australian & New Zealand Bone & Mineral Society (ANZBMS), August 18-20, 2008, Melbourne, Australia

Weber AJ, Li G, Kalak R, Street J, Dunstan CR, Buttgereit F, Zhou H, Seibel MJ. Normal intramembranous fracture healing in mice with transgenic osteoblast-targeted disruption of glucocorticoid signalling: analysis by microcomputed tomography. The American Society for Bone & Mineral Research (ASBMR) 30th Annual Meeting, September 12-16, 2008, Montréal, Québec, Canada

Weber AJ, Li G, Kalak R, Street J, Dunstan CR, Buttgereit F, Seibel MJ, Zhou H. Osteoblast/ Osteocyte-targeted disruption of glucocorticoid signalling in mice: normal intramembranous bone repair of a cortical tibia defect. Annual European Congress of Rheumatology, The European League Against Rheumatism (EULAR), June 10-13, 2009, Copenhagen, Denmark

Weber AJ, Li G, Kalak R, Street J, Dunstan CR, Buttgereit F, Seibel MJ, Zhou H. Normal intramembranous bone repair of cortical bone defects in mice with osteoblast-targeted disruption of glucocorticoid signalling in mice. The American College of Rheumatology (ACR) Scientific Meeting 2009, October 17-21, 2009, Philadelphia, USA

9.2 Curriculum Vitae

Mein Lebenslauf wird aus datenschutzrechtlichen Gründen in der elektronischen Version meiner Arbeit nicht veröffentlicht.

9.3 Acknowledgements

This work was conducted at the Charité University Hospital, Berlin, Germany in cooperation with the ANZAC Research Institute, The University of Sydney, Sydney, Australia.

I am very grateful to my supervisors Prof. Dr. Frank Buttgereit and Prof. Dr. Markus Seibel for the opportunity to participate in this interdisciplinary continuing research cooperation as the first student. I greatly appreciate the many opportunities to present and discuss this work at national and international congresses.

I am very thankful to Prof. Dr. Frank Buttgereit for his valuable and constructive comments on this work.

My warm thanks go to Prof. Dr. Markus Seibel for his constant support and dedicated guidance during my research in Australia.

I am thankful to Dr. Hong Zhou for introducing me into the methodology and the possibility to discuss the laboratory results.

I am very grateful to the Bone Biology group, especially to Janine Street and Dr. Robert Kalak who made me familiar with various technical methods.

My special thanks go to Bjornar Sandnes from the Macquarie University, Sydney, Australia for producing the SHIM pictures.

My warm thanks go to Dr. Gang Li from the Chinese University Hong Kong, Hong Kong, PR China for his kindful and precise introduction into his fracture healing model.

I thank the Charité University Hospital and the Bone Biology group of the ANZAC Research Institute to provide financial support.

Finally, I thank my family and friends for their constant support and encouragement.

9.4 Statement/ Erklärung an Eides Statt

„Ich, Agnes Weber, erkläre, dass ich die vorgelegte Dissertation mit dem Thema: „Fracture Healing and Glucocorticoids in HSD2 tg mouse model“ selbst verfasst und keine anderen als die angegeben Quellen und Hilfsmittel benutzt, ohne die (unzulässige) Hilfe Dritter verfasst und auch in Teilen keine Kopien anderer Arbeiten dargestellt habe.“

Berlin, den 01.10.2010

Agnes Weber